ASTEROID SURFACE MATERIALS: MINERALOGICAL CHARACTERIZATIONS FROM REFLECTANCE SPECTRA

By

Michael J. Gaffey
Thomas B. McCord

NSG-7310

University of Hawaii at Manoa

Institute for Astronomy
2680 Woodlawn Drive • Honolulu, Hawaii 96822
Telex: 723-8459 • UHAST HR

November 18, 1977

NASA Scientific and Technical
Information Facility
P.O. Box 8757
Baltimore/Washington Int. Airport
Maryland 21240

Gentlemen:

RE: Spectroscopy of Asteroids, NSG 7310

Enclosed are two copies of an article entitled "Asteroid Surface Materials: Mineralogical Characteristics from Reflectance Spectra," by Dr. Michael J. Gaffey and Dr. Thomas B. McCord, which we have recently submitted for publication to Space Science Reviews. We submit these copies in accordance with the requirements of our NASA grants.

Sincerely yours,

Thomas B. McCord
Principal Investigator

TBM:zc

Enclosures

ASTEROID SURFACE MATERIALS: MINERALOGICAL CHARACTERIZATIONS FROM REFLECTANCE SPECTRA

By

Michael J. Gaffey

Thomas B. McCord

Institute for Astronomy
University of Hawaii at Manoa
2680 Woodlawn Drive
Honolulu, Hawaii 96822

Submitted to Space Science Reviews

Publication #151 of the Remote Sensing Laboratory

Abstract

The interpretation of diagnostic parameters in the spectral reflectance data for asteroids provides a means of characterizing the mineralogy and petrology of asteroid surface materials. An interpretive technique based on a quantitative understanding of the functional relationship between the optical properties of a mineral assemblage and its mineralogy, petrology and chemistry can provide a considerably more sophisticated characterization of a surface material than any matching or classification technique for those objects bright enough to allow spectral reflectance measurements. Albedos derived from radiometry and polarization data for individual asteroids can be used with spectral data to establish the spectral albedo, to define the optical density of the surface material and, in general, to constrain mineralogical interpretations.

Mineral assemblages analogous to most meteorite types, with the exception of ordinary chondritic assemblages, have been found as surface materials of Main Belt asteroids. C1- and C2-like assemblages (unleached, oxidized meteoritic clay minerals plus opaques such as carbon) dominate the population ($\sim$80%) throughout the Belt, especially in the outer Belt. A smaller population of asteroids exhibit surface materials similar to C3 (CO, CV) meteoritic assemblages (olivine plus opaque, probably carbon) and are also distributed throughout the Belt. The relative size (diameter) distributions for these two populations of objects are consistent with an origin by sequential accretion from a cooling nebula ('C2'

as surface layers, 'C3' as interior layers or cores). Based on information from meteoritic analogues and on qualitative models for the behavior of these materials during a heating episode, it seems unlikely that these 'C2'- and 'C3'-like asteroidal bodies have experienced any significant post-accretionary heating event either near surface or in the deep interior.

The majority of remaining studied asteroids (20) of 65 asteroids exhibit spectral reflectance curves dominated by the presence of metallic nickel-iron in their surface materials. These objects are most probably the several end products of an intense thermal event leading to the melting and differentiating of their protobodies. These thermalized bodies are concentrated toward the inner part of the Asteroid Belt but exist throughout the Belt.

The size of the proto-asteroid has apparently exercised control over the post-accretionary thermal history of these bodies. The available evidence indicates that all asteroids larger than about 450 kilometers in (present) diameter have undergone a significant heating episode since their formation. The post-accretionary thermal history of the asteroidal parent bodies was apparently affected by both distance from the sun and body size.

The C2-like materials which dominate the main asteroid belt population appear to relatively rare on earth-approaching asteroids. This suggests that most of these Apollo-Amor objects are not randomly derived from the main belt, but (a) may derive from a single event in recent time ($\sim 10^7$ years), (b) may derive from a favorably situated source body, (c) may derive from a particular,

compositionally anomalous region of the belt, or (d) may derive from an alternate source (e.g. comets).

I. Introduction

The asteroids are of special interest to the astronomical and cosmological communities as a possible window back to the very early stages of the evolution of the solar system. For example, the understanding of the relationship between the asteroids and the terrestrially available meteoritic materials would permit the expansion of the cosmological insights gained by the study of the meteorites to specific locations in the solar nebula. The significance of meteorites in understanding the origin and evolution of the solar system lies both in their antiquity and in the contraints which their detailed petrology, mineralogy and mineral chemistry place on the processes in the solar nebula and early solar system. The sophistication with which asteroids can be used as similar, but in situ, probes of the early solar system is therefore a direct function of the sophistication of the mineralogical and petrological characterizations which can be made for asteroidal materials. Until a number of asteroid sample return missions have been accomplished, remote sensing will remain our only method of characterizing such materials.

The interpretation of visible and near-infrared reflectance spectra is the most definitive available technique for the remote determination of asteroid surface mineralogies and petrologies. This technique utilizes electronic absorption features present in the reflectance spectra which are directly related to the mineral phases present. McCord et al. (1970) first measured the detailed reflectance spectrum (0.3 - 1.1μm) for the asteroid

Vesta and showed that this spectrum was diagnostic of a surface mineral assemblage similar to certain basaltic achondritic meteorites. In five subsequent papers (Chapman et al., 1973a, b; McCord and Chapman, 1975a, b; Pieters et al., 1976) the narrow bandpass filter spectra for approximately 100 additional asteroids were made available. UBV colors are available for about 300 asteroids (Zellner et al., 1975; Zellner et al., 1977b; Zellner and Bowell, 1977). In addition, observational work has been initiated for the 1-3μm region with the broad-band JHK filters (1.25, 1.65 and 2.2μm respectively) for more than 30 asteroids (Johnson et al., 1975; Chapman and Morrison, 1976; Matson et al., 1977a) and with higher resolution interferometric observations of three bright asteroids: 4 Vesta (Larson and Fink, 1975), 433 Eros (Larson et al., 1976) and 1 Ceres (Larson, 1977).

Since 1970, a number of papers (e.g. Chapman and Salisbury, 1973; Johnson and Fanale, 1973; Chapman et al., 1975; Chapman, 1976, 1977; Zellner and Bowell, 1977) have been published describing asteroid surface materials as derived from these and other observational data sets, principally, radiometric and polarimetric albedos and diameters. The present paper will attempt to achieve a significant advance over previous efforts in the sophistication of such characterizations. Two general approaches have been utilized in the various discussions of the asteroid surface materials, the classification or matching approach and the interpretive approach. Early efforts to match observational data of asteroids with laboratory spectral measurements of possible comparison materials, especially meteorites, are being replaced

by characterizations based on the identification and quantification of spectral features which are diagnostic of the presence and composition of specific mineral phases. In the limiting case, the pure matching approach to characterizing a material from spectral, albedo or polarization data does not require any understanding of the functional relationship(s) between the observed optical parameters and the mineralogic, petrologic or physical properties of the material. Sytinskaya (1965) provides a good example of a nearly pure matching characterization of asteroids. This type of comparison selects for materials which are similar with respect to the chosen optical parameters but which may be quite different with respect to other properties of the materials (e.g. mineralogy).

The interpretive approach requires the identification of some feature in the reflectance spectrum (such as an absorption band) which is diagnostic of a specific mineral or mineral assemblage. To utilize this approach, it is necessary to have at least a qualitative understanding of the mineralogical significance of the parameters of these features (i.e., wavelength position, symmetry, halfwidth, etc.).

The accuracy, uniqueness and completeness of a mineralogic interpretation of the reflectance spectrum of an asteroid depends on the precision to which the relevant features in the spectrum can be measured. A certain minimum spectral coverage, spectral resolution and photometric precision is required. This can be graphically illustrated (Figure 1) by comparing the spectral resolution and coverage of the several existing observational

spectral data sets for asteroids to the spectral reflectance curves of several interesting meteorite types. The parameters describing the mineral absorption features for pyroxene, olivine and feldspar, for example, are functions of mineral chemistry and relative mineral abundance. The slope and curvature of the visible spectral continuum indicates, among other things, the relative abundance of metals and silicates. To determine detailed mineralogical or petrological properties of an asteroid surface material, the spectral measurements must have spectral coverage and resolution sufficient to detect and define these spectral features. Broadband, low spectral coverage data, such as UBV measurements, usually cannot measure the necessary parameters.

It is important to note that the correlation between the mineralogical, petrological or physical properties of a material and its spectral, albedo and polarimetric properties is neither a simple nor a single-valued function for most cases. Thus the albedo of a powdered surface, while related to the mineral assemblage present, is strongly controlled by particle size and packing (Adams and Filice, 1967). The amplitude of the negative branch of a polarization vs. phase angle curve at small phase angles (P_{min}) results from multiple scattering and shadowing in a particulate surface layer and is thus controlled by mineral optical density, grain size, particle packing and petrology (Wolff, 1975; Egan et al., 1973; Zellner et al., 1974; Dollfus and Geake, 1975). Spectral colors are also functions of several material characteristics. Hapke (1971) noted the large variation of UBV colors of a material with particle size. Zellner et al. (1975) shows that

the scatter of UBV colors for specimens of a variety of diverse meteorite types (e.g. Eucrites, Howardites, H, L, LL and C3 chondrites) is larger than the difference in mean colors between types. UBV colors cannot unambiguously differentiate among a significant range of meteorite types even under laboratory conditions. On the other hand, many characteristics of mineral absorption bands (see for example, Burns 1970b; Adams, 1974) are functions only of mineral chemistry and are not affected to any significant degree by the physical properties of the surface layer.

II. Additional information sources

In addition to spectral reflectance, several other observational or theoretical techniques can provide information on the surface properties of asteroids or their relationship to meteorites. The two most extensively applied complimentary observational techniques involve polarimetric and infrared radiometric measurements to define surface properties (e.g., albedo, optical density, object diameter) which are not unique functions of mineralogy or petrology.

Measurements of the polarization of light reflected from the surface of asteroids as a function of phase angle have been made by Lyot (1934), Gehrels et al. (1970), Veverka (1970, 1971a, b, 1973), Dunlap et al. (1973), Dunlap (1974), Zellner et al. (1974) and Zellner and Gradie (1976a, b). Polarimetric measurements of laboratory comparison materials have been used as a basis for interpreting these data by Dollfus (1971), Dollfus and Geake (1975), Veverka and Noland (1973), Bowell and Zellner (1973) and Zellner and Gradie (1976a). At least three parameters of a polarization-versus-phase-angle curve have been empirically related to specific properties of the observed surface materials of asteroids. (a) The existence of a negative branch in the polarization-versus-phase-angle-curve at small phase angles for most asteroids indicates the existence of at least a thin powdered or dusty surface layer. (b) The depth of the negative branch (P_{min}) is a function of the optical density or absorbance of the surface grains. Asteroid surface materials exhibit a range of optical densities comparable

to that for meteoritic materials. (c) The slope of the ascending branch of the phase-polarization curve (at larger phase angles) is a function of the albedo of the surface materials. Polarimetricly derived asteroid albedos have the same general range (3-30%) as do meteoritic materials. By combining the measured visual brightness with the calculated albedo, it is possible to derive the effective diameter of an asteroid. Wolff (1975) has begun to define quantitatively the functional relationships between phase-polarization behavior and surface properties.

Measurements of the brightness of an asteroid in the thermal infrared (e.g., at wavelengths of 10 and 20μm) can be used to determine a model radiometric diameter, that is, the size of an object required to produce the measured flux using certain assumptions concerning temperature, emissivity and geometric factors. This technique was developed by Allen (1970, 1971) and by Matson (1971, 1972) and has been applied extensively by Cruikshank and Morrison (1973), Jones and Morrison (1974), Morrison (1973, 1974, 1977a, b), Morrison and Chapman (1976), Hansen (1976, 1977), Cruikshank (1977) and Cruikshank and Jones (1977). These results are reviewed by Morrison (1977c).

The values for asteroid diameters and albedo obtained by these two techniques have agreed well for objects with albedos higher than about 7%, but until recently have diverged significantly for objects with lower albedos. Chapman et al. (1975) adopted a weighting scheme to combine the radiometric and polarimetric values to produce their final published values for albedos and diameters.

Zellner and Gradie (1976a), Morrison (1977a) and Hansen (1977) have discussed this discrepancy. Recently Zellner et al. (1977a) concluded that a single polarization-phase curve slope-albedo relationship cannot be used for the range of asteroid albedos. The new slope-albedo relationship for low albedo surfaces reconciles the polarimetric values to the radiometric values.

The albedo or optical density of an asteroid surface material cannot be interpreted to define unambiguously surface mineralogy or petrology. However, an albedo determined from radiometry or polarimetry is valuable for constraining and testing the mineralogical interpretation of reflectance spectra and is used here in this manner.

A completely different approach to the problem of determining the relationship between the meteorites and possible asteroidal source bodies involves the investigation of origin and orbital evolution of the meteorites and asteroidal fragments. Wetherill (1974) has reviewed the effort in this area. The shock history, cosmic ray exposure age, collisional lifetime, orbital elements and orbital evolution data for meteoritic specimens tend to select or eliminate specific celestial objects as the source bodies of particular meteorites. The major uncertainty in evaluating any particular asteroidal object as a source of some portion of the terrestrial meteorite flux lies in the incomplete understanding of the mechanism which converts the original orbit into one which intersects that of the earth. A variety of mechanisms have been proposed including close encounters with Mars (Anders, 1964; Arnold, 1965), secular perturbation (Kozai,

1962; Williams, 1969), resonant perturbations (Zimmerman and Wetherill, 1973), secular resonant accelerations (Williams, 1973) and non-gravitational accelerations (Peterson, 1976). Several authors predict that specific asteroids should be providing a significant contribution to the terrestrial flux if their mechanism is dominant. Some of these predictions are given on Table I. Detailed mineralogical characterizations of the surface materials of these asteroids can be utilized to test such predictions.

III. Previous characterizations of asteroid surface materials

McCord et al. (1970) measured the 0.3-1.1μm spectrum of the asteroid 4 Vesta and identified an absorption feature near 0.9μm as due to the mineral pyroxene. They suggested that the surface material was similar to basaltic achondritic meteorites. Hapke (1971) compared the UBV colors of a number of asteroids to a variety of lunar, meteoritic and terrestrial rocks and rock powders. He concluded was that the surface material of these asteroids could be matched by powders similar to a range of the comparison materials but not by metallic surfaces. Chapman and Salisbury (1973) and Johnson and Fanale (1973) by comparing narrow band filter, 0.3-1.1μm asteroidal spectra to laboratory meteorite spectra were able to make much more specific statements concerning the asteroid surface materials. Chapman and Salisbury (1973) indicated that some matches between asteroid and meteorite spectra were found for several meteorite types including enstatite chondrites, a basaltic achondrite, an optically unusual ordinary chondrite and, possibly, a carbonaceous chondrite. Johnson and Fanale (1973) showed that the albedo and spectral characteristics of some asteroids are similar to C1 and C2 carbonaceous chondrites and to iron meteorites. They both noted the problem of defining precisely what constituted a 'match,' and both raised the question of subtle spectral modification of asteroid surface materials by in situ space weathering processes. Salisbury and Hunt (1974) raised the question of the effects of terrestrial weathering on meteorite specimens and the validity of matches between the spectra of such specimens and the asteroids. McCord

and Gaffey (1974) utilized absorption features and general spectral properties to characterize 14 asteroids and identified mineral assemblages similar to carbonaceous chondrite, stony-iron, iron, basaltic achondrite and silicate-metal meteorites. At that time it was possible to establish the general identity of the spectrally important minerals in an assemblage, but very difficult to establish their relative abundances.

Chapman et al. (1975) utilized spectral, albedo and polarization parameters to define two major groups which include most asteroids. The first group was characterized as having low albedos ($\leq$0.09), strong negative polarizations at small phase angles (>1.1%) and relatively flat, featureless spectral reflectance curves. These parameters were similar to those for carbonaceous chondrites and these asteroids were designated as 'carbonaceous' or 'C' type. The second group was characterized as having higher albedos ($\geq$0.09), weaker negative polarizations (0.4-1.0%) and reddish, sometimes featured spectral curves. These parameters were comparable to those for most of the meteorites which contain relatively abundant silicate minerals, so this group was designated 'silicaceous or stony-iron' or 'S' types. A small minority ($\sim$10%) of the asteroids could not be classified in this system and were designated 'unclassified' or 'U' types.

This simple classification scheme can be quite useful since it does seem to often separate these two major types of objects and the observational parameters on which the scheme is based can be measured at present for objects fainter than those for which

complete spectra can be obtained. The choice of terminology is unfortunate, however, since it implies a specific definition of surface materials in meteoritic terms, which was not intended. Any 'flat-black' spectral curve would be designated 'C' type whether or not the surface material would be characterized as carbonaceous by any other criteria. Thus, asteroid surface materials similar to such diverse meteoritic assemblages as ureilites, black chondrites and the carbon-poor C4 meteorite Karoonda would all be lumped under the label 'carbonaceous'.

The problem is complicated by the terminology for the meteorites themselves. As Mason (1971) noted, the term 'carbonaceous' immediately implies the presence of carbon or carbonaceous compounds as a distinctive component. However, a number of the carbonaceous chondrites, especially types C3 and C4, contain less carbon than many non-'carbonaceous' meteorites. Indeed, the presently accepted definition of the carbonaceous chondrites ($SiO_2/MgO < 1.5$ (weight) - Van Schmus and Wood, 1967) has little or nothing to do with carbon. It is essential to realize that the term 'carbonaceous asteroid' is not necessarily equivalent to 'carbonaceous meteorite' (as broad as that latter classification is). 'Carbonaceous' as presently used is a spectral classification designation with respect to asteroids and a compositional designation with respect to meteorites. A similar objection can be raised with respect to the 'silicaceous' terminology since it implies a degree of specificity not present in the classification criteria. It must also be noted that the criticism is with respect to the terminology and the confusion

which it engenders and not with respect to identification of these two major groups, defined by the parameters chosen (e.g. albedo, polarization, etc.), which appear to be significant.

Thus while the 'C' and 'S' classification of asteroids cannot be viewed as descriptions of mineralogy or petrology, it does provide valid characterizations with respect to the chosen parameters. Since the groups appear in each of the data sets used, (albedo, polarization, color) a single measurement such as UBV color can be used to classify the asteroid (Zellner et al., 1975; Zellner et al., 1977b; Zellner and Bowell, 1977; Morrison, 1977a, b). This approach can also be utilized to identify anomalous objects (Zellner, 1975; Zellner et al., 1977c) or to establish possible genetic relationships between members of asteroid dynamical families (Gradie and Zellner, 1977). Chapman (1976) utilized the basic 'C-S' classification system but identified subdivisions based on additional spectral criteria ('Slope', Bend' and 'Band Depth' - McCord and Chapman, 1975a, b) which are mineralogically significant.

Johnson et al. (1975) measured the infrared reflectance of three asteroids through the broad bandpass J, H and K filters (1.25, 1.65 and 2.2 μm) and concluded that these were consistent with the infrared reflectance of suggested meteoritic materials. Matson et al. (1977a, b) utilized infrared H and K reflectances to infer that space weathering or soil maturation processes were relatively inactive on asteroid surfaces in contrast to the Moon and Mercury.

A very favorable apparition in early 1975 permitted the measurement of a variety of spectral data sets for the earth-approaching asteroid 433 Eros. Pieters et al. (1976) measured the 0.33-1.07μm spectral reflectance of Eros through 25 narrow-bandpass filters. This curve was interpreted to indicate an assemblage of olivine, pyroxene and metal, with metal abundance equal to or greater than that in the H-type chondrites. Veeder et al. (1976) measured the spectrum of Eros through 11 filters from 0.65-2.2μm and concluded that their spectral data indicated a mixture of olivine and pyroxene with a metal-like phase. Wisniewski (1976) concluded from a higher resolution spectrum (0.4-1.0μm), that this surface was best matched by a mixture of iron or stony-iron material with ordinary chondritic material (e.g. iron + pyroxene + olivine), but suggested that olivine is absent or rare. Larson et al. (1976) measured the 0.9-2.7μm spectral reflectance curve for Eros and identified Ni-Fe and pyroxene, but found no evidence of olivine or feldspar. The dispute over the olivine content arises because of slight differences in the observational spectra near 1μm, and the uncertainty in the metal abundance is due to incomplete quantitative understanding of the spectral contribution of metal in a mixture with silicates.

The evolving characterization of the surface mineralogy of the asteroid 4 Vesta is illustrative of the improving sophistication of the interpretative process.

(a) McCord et al. (1970) measured the reflectance spectrum of Vesta with moderate spectral resolution and coverage (0.40 - 1.08 μm, ∿24 filters). They identified a deep absorption band (∿0.92μm) which they interpreted as diagnostic of a pigeonite (pyroxene with moderate calcium content). The spectrum was matched to that of a eucritic basaltic achondrite (pyroxene + plagioclase). A second pyroxene band was predicted near 2.0 μm.

(b) Chapman (1972) obtained a spectral curve of Vesta with the absorption feature centered near 0.95μm which was interpreted to indicate a more calcium- or iron-rich pigeonite.

(c) Chapman and Salisbury (1973) compared this spectrum to a range of meteorites and concluded that it was best matched by a laboratory spectrum of the howarditic basaltic achondrite, Kapoeta.

(d) Veeder et al. (1975) measured a high-resolution (∿50Å) 0.6 - 1.1 μm reflectance spectrum of Vesta, determined the absorption band position to be 0.92±0.02 μm and interpreted this to represent a calcic pyroxene or eucritic basaltic achondrite.

(e) Johnson et al. (1975) measured the broad bandpass reflectance of Vesta at 1.65 and 2.20 μm (H and K filters) and concluded that these data matched that expected for a basaltic achondritic surface material. They emphasized the need for higher-resolution spectra beyond 1.0 μm.

(f) Larson and Fink (1975) determined that 1.1 - 3.0 μm reflectance of Vesta relative to the Moon. They identified the predicted second pyroxene band and confirmed the existence of pyroxene in

the surface material. They indicated that no absorption bands for olivine, feldspar or ices were seen in the spectrum. Their band position (2.06 ± .01 μm) was artificially shifted toward longer wavelengths because of the slope in the lunar spectrum used as the standard.

(g) McFadden et al. (1977) measured the high-resolution (20-40Å) 0.5 - 1.06 μm spectrum and determined the band position to be 0.924 ± 0.004 μm. They determined the presence of a 10-12 mole % Ca pyroxene and they suggested that the symmetry of the absorption feature indicated little or no olivine.

(h) Larson (1977) presents the 1.0 - 2.5 μm reflectance curve of Vesta relative to the Sun. The band minimum (2.00 ± 0.05 μm) is within the field of eucrite meteorites, although it may overlap with the howardite field.

Improvements in the mineralogical and petrological characterization of the surface materials of 4 Vesta are the result of observational spectra with improved spectral resolution and coverage coupled with an improved understanding of the mineralogical significance of the spectral behavior of the reflectance curve. The recent effort has concentrated on characterizing the mineral absorption features more precisely, but the original interpretation (McCord et al., 1970) still appears valid.

IV. Asteroid Spectral Groups

The nearly 100 asteroid spectra available in the literature can be classified into a small number of groups based on shared spectral characteristics. The number of groups defined by this method depends on the sensitivity of the discriminating parameters. Chapman et al. (1973a) classified their spectra into three general groups based on color (slope of spectral curve) with subgroups distinguished by slope, absorption band position, location of UV dropoff and other spectral characteristics. McCord and Chapman (1975a, b) identified a series of spectral groups based on spectral curve slope (R/B), curvature (bend), IR reflectance and IR band depth as defined by the ratios of reflectances at specific wavelengths in the spectrum. The spectral parameters were selected to provide the maximum degree of compositional or mineralogical discrimination. The labeling terminology ('R' = Red or steep slope, 'M' = Medium or intermediate slope, 'F' = Flat or non-sloped spectral curve) is specifically spectral and does not draw an inference that these groups are unique or homogeneous compositional groups. The spectral parameter R/B was also used to define the more general 'C', 'S', 'M', etc. classes (Chapman et al., 1975). Chapman (1976) redefined the 'R', 'M' and 'F' groups in more compositional terms along the lines of the 'C' and 'S' groups, but maintained the larger number of subtypes.

While the reflectance spectrum of an assemblage is primarily a function of mineralogy, it can be significantly modified by non-mineralogical factors such as relative particle size and packing (e.g. Adams and Filice, 1967). Thus a relatively large

spectral variation may have no mineralogical significance while a relatively minor variation may represent a major change in mineralogy. Although, current understanding of these relationships is incomplete, major progress has been made since the classifications discussed above were derived. The evolving type of interpretation utilized by McCord and Gaffey (1974), Pieters et al. (1976), Gaffey and McCord (1977) and the present paper attempts to take these factors into consideration.

For purposes of this interpretation, a spectral classification system has been defined. These spectral groups parallel those defined by Chapman et al. (1973) and McCord and Chapman (1975a, b) but recognize somewhat different subdivisions. Type-example spectra of these groups are shown on Figure 2. These spectra are displayed in several ways to enhance certain spectral parameters. All data are plotted as reflectance (scaled to unity at 0.56μm) versus both wavelength (μm) and energy (wavenumber, cm^{-1}). The energy scale is of particular interest because the linearity or curvature of the spectral continuum and the symmetry of absorption features, both powerful diagnostic tools, are dependent on energy. An arbitrary continuum (linear in energy space and fitted through 0.43 and 0.73μm) has been subtracted from the reflectance spectra to reveal the continuum curvature and to isolate and allow enhancement of absorption features.

The available asteroidal spectra have been arranged into approximately a dozen groups. The spectral criteria used to choose group membership will be discussed in this section. The compositional interpretation of individual spectra of each group and the details of the interpretive methodology will be discussed in a subsequent section. The most important spectral parameters utilized in discriminating between groups are the presence, position and symmetry of the absorption feature near 1μm and the linearity or curvature of the spectral continuum at energies higher than about 14,000 cm^{-1} ($\lambda<0.7\mu m$).

The following groupings of asteroid reflectance spectra are designated on the basis of the mineralogically important features.

Group RA - The spectra of these asteroids (Figure 2A, B) are characterized by a linear increase in reflectance toward lower energy (R = red) and well-defined absorption features (A = absorption) near 1μm. The absorption features range from narrow, symmetric pyroxene features (λ center $\leq 0.95\mu m$) through olivine-broadened pyroxene features to a broad olivine feature (λ center $\sim 1.0\mu m$). Included are asteroids 3 Juno, 8 Flora, 15 Eunomia, 39 Laetitia and 354 Eleonora.

Group RR - These asteroid spectra (Figure 2C) are characterized by a relatively featureless continuum with increasing reflectance across the interval 0.35 to 1.1μm. Included are asteroids 16 Psyche and 140 Siwa.

Group RF - The spectra of these asteroids (Figure 2D) are characterized by increasing reflectance through the visible (R)

and a plateau of nearly constant reflectance (F = flat) in the infrared. Included are 9 Metis, 11 Parthenope and 230 Athamantis.

Group A - These asteroid spectra (Figure 2E, F) are characterized by a very strong absorption feature (A) near 1μm. Included are 4 Vesta and 349 Dembowska.

Group F - These asteroids (Figure 2G) are characterized by a nearly flat spectral reflectance curve (F) with a variable UV falloff shortwards of 0.4μm. Includes - 1 Ceres, 2 Pallas and 85 Io.

Group T - The spectra of these asteroids (Figures 2H, I, J, K, L) appear to represent a relatively smooth transition (T) from type 'F' to type 'R' spectra. The position of the break-in-slope between a steeply sloping blue and UV continuum and a relatively flat infrared continuum is used to subdivide the 'T' group into five subgroups-'TA', 'TB', 'TC', 'TD', and 'TE'. Type 'TA-TB-TC' spectra are distinguished from type 'F' by the relatively longer wavelength of the break-in-slope ($\lesssim$0.55 m). The type 'TE' spectra are distinguished from type 'RF' spectra by the normalized reflectance of the IR continuum plateau ($\leq$1.1 vs.$\geq$1.2, respectively). The majority of the asteroid spectra are included in type 'T'.

The spectral reflectance curves of some asteroids cannot be unambiguously assigned to a specific spectral group either because those spectra exhibit characteristics of more than one group or because no sharply defined boundaries exist between similar spectral groups. These are discussed more fully in subsequent sections. It must be emphasized that these spectral groups should not be viewed as necessarily equivalent to compositional groups.

V. Interpretive Procedure

It has been persuasively argued that asteroidal bodies must be the source of at least some of the meteoritic material which arrives at the Earth's surface (e.g., Anders, 1971; Wetherill, 1974). Thus previous investigators have reasonably concluded that the meteorites constiute the best available set of comparison materials for asteroid surface materials. But, the technique of matching laboratory meteorite spectra to observed asteroid spectra has met with only limited success, for several reasons. The most serious uncertainty in any curve matching approach lies in the problem of deciding what constitutes a 'match'. In an empirical curve matching program, there is no basis for deciding when the deviation from a precise match is mineralogically significant. Hapke (1971) pointed out the large variation in the UBV colors of a material due to particle size variations. Salisbury and Hunt (1974) discussed the uncertainty introduced by terrestrial weathering of meteorites. Chapman and Salisbury (1973) and Johnson and Fanale (1973) discussed space weathering as a possible source of mismatch. The problem is compounded by the virtual certainty that the selection of meteoritic material arriving at the Earth's surface is both biased and incomplete with respect to the distribution of asteroidal materials (Chapman and Salisbury, 1973; Johnson and Fanale, 1973; McCord and Gaffey, 1974).

The approach used in this paper avoids, or makes less severe, these problems. The diagnostic spectral parameters (absorption feature characteristics and continuum behavior) utilized in these

mineralogical interpretations are insensitive to the physical properties (e.g., particle size) of the surface material (Gaffey, 1976). Additionally, this interpretive approach does not require a collection of comparison materials containing samples of all possible asteroidal materials; only the range of possible mineral assemblages must be defined. The meteorite spectra are used to calibrate the interpretive procedures. Gaffey (1974, 1976) compiled an extensive collection of unaltered meteorite reflectance spectra and discussed the variations of these spectra for the range of meteorite classes in terms of the type, composition, abundance and distribution of the constituent mineral phases. A collection of these meteorite spectra is shown in Figure 3.

The spectra of several types of meteoritic material are shown on Figure 4 in the same format as the asteroid spectra of Figures 2 and 6. A brief discussion of the diagnostic spectral parameters which characterize the mineral assemblages contained in these meteorite types is presented here. A more extensive discussion of the quantification of the relationship between these diagnostic spectral features and the mineralogy and petrology of meteoritic material is in preparation by Gaffey.

Since the early 1960's a major effort has been underway to define the physical processes which govern the interaction of light with the common rock-forming silicate minerals (e.g. White and Keester, 1966, 1967; Burns, 1970a; Bell et al., 1974). This work, based on crystal field theory, ligand field theory and molecular orbital theory, was summarized for mineralogical systems by Burns (1970b).

Elements of the first transition series (Ti, V, Cr, Mn, Fe, Co, Ni, Cu) and their petrologically important cations (esp. Fe^{2+}, Ti^{3+}) have an outer unfilled d-shell in their electron distribution. When such a cation is located in a crystal site surrounded by anions, certain electronic orbitals experience strong repulsions and undergo splitting to higher energy. The orbitals undergoing the least electronic repulsion become the groundstate orbitals in which the electrons tend to reside. The energy difference between the groundstate and any excited state is termed the crystal field splitting energy and is a direct function of the particular cation and the crystal site in which it resides. A photon whose energy corresponds to the splitting energy of a particular cation can be absorbed. This gives rise to specific absorption features in the reflectance spectra of transition-metal silicates such as olivine, pyroxene and feldspar. Adams (1975) has shown that the positions of these bands are distinctive for each type of mineral. Adams (1974) has calibrated the precise positions of the two pyroxene bands with respect to the mineral chemistry (iron and calcium content) of the specimens.

Quantification of the spectral characteristics of mineral mixtures in order to interpret reflectance spectra for mineral abundance as well as composition, is a more complex problem. For example, Adams and McCord (1970), Nash and Conel (1974) and Gaffey (1974, 1976) have noted that the relative abundance of a mineral phase does not in general correlate exactly with its

apparent spectral abundance. Johnson and Fanale (1973) and Nash and Conel (1974) used laboratory mixtures to show that an opaque phase (carbon and magnetite, respectively) would dominate the reflectance spectrum of a mixture even when present in small amounts. Gaffey (1976) showed how the relatively more optically dense pyroxene phase dominates the spectrum of a pyroxene-olivine-feldspar assemblage (L6 chondrite), but that the pyroxene spectrum is modified by the olivine and feldspar features. The olivine feature tends to lower the reflectance of a mixture near 1 μm, distorting the long wavelength wing of the 0.9 μm pyroxene feature (Chapman and Salisbury, 1973; Gaffey, 1976).

Three general classes of minerals are important in controlling the optical properties of meteoritic mineral assemblages: (1) nickel-iron minerals, (2) silicate phases (olivine, pyroxene, feldspar, and clay minerals or 'layer-lattice' silicates) and (3) opaque phases (carbon, carbon compounds, magnetite). Of these minerals, the Fe^{2+} silicates exhibit the best understood and most easily interpreted diagnostic spectral features.

The apparent contribution of a specific mineral phase to the reflectance spectrum of a mixture is a function of the

wavelength-dependent optical properties and of the relative abundance and distribution of that phase. The mineral phase with the greatest optical density tends to dominate the reflectance spectrum of a mixture. This can be shown by comparison of the spectra of pyroxene, olivine and a pyroxene-olivine mixture. The pyroxene spectral reflectance curve (Figure 4A) is characterized by a relatively narrow, symmetric absorption feature centered near 0.90 μm, while an olivine spectrum (Figure 4C) is characterized by a broad, asymmetric feature centered near 1.00 μm. The optical density of the pyroxene phase is nearly an order of magnitude greater than that of the olivine phase. A mineral assemblage containing approximately equal amounts of olivine and pyroxene (Figure 4B) produces a spectral curve which is essentially that of the pyroxene phase, with the long wavelength edge of the pyroxene feature somewhat depressed by the weaker absorption of the olivine phase. The broadening and asymmetry of the resulting feature is a function of the relative abundance of olivine and pyroxene. A preliminary calibration of this functional relationship (from Gaffey, 1977, in preparation) is shown in Figure 5a. Computer deconvolution techniques can be utilized to resolve a spectrum into its superimposed component spectra. This technique can be used to extract continuum and strong absorptions to reveal weak absorption features such as that of feldspar. The relative intensity of the pyroxene and feldspar absorption features can be correlated to the relative abundance of these mineral phases.

The feldspar minerals of the lunar surface materials (Bell and Mao, 1973) and most meteorites (Gaffey, 1974, 1976) incorporate a minute amount of Fe^{2+} into their structure giving rise to an absorption feature near 1.25 μm. This feature lies outside the 0.3 - 1.1 μm spectral region for which most asteroidal spectra have been obtained, so that no feldspar feature can be seen in these asteroid spectra. The effect of feldspar on the observed spectral range would be minor, except a slight depression of the spectrum beyond 1.0 μm. However, the calcium component of a magma crystallizing into a plagioclase feldspar will also partition to some degree into the other minerals being formed. The pyroxene absorption feature near 1.0 μm is especially sensitive to the calcium content of the pyroxene, as discussed by Adams (1974), which in an equilibrium or quasi-equilibrium crystallization event is related to the calcium content of the melt and thus to the plagioclase abundance of the resulting mineral assemblage. It can be argued that if one assumes that the asteroid surface material for any given body is derived from an equilibrated mineral assemblage, the wavelength position of the 1.0 μm pyroxene band is some measure of the pyroxene/plagioclase abundance of the

surface material. This approach provides an alternate indirect measure of feldpsar abundance which can be applied to the existing asteroidal spectra.

The metallic nickel-iron (NiFe) phases are significant or dominant mineralogical constituents in a variety of meteoritic assemblages. The 0.35-2.5μm reflectance spectra of these minerals (Johnson and Fanale, 1973; Gaffey, 1974, 1976) exhibit no discrete diagnostic electronic absorption features. The overall shape of the reflectance spectrum is distinctive for the general group of NiFe minerals containing less than 25% nickel. A typical NiFe spectral curve (Figure 4D) is characterized by a linearly (in energy space) increasing continuum reflectance at wavenumbers greater than 10,000-12,500 cm^{-1} (λ<0.8-1.0μm). At lower wavenumbers (<10,000 cm^{-1} or λ>1.0μm), the energy space spectrum exhibits an upward (positive) curvature with decreasing frequency. The degree of positive infrared curvature seems to be inversely proportional to the Ni content of the alloy (Gaffey, 1976).

By contrast, an assemblage primarily made up of silicate minerals such as pyroxene, olivine and feldspar (Figure 4B) has a distinctly non-linear spectral reflectance curve in the region shortwards of the 0.9μm absorption feature, (figure 4B-right). This strong blue and ultraviolet decrease is the result of increasingly efficient charge transfer absorptions toward higher energy between the various cations and anions in the silicate structure. Such curvature and blue-UV absorption is typical of most silicate assemblages.

The major exceptions to this rule are pure or nearly pure olivine assemblages (>90% olivine) which exhibit spectral curves (Figure 4C) with a generally linear continuum shortwards of 0.7μm (>14,000 cm^{-1}). A series of relatively weak absorption features between 0.4 and 0.6μm introduce a series of discontinuities or steps in the continuum. These steps and the strong olivine $\frac{1}{2}$ feature leave little probability of confusion of the olivine spectral curve with a linear NiFe spectral curve.

As a general rule, a linear continuum indicates a mineral assemblage with a spectrally dominant NiFe metal component, while a curved continuum with a blue-UV absorption indicates a mainly silicate assemblage. For mixtures of metal and silicate phases where neither is spectrally dominant, the relationship between apparent spectral abundance of the metal phase and its actual mineralogical abundance is a complex function of abundance, grain size, distribution and oxidation state. The complexity of this relationship can be illustrated by an example.

The metal abundance for L-type chondritic assemblages is approximately 10%, but the apparent spectral contribution of the metal phase, judged by the linearity of the continuum, is significantly different between an L6 assemblage (Figure 4B) and an L4 assemblage (Figure 4E). Measurements of metal grain-size (Dodd, 1976) imply an increase in median grain size with increasing degree of metamorphism (judged by the compositional homegeneity of the silicate grains) by a factor of at least 2 or 3 from L4 to L6. This would represent at least an order of magnitude difference in the surface area of metal grains. This is, to first order,

spectrally equivalent to a larger metal abundance with the same grain size distribution. The special behavior of the L4 assemblage is further complicated by the possible presence of a spectral blocking (opaque) phase (Gaffey, 1976). Such a component would tend to suppress the higher albedo portions of the spectrum and reduce the blue-UV falloff as well as the absorption band depth.

The enstatite chondrites consist of assemblages of NiFe metal and enstatite, a transition metal-free pyroxene (Fe^{2+} $<$0.05%, Reid and Cohen, 1967; Keil, 1968). The reflectance spectrum of enstatite (Figure 4H) exhibits no discrete absorption features except for a UV absorption due to charge transfers at very high energy. This flat, featureless, high albedo spectrum is characteristic of a powdered material for which the optical density is very low and not strongly wavelength dependent. In such a material a photon can pass through many grains and encounter many scattering boundaries and thus has a high probability of escaping the material before absorption. The E4 (Figure 4F) and E6 (Figure 4G) assemblages, consisting of metal and enstatite, exhibit only the metal spectrum. The relatively low albedos of these assemblages (7-17%) is probably the result of an absorbing FeO layer coating the metal grains, analogous to the darkening of iron upon exposure to air. The difference in the IR spectral curve between E4 and E6 spectra is probably the effect of increasing the metal grain size.

The spectral behavior of mineral assemblages containing a significant component of an opaque phase also presents a complex problem. The carbonaceous chondrites have been cited as examples

of assemblages whose spectral properties are dominated by the presence of opaque phases (e.g., Chapman and Salisbury, 1973; Johnson and Fanale, 1973; Gaffey, 1974, 1976). Johnson and Fanale (1973) attempted, with some success, to model the spectral properties of the C-Type assemblages with a mixture of a clay mineral (montmorillonite) and carbon black. The presence of an opaque component in a mineral assemblage tends to decrease the mean free path of a photon and to increase the probability that a photon will be absorbed before it is scattered out of the material. For purposes of this discussion, an opaque phase will be defined as any mineral whose grain size is many optical depths at all wavelengths of interest.

However, even the relatively restricted group of opaque-rich cosmicly-occuring assemblages represented by the carbonaceous chondrites are far from a simple system. From the point of view of optical properties, the C-Type materials can be subdivided into at least three distinct subtypes following the meteoritic subdivisions C1-C2 (CI, CM), C3 (CO and CV) and C4. The C1-C2 assemblages appear to represent agglomerations of minerals at low temperatures. Hydrated layer-lattice silicate or clay mineral grains comprise the bulk of these materials, with carbon and carbon compounds present both as discrete grains and as coatings on the silicate grains. The clay-mineral grains contain both bivalent and trivalent iron giving rise to an intense charge transfer absorption in the blue which extends across the visible portion of the spectrum. Thus even with the very low albedos (3-6%) induced by the carbon, this strong charge transfer band

is evident from the sharp decrease of reflectance shortwards of about 0.5μm (Figure 4I). The weak features near 0.65 and 0.9μm represent large increases in the bulk optical density near these wavelengths in order to impose these features on a very low albedo spectral curve. It is probable that these features arise from charge transfer transitions between Fe^{2+} and Fe^{3+} or within the Fe^{3+} cations.

The asteroid and meteorite absorption features in the 0.6-0.7 spectral region have been an area of investigation and controversy for several years. The major problem lies in the fact that a variety of crystal field and charge transfer transitions can and do take place in this spectral region. We can rule out the relatively weak 'forbidden' crystal field transitions of the appropriate transition metal ions (e.g., Ti^{3+}, Mn^{3+}, etc.) except where the symmetry of the cation site makes the transition 'allowed' (see Burns, 1970). The strong titanium absorption feature in the spectrum of a titanium pyroxene from the meteorite Allende is sufficiently intense, but the specific nature of the transition (and hence the likelihood of the existence of this mineral in an assemblage of any given oxidation state and equilibrium state) is still unsettled. For example, Burns and Huggins (1973) assign the strong ∿0.6μm absorption in this mineral to a d-shell electronic transition in Ti^{3+} in a distorted octahedral crystal site. Dowty and Clark (1973a, b) and Mao and Bell (1974a) assign this transition to a Ti^{3+}-Ti^{4+} charge transfer transition.

Alternatively, the iron oxide minerals goethite (αFeOOH) and lepidocrocite (γFeOOH) exhibit strong, ∿0.7μm absorption features

which have been assigned to a crystal field transition in Fe^{3+} ions (Mao and Bell 1974b). The laboratory spectra of iron-bearing terrestrial 'clay minerals' or 'layer-lattice silicates' including talc, chlorite, and serpentine (Hunt and Salisbury, 1970) exhibit absorption features (mostly weak) near 0.6μm which may be related to the absorption features near 0.6μm in the laboratory spectra of the C2 (CM) meteorites (Gaffey, 1976).

The C3 (CO and CV) assemblages are composed primarily of mafic silicate grains with coating layers of graphite or carbon (e.g., Green et al., 1970). The relatively low optical density of the olivine grains and the relatively small amount of carbon (C3∿0.5%, C2∿2.5% - Vdovykin and Moore, 1971) contribute to the relatively high albedo of these meteorites (7-17%). The small amount of the opaque phase permits the weak blue-visible charge transfer absorptions of the olivine to dominate the spectrum (Figure 4J) and permits the presence of a 10% deep absorption feature near 1.0μm. There is also evidence of a pyroxene feature near 0.9μm. The curved continuum due to a dominately silicate assemblage is clearly evident.

The C4 assemblage represented by the meteorite Karoonda (Van Schmus, 1969) is composed dominately of olivine with magnetite as the opaque phase (Mason and Wiik, 1962). Herndon et al. (1976) notes that the magnetite content of Karoonda (∿8%) is significantly higher than those of the C3 assemblages (∿2-4%). This opaque component is sufficient to flatten the reflectance spectrum and suppress the spectral features (Figure 4K), due to

the olivine component. The albedo is reasonably high (9.4%), indicating the relatively small decrease in mean photon path length required to suppress the spectral contrast of the low optical density mafic silicate spectra. By contrast, the unleached clay mineral assemblages (C2-Type) maintain significant spectral contrast at significantly lower albedos. Thus the combination of absorption feature strength and albedo can be utilized to constrain the interpretation of the optical density of the non-opaque phase and of the abundance of the opaque phase.

VI. Asteroid Spectra: Mineralogical and Petrological Interpretations

Introduction

In this section, the application of the interpretive methodology (section V) to the spectral reflectance data for individual members of the asteroidal spectral groups (section IV) is described. For several interesting objects, the interpretive procedure is described in some detail in order to provide an insight into the power and limitations of this approach. Where available, polarization and radiometric data (section II) are utilized to constrain or refine the interpretations.

Type 'RA' Asteroid Spectra

All members of this group are characterized by a relatively linear (in energy space) spectral reflectance continuum between 0.40 and 0.80μm (with a range of slopes) as well as the silicate absorption features near 1μm. The linearity of the visible portion of these spectra is most easily interpreted in terms of a significant spectral contribution by a metallic (NiFe) phase. This interpretation is reinforced by the absence of a significant UV absorption feature, which is present in the reflectance spectra of primarily silicate assemblages. Several mineralogical or petrological subgroups within the RA asteroid type are distinguished on the basis of interpreted silicate mineralogy.

3 JUNO - This relatively linear reflectance spectrum with a shallow slope ($0.39 \times 10^{-1}/cm^{-1}$ between 23000 cm^{-1} (0.434μm) and 13700 cm^{-1} (0.73μm)) and with no strong IR excess (figure 6A)

is typical of either a metal-rich assemblage with silicates or a primarily silicate assemblage with a small amount of an opaque phase (e.g., a low-grade ordinary chondritic-like assemblage).

The absorption feature with a minimum near 0.95μm is broadened toward longer wavelengths indicating a silicate assemblage containing both pyroxene and olivine. In the case of the first alternative (metal plus silicates), the absorption band intensity (below a linear continuum) is ∿20%, and olivine must dominate (Px/Ol ∿0.1). Depending on the mean particle size of the particular phases, the metal/silicate ratio could fall between 2/1 and 1/2 (∿30-70% metal).

In the case of the second alternative (silicates plus an opaque phase) the band depth (below the relative maximum at 0.8μm) is ∿10%. This absorption feature is weaker than typical for the lowest grade ordinary chondrites, indicating a shorter mean path length for photons. The band depth is comparable to that of the olivine-carbon C3 assemblages (figure 4J). The band shape would indicate a pyroxene/olivine ratio of approximately 0.5 to 1.0.

At least five pieces of observational evidence bear on the problem of distinguishing between these two alternatives:

(a) Even for the lowest grade ordinary chondritic assemblages, the spectrum exhibits a slight curvature and a weak (∿5%) UV fall-off (below a linear continuum) at 0.35μm, neither of which are seen in the spectrum of 3 Juno (see figure 4E-right).

(b) The ratio of the band depth of the silicate Fe^{2+} absorption feature to that of the blue-UV charge transfer region (Figure 5B) for Juno is lower than that of an ordinary chondritic or primarily silicate assemblage. This would indicate that the olivine-pyroxene mixture is diluted by a material which is relatively absorbing in the blue-UV region but which does not exhibit a 1μm absorption feature.

(c) The normalized reflectances near 0.8μm (1.19±0.03) and at the minimum in the absorption band (1.07±0.03) are higher than those exhibited by the ordinary or carbonaceous chondritic assemblages, and indicate a significant reddening agent in the surface material of the asteroid.

(d) The radiometric albedo (15%) is somewhat high for an assemblage with a shallow absorption feature resulting from an opaque phase suppressing the normal band intensity of a silicate assemblage.

(e) The relatively shallow negative branch of the polarization-phase curve (P_{min} = -0.75%) indicates a reasonably non-shadowing surface material such as a relatively transparent silicate assemblage or metal-rich assemblage.

(f) A primarily silicate assemblage will have a normalized reflectance beyond 1.0μm of 1.3 or less, while an assemblage with a significant metal component will have a normalized reflectance near 2.0μm of 1.3 or greater, if

the metal is coated with an oxide surface layer (fine-grained crystal assemblage) or 1.5 or greater if the metal is without an oxide surface layer (e.g., crushed, coarse-grained assemblage). Based on a preliminary IR measurement (Matson et al., 1977a), the normalized reflectance of 3 Juno at 2.2μm is about 1.3.

In general, the available observational data supports the characterization of surface material of 3 Juno as a metal-silicate assemblage (metal/silicate $\approx$ 1.0, olivine > pyroxene) rather than any type of chondrite-like assemblage, (i.e., undifferentiated metal/silicate $\leq$0.25) unless some physical property of the surface material (e.g., particle size) can act to accentuate the spectral contribution of the metal phase.

15 EUNOMIA - The spectrum of this asteroid (Figure 6A) is quite similar to that of 3 Juno and the general compositional interpretation is similar - a metal-rich silicate assemblage. The absorption features may be slightly shifted toward longer wavelengths (λmin $\sim$ 1.0μm) indicating that olivine is the dominant mineral.

39 LAETITIA - This spectrum (Figure 6A) is characterized by a linear, steep (0.47) continuum with a broad, relatively weak (0.08), asymmetric absorption feature with a minimum near 0.96μm. The steep linear slope indicates a strong spectral contribution from elemental iron metal. The high albedo (0.17%) and the high normalized spectral reflectance at about 0.80μm (1.27) and at the absorption band minimum (1.18) support this conclusion. The absorption band shape indicates an olivine-pyroxene ($\sim$1/1) silicate assemblage. The ratio of metal to

silicate should be 1.0 to 2.0, depending on particle size in the surface material.

7 IRIS - This spectrum (Figure 6A) is similar to that of 39 Laetitia differing mainly in the character of the silicate absorption feature. The continuum is linear and steep (0.45) with no UV falloff, indicating that elemental iron metal comprises a major fraction of the surface material. The absorption feature is stronger and shifted toward longer wavelength (λmin $\geq$1.0μm) indicating that olivine predominants over pyroxene in the silicate assemblage. The relatively low optical density characteristic of olivine minerals in general suggests three metal/olivine alternatives for the surface assemblage: (a) a relatively low metal/silicate (olivine) ratio ($\sim$0.5-1.0), (b) a relatively coarse-grained surface material, or (c) a relatively iron-rich (fayalitic) olivine with a high optical density. A relatively high spectral resolution, high signal-to-noise spectrum of the 1μm (0.7-1.2μm) region of 7 Iris should resolve this ambiguity.

354 ELEONORA - This spectrum (Figure 6A) is quite similar to that of 7 Iris except that the IR absorption band is stronger. The continuum is linear and quite steep (0.53) with no distinct UV absorption feature indicating that, as in the case of 39 Laetitia and 7 Iris, elemental iron is a major surface component. The absorption feature is relatively strong (0.15) and broad with a minimum (λmin) $\geq$1.0μm, which indicates a strong spectral contribution from olivine. The quite weak negative branch of

the polarization-phase curve (P_{min} = -0.4%) is consistent with an olivine-metal assemblage (~1/1). If our evaluation of the elementral iron origin of the steep linear slopes is correct, the surface material of 354 Eleonora is derived from a coarse-grained substrate of olivine and metal structurally analogous to the pallasite meteorites.

These five asteroids (3 Juno, 7 Iris, 15 Eunonia, 39 Laetitia and 354 Eleonora--designated 'Type RA-1') share three compositionally important spectral characteristics: (a) a linear continuum and reddish color, (b) a broad absorption feature centered near 1μm ($\bar{>}$0.95μm) and (c) a relatively high normalized IR reflectance. These spectral data are interpreted to indicate surface materials on these asteroids consisting of metal-silicate mixtures, spectrally and (presumably) petrologically dominated by the metal component (metal/silicate $\bar{>}$1) with the silicate component dominantly olivine (olivine/pyroxene>1). The range of slopes for the continua of the normalized spectral reflectance curves (0.39 to 0.53 x 10^{-4}/cm^{-1}) is probably a function of the bulk oxidation state of the metal (FeO/Fe^0) related to the physical dimensions of the metal particles in the parent material from fine (low slope) to coarse (high slope). The general similarity of the surface materials of these five objects is supported by the limited range of measured albedos (0.148 to 0.169) and P_{min} (-0.55 to -0.75%) as compared to the asteroids as a whole.

If material with these mineral assemblages were derived from a single source region (e.g., layer or spherical shell) on each asteroid, rather than

several heterogeneous source regions (e.g., silicate region plus metal region), then that single source region would be analogous to (or intermediate between) the pallasite (olivine stony-iron) and lodranite (olivine-pyroxene stony-iron) meteorites. With the current understanding of the optical properties of metal-silicate mixtures, it does not appear possible that the metal/silicate ratio for these surface materials could be as low as even the most metal-rich ordinary chondritic assemblages (∿1/3) which were suggested as candidates by Gradie and Zellner (1977).

These objects could be observed profitably (a) at higher spectral resolution through the 1μm region (∿0.75 - 1.25μm) to better define the shape and position of the absorption feature, (b) in the IR to evaluate the presence, position and intensity of the second pyroxene feature, and (c) in the UV to better define the spectral reflectance below 0.4μm. These observations, though difficult and time consuming, would permit a much more precise definition of the modal abundances of the mineral phases in the surface material. Such quantitative interpretations of the mineral components of the surface material at several well-spaced rotational phase angles, would provide a measure of surface homogeneity.

8 FLORA - This asteroid exhibits a type 'RA' spectrum (Figure 6B) quite distinct from those discussed above in that the linear continuum is steep (0.46) with a relatively stronger (∿0.20 below the 0.8μm relative maximum, ∿0.30 below a linear

continuum), narrower (width at half-height ∿1600 cm^{-1}), more symmetric absorption feature (λmin = 0.90 - 0.95μm). The absorption feature is typical of a relatively calcic pyroxene (Wo_{10-25}) where the average photon has passed through ∿30 microns of the pyroxene phase. The very linear, relatively steeply sloping continuum suggests a significant elemental iron component of the surface material. This interpretation is supported by the high normalized reflectance (1.20) near 0.8μm and beyond the absorption feature of 1.05μm. The spectral evidence implies a well-developed metal-clinopyroxene assemblage. The relatively high albedo (0.14), shallow P_{min} (-0.60%) and relatively high IR reflectance (1.46 ± .09 at 1.6μm and 1.59 ± .11 at 2.2μm - Matson et al., 1977a) are consistent with this interpretation. A well-defined pyroxene feature should be present near 1.9 - 2.0μm.

6 HEBE - This spectral reflectance curve (Figure 6B), while somewhat irregular, consists of a relatively linear, shallow sloped (0.37) continuum with a weak (∿0.10 below the 0.8μm maximum ∿0.20 below a linear continuum), relatively broad (∿2300 cm^{-1}) absorption feature (λ_{min}∿0.90 - 0.95μm). The shape and position of the absorption feature indicates that the dominant silicate is a pyroxene, either clinopyroxene (Wo_{10-25}) alone or with a minor amount of accessory olivine, in order to account for the width of the feature. The relatively linear continuum, the lack of any UV falloff and the high reflectance at 0.8μm (∿1.15) and beyond the absorption feature near 1.1μm (∿1.2)

indicate the presence of a significant metal component in the surface material. The relatively high albedo (0.16) and relatively shallow P_{min} (-0.80%) are consistent with this interpretation.

17 THETIS - Although the IR portion of the spectrum (Figure 6B) of this asteroid is rather poorly characterized, the absorption feature resembles that of 6 Hebe. This asteroid deserves additional observational work.

40 HARMONIA - The spectrum of this asteroid (Figure 6B) is, in general, similar to that of 6 Hebe except for the spectral region in and beyond the absorption feature near 1μm. The continuum is reasonbly linear and steep (0.44) with a high normalized reflectance at 0.8μm (∿1.2) and a very high reflectance beyond the absorption feature near 1.1μm (∿1.4). These characteristics would indicate a large component of elemental iron in the surface material. The absorption feature (λ_{min} ∿0.93 ± 0.03μm) is narrow and reasonably symmetric, indicating that a pyroxene is the major or only silicate present. The weakness of the absorption feature (∿0.06 below the 0.8μm maximum or ∿0.13 below a linear continuum) indicates that the surface material has a high metal/pyroxene ratio (∿2-4). The surface material of 40 Harmonia is best described as a metal with 20-30% pyroxene. The albedo (0.12) and the P_{min} (-0.75%) are consistent with this interpretation. The reflectance should continue to increase across the spectral interval 1.1 - 2.5μm

and a well developed but weak pyroxene band should be present near 1.9μm.

79 EURYNOME - The spectrum of this asteroid (Figure 6B) is most similar to that of 40 Harmonia. The slope of the approximately linear continuum is lower (0.38) and the absorption feature is stronger (∿10%), broader and at slightly longer wavelength (λ_{min}∿0.96μm). The combination of factors suggest a slightly more calcic pyroxene in somewhat higher abundance relative to a metallic iron phase.

192 NAUSIKAA - This spectral curve (Figure 6B) is in general similar to that of 40 Harmonia and 79 Eurynome except that the maximum near 0.7 - 0.8μm is broader. The nearly linear continuum has an intermediate slope (0.41), the normalized IR reflectance is relatively high (1.18 at 0.8μm, 1.08 at the center of the feature), and the absorption feature is relatively broad (λ_{min}∿0.95μm) and relatively strong (∿0.10 below 0.8μm shoulder, ∿0.20 below linear continuum). The absorption feature indicates dominant pyroxene (olivine/pyroxene ∿1/2) as the silicate component in a metal-rich (metal/silicate >1/2) assemblage. The albedo (0.16) is appropriate for such an assemblage.

25 PHOCAEA and 27 EUTERPE - The spectra (Figure 6B) of these two objects are considered together. They are essentially identical within their somewhat large error bars. They have a linear, very steep (0.52-0.53) continuum with a relatively high normalized reflectance at the 0.8μm shoulder (∿1.2), at the absorption center (∿1.05-1.1) and beyond the band near 1.1μm (∿1.3),

indicating a significant component of elemental iron in the surface material. The absorption features are relatively strong (∿0.15 below the 0.8μm reflectance) and are very broad with no well-defined minimum (λ_{min}∿0.85 - 1.00μm). Such an absorption feature could arise from the sum of two relatively narrow, equally strong gaussian-shaped absorption features centered near 0.90μm and 1.00μm. An appropriate mixture of low-calcium orthopyroxene (e.g., Fs_{10}, λ_{min} ∿0.90μm) with either a calcic clinopyroxene (e.g., Fs_{10} Wo_{40}, λ_{min} ∿1.00μm) or a fine-grained olivine (<40 micron, in order to isolate the intense center transition feature near 1.00μm from the weaker transitions on either side) would produce such a feature. Improved (spectral resolution, signal-to-noise) observations in the 1μm region would serve to verify the distinctive shape of these absorption bands, but would not provide the basis to distinguish between the two interpretations. A spectrum near 2μm in order to characterize the second pyroxene band is required in order to select between these alternatives.

The preceeding eight asteroids (8 Flora, 6 Hebe, 17 Thetis, 40 Harmonia, 79 Eurynome, 192 Nausikaa, 25 Phocaea and 27 Euterpe--designated type 'RA-2'--are distinguished from the type 'RA-1' asteroids by the nature of the absorption feature. For these latter eight objects, the absorption feature is generally narrow, relatively symmetric, centered at shorter wavelengths (λ_{min}∿0.90 - 0.96μm) and is entirely contained within the spectral interval below 1.1μm. The spectral features

indicate that the major silicate phase must be a pyroxene. Without a more precisely defined band position, a detailed mineralogical characterization of this phase is not possible other than to suggest that the range of band positions are typical of an ortho- or clinopyroxene (Wo_{20}). The linear continuum, lack of a discrete UV absorption feature and high IR reflectance at the 0.8μm maximum, at the band minimum and beyond the absorption feature, all strongly indicate a major metal component of the surface material. The range of continuum slopes ($0.36 - 0.53 \times 10^{-4}/cm^{-1}$) is probably related to a range in the oxidation state of the metal and hence to the physical dimensions of the metal matrix with respect to the included silicate grains, that is, low slope for fine-grained and high slope for coarse-grained parent material. The relatively limited range of albedos (0.10-0.17) and P_{min} (-0.60 to -0.80%) as compared to the asteroids as a whole, is consistent with a limited range of surface materials. The surface material of these objects is interpreted to be a metal (Fe-Ni) with admixed pyroxene. If the surface materials of these asteroids are derived from a single source region on each asteroid, then the assemblages in those source regions are generally analogous to the mesosiderite (metal + pyroxene + plagioclase) or siderophyre or IVA Iron with silicate inclusions (Schaudy et al., 1972) (metal ± pyroxene) meteoritic assemblages.

The relatively calcic pyroxene interpreted from the absorption feature in the spectral reflectance curve of 8 Flora would

generally be considered to be the result of crystallization (or partial melting) of a relatively calcic parent material. This would also imply that a plagioclase feldspar should co-exist with the calcic pyroxene in the surface material of 8 Flora. This would be analogous to a mesosiderite assemblage and the 1.25μm feldspar band should be present in the spectrum of this asteroid.

McCord and Chapman (1975a) presented the spectral curve of 8 Flora with the comment that

> '8 Flora shows the deepest absorption band of any asteroid except 4 Vesta, and its spectrum more closely resembles that for 1685 Toro and ordinary chondrites than any other main-belt asteroid yet measured.'

The resemblance referred to by McCord and Chapman (1975a), based largely on the presence of an absorption band in a reddish continuum, was cited by Levin et al. (1976) as observational support for the 8 Flora family of asteroids as possible parent bodies for the L-type chondrite, Farmington. Wetherill (1976) discussed this suggestion and concluded, on the basis of orbital criteria and spectral mismatch, that this relationship was unlikely.

The current interpretation of the spectral reflectance curve of 8 Flora (metal + calcic pyroxene) would rule out this asteroid as a source of ordinary chondritic material. This pyroxene (Wo_{10-25}) is much more calcium-rich than the pyroxenes typical of the ordinary chondrites ($<Wo_1$ -Keil and Fredriksson, 1964; Binns, 1970). Olivine, if present in the surface material

of 8 Flora, is only an accessory mineral. The silicate fraction of the surface material of this asteroid would more closely resemble a basaltic achondritic assemblage than any type of chondritic assemblage. There is thus no spectral evidence to link 8 Flora to Farmington or any other ordinary chondrite.

The surface material of 192 Nausikaa apparently contains the largest olivine component ($\sim$1/3) found in the silicate phase of the surface materials of typical type 'RA-2' asteroids. As such, 192 Nausikaa may be transitional to the more pyroxene-rich members of the type 'RA-1' asteroids.

The characterization of surface mineralogy of these asteroids can be significantly improved and quantified by measuring improved spectra (spectral resolution, signal-to-noise) near 1μm (0.7-1.1μm) and by obtaining spectra to characterize the second pyroxene band and the feldspar band (1.0 - 2.5μm). To fully utilize such improved spectra, an improved quantitative understanding is needed of the spectral properties of metal-silicate mixtures as a function of phase abundance and type, particle size and oxidation state.

14 IRENE and 63 AUSONIA - The spectra of these two asteroids (Figure 6C) share several distinctive spectral characteristics and will be considered together. The important distinguishing characteristic is the flatness or lack of spectral contrast of the continuum beyond about 0.75μm with a weak, narrow, but well-defined, absorption feature ($\lambda_{min} \sim 0.93\mu m$). The continuum (13000 - 25000cm^{-1}) is quite linear with the UV portion of the

63 Ausonia curve having a higher reflectance than the extrapolated continuum. On cursory examination, these spectra (designated Type 'RA-3') would appear quite similar to type 'RF' and 'TD-TE' spectral curves with the addition of the narrow absorption feature. The relatively high normalized reflectance of the IR plateau (∿1.2-1.3) is suggestive of the type 'RF' spectra.

Utilizing the interpretive criteria as above, these spectra indicate a surface material made up predominately of metal with pyroxene ($\sim Wo_{15}$). However, these spectra are sufficiently distinct from other type 'RA' and 'RF' spectra to warrant an extended discussion.

The linear continua and relatively high IR reflectance of the 14 Irene and 63 Ausonia spectra indicate a major metal component in their surface materials. The IR plateau in the spectra indicates that the metal-rich assemblage is different than those for the other type 'RA' discussed above. A relatively high reflectance IR plateau in a spectrum can result from at least three mineralogical and petrological assemblages. (a) The observed effect of increasing the nickel content of Ni-Fe metals is to suppress the IR reflectance (Gaffey, 1976, p. 913), so that the spectral curve of 63 Ausonia and 14 Irene could be produced by a surface of NiFe metal (∿20% Ni) mixed with a very fine-grained (∿20 microns) or iron-poor ($\sim Fs_{1-5}$) pyroxene. The narrowness of the absorption band would require the isolation of the intense central portion and suppression of the weaker

wings of the pyroxene feature. This effect can be achieved by decreasing the average number of absorbing elements (Fe^{2+} cations encountered by a photon. The probability of absorption is proportional to the number of absorbing elements multiplied by a distribution function which decreases away from the optimal crystal field transition energy. As the number of absorbing cations encountered by the average photon is decreased, the center of the feature will persist long after the wings have become negligible. (b) A fine-grained (∿100 micron) mixture of iron metal and silicate which has been in intimate contact at high temperature will result in a thick (∿0.01-0.1 micron) dark coating of wustite (FeO) around each metal grain produced by oxygen depletion of the enclosing silicate materials. This wustite layer will flatten the spectrum, suppressing the spectral contrast. The relatively flat IR portion of the spectral curve of high grade (E6) enstatite chondrites (Figure 4G) is probably a result of this effect. Such spectra have a reasonably linear visible continuum (low slope ∿0.2-0.3) with some UV upturn relative to the linear continuum. The normalized reflectance of the IR plateau is 1.1-1.2. The spectral curve of the E6 assemblages exhibit a very weak (∿1%) absorption feature near 0.85μm, arising from trace amounts ($\lesssim$0.1%) of Fe^{2+} in the silicate (enstatite) of these meteorites. The characteristics of the absorption feature present in these asteroidal spectra would require a pyroxene phase with higher iron ($\sim Fs_{1-3}$ to provide the relatively strong Fe^{2+} feature) and calcium ($\sim Wo_{10-15}$ to shift the band

center to 0.93μm--Adams, 1974) contents than typical of the E-type assemblages ($\sim Fs_{0.01}$ and $Wo_{0.02}$ respectively--Keil, 1968). (c) The spectral reflectance curve of an assemblage of elemental iron particles (e.g., no wustite coating) and a low-iron, high-calcium pyroxene (e.g., Fs_{1-3}, Wo_{10-15}--see above) could be modified by the addition of a minor opaque phase diffused in the silicate component. The opaque phase would have the effect of increasing the optical density of the silicate and decreasing the overall spectral contrast but most strongly effecting the IR where the photon mean path is longest, producing an IR plateau.

The steep slope of the continuum (0.60) of the 63 Ausonia spectral curve would tend to support weakly interpretation 'a' over 'b' or 'c'. The relatively high albedo (13%) and shallow P_{min} (-0.65%) are not inconsistent with either interpretation. While the abundance and distribution of the metallic phase is not well defined, the presence of a clinopyroxene (Wo_{10-15}) is required as the spectrally dominant silicate phase.

The lower slope of the continuum (0.35) of the 14 Irene spectral curve would tend to support weakly interpretations 'b' or 'c' over 'a'. The wavelength position of the elbow between the IR plateau and the visible continuum is significantly longer in the spectrum of 14 Irene ($\sim$0.75μm) than in the spectral curve of the E6-assemblage ($\sim$0.60μm) discussed in alternative 'b'. This would require less wustite coating ('b') or a lower opaque component ('c'). The relatively high albedo of 14 Irene (16%) is reasonable for all three interpretations.

It should be noted that the calcic pyroxene present as a major silicate phase on 14 Irene and 63 Ausonia, is evidence that this material is not a primitive accretionary or proto-accretionary product such as the enstatite chondrite assemblages, but rather, has undergone significant post-accretionary modification from the low calcium pyroxene of primitive nebular condensate.

Type 'RR' Asteroidal Spectra

These spectra (16 Psyche and 140 Siwa--Figure 6D) are characterized by a linear curve with increasing reflectance across the visible and into the IR ('RR' - red visible, red IR), with no detectable silicate absorption features. The slopes in these spectra tend to be low ($0.18 - 0.26 \times 10^{-4}/cm^{-1}$). As discussed above, this type of spectral reflectance curve is characteristic of a metal (Ni-Fe) rich assemblage and the shallow curve slope is indicative of a significant oxide coating (wustite) on the metal surfaces, or of an opaque component diffused throughout an iron-free silicate. The intermediate P_{min} (-0.95%) and albedo (9%) of 16 Psyche are consistent with these interpretations. The relatively low albedo (5%) of 140 Siwa is lower than the range of albedos observed for intimate associations of metal and transition-metal free silicates (6-18%).

The spectral reflectance curve of 16 Psyche has been considered by several other authors. Johnson and Fanale (1973) noted that the reflectance spectrum of a particulate metal (NiFe from the Odessa iron meteorite) provided a good match

to the spectrum of 16 Psyche. Chapman and Salisbury (1973) matched the spectral reflectance curve of an E4 chondrite (Abee) to 16 Psyche. As noted by Gaffey (1976) the spectral behavior of the E chondrites is dominated by their metal component, so that the suggestions of these authors are equivalent in terms of the identification of the spectrally dominant phase (metal). If the proposed 'slope-oxidation state' relationship is valid for the Ni-Fe metals, the low slope of the 16 Psyche spectrum would indicate that the surface material is derived from a substrate of fine-grained metal in intimate association with an oxide (silicate) phase. A reduced (transition metal free) silicate such as the enstatite of the E-type chondrites would suffice.

A more complete understanding of effects of thin oxide layers on the spectral reflectance properties of the Ni-Fe metals is necessary to fully interpret this spectrum. Moreover, the presence of a broad, weak absorption feature near 0.6-0.7μm in this spectrum, if verified by new measurements, should provide additional constraints on the surface mineralogy of these objects.

Type 'RF' Asteroidal Spectra

These spectra (Figure 6E) are characterized by an increasing reflectance with increasing wavelength through the visible ('R') and a nearly constant reflectance in the infrared ('F'). These spectra are distinguished from the type 'RA' spectra by the lack of any clearly defined absorption feature in the 1.0μm spectral region and from the type 'TD-TE' (see below) by the relatively high normalized reflectance of the IR plateau ('RF'

$\geq$1.2, 'TD-TE' <1.20). The 'RF' reflectance curve is linear through the visible portion of the spectrum while the type 'TD-TE' curve exhibits a degree of curvature.

The general interpretation of the 'RF' spectra is that they are produced by a surface material spectrally dominated by metal with the IR spectral constrast suppressed. At least three NiFe-rich assemblages can produce these spectral properties: (a) a relatively nickel-rich ($\sim$20% Ni) NiFe metal, (b) a mixture of metal with an opaque phase (probably carbon or magnetite) diffused in a relatively featureless silicate, or (c) a metal coated with wustite mixed with an iron-free silicate (see above). Improved quantitative understanding of the optical properties of metal-silicate mixtures is needed before a selection can be made between these options. At least three asteroids belong to this group (9 Metis, 11 Parthenope, 230 Athamantis). Several other asteroids including 30 Urania, 462 Eriphyla and 674 Rachele, are candidates but on the basis of the available spectra they cannot be distinguished from Type 'TD-TE'.

Strongly-Featured Asteroidal Spectra

Two asteroids, 4 Vesta and 349 Dembowska, exhibit spectral curves dominated by a strong mafic silicate absorption feature near 1μm. The asteroid 4 Vesta has been extensively investigated and it's surface material characterized, most recently by McFadden et al., 1977. Vesta will, therefore, not be discussed further (see section III). 349 Dembowska has not been subjected to this interpretive procedure and will be discussed here.

349 DEMBOWSKA - The spectral reflectance curve for this asteroid (Figure 6F) is distinctive for the strong silicate absorption feature near 1.0μm. This feature is broad (>2500 cm^{-1}), somewhat asymmetric and centered near 0.95-1.0μm. A second, weak but well-defined absorption feature is located near 0.65μm at the edge of a steep, reasonably linear, UV-visible continuum.

The comparison of this spectral curve with that of 4 Vesta (Figure 6F) is useful for interpretative purposes. The major difference is in the behavior of the UV and visible continuum. The strong curvature of the UV-visible portion of the Vesta spectrum is characteristic of well-developed, predominantly silicate assemblage such as the basaltic achondrites and high-grade ordinary chondritic assemblages. The relatively linear (considering the strong 1.0μm feature) UV-visible continuum of 349 Dembowska could result from three possible mineral assemblages: (a) a metal-rich assemblage, (b) a silicate assemblage with an opaque phase, or (c) a predominantly olivine assemblage.

The first alternative, a metal-rich assemblage, is unlikely because of the strength of the silicate feature, the steepness of continuum ($0.53 \times 10^{-4}/cm^{-1}$) and the relatively low normalized IR reflectance. The relatively high spectral reflectance of a metallic Ni-Fe phase should extend across the region of the absorption feature, resulting in a relatively high normalized reflectance even at the band center (e.g., 3 Juno and 39 Laetitia). The relatively low normalized reflectance at the band center places an upper limit on the abundance of any reddening agent (e.g., metal). Moreover, if the absorption feature is imposed on a steep linear metal continuum, then the observed minimum of the feature has been strongly shifted towards the shorter wavelengths. This would imply that olivine is the predominant silicate. Since the optical density of olivine is relatively low, the effect of any reddening agent is enhanced. This would place an even more stringent upper limit on the abundance of a metallic phase, and most probably rules out any major NiFe component.

The second alternative, a silicate assemblage with an opaque phase to suppress the UV absorption and continuum curvature, is analogous in spectral behavior of that for the lower metamorphic grade ordinary chondrites (e.g., L4). The major failure of this assemblage in explaining the spectral properties of 349 Dembowska is that the continuum slope and absorption band intensity are also decreased by the presence of a spectral blocking phase. Additionally,

the shallow negative branch of the phase-polarization curve (P_{min} = -0.35%) argues against any assemblage with a significant component of opaques.

The third alternative, an olivine-rich assemblage, could provide a reasonably linear, relatively steep continuum through this region as well as a shallow P_{min}. The broadness of the absorption feature is consistent with an olivine-pyroxene or an olivine assemblage but the wavelength position of the band minimum seen in this spectrum (∿0.95μm) is somewhat short for a pure olivine assemblage. This broad absorption with an approximately 0.95μm band minimum can arise from olivine-rich assemblages with either a metal or pyroxene present as a minor component. The wavelength in the continuum with the same reflectance as the band minimum (and hence the same effective bulk optical density) is approximately 0.50μm as compared to approximately 0.40μm (0.35 - 0.45μm) for silicate assemblages (pyroxene: eucrite; olivine:chassignite; olivine-pyroxene:H,L,LL chondrites). This relatively long wavelength position indicates the presence of at least some reddening agent. The presence of such a reddening agent is also indicated by the position of 349 Dembowska on Figure 5B, which is outside the field of silicate assemblages. The most common reddening agent in meteoritic assemblages is metal.

Thus, the surface material of 349 Dembowska is most probably an olivine-rich assemblage with metal or metal and pyroxene

present. Olivine should comprise 80-90% of the surface assemblage. The main observational tests of this interpretation lie in the improved resolution of the absorption band near 1.0μm and in the spectral behavior further into the IR (1.0 - 2.5μm). The absence (or extreme weakness) of the second pyroxene band near 2.0μm is an important test of this assemblage.

It must be noted that McCord and Chapman (1975b) suggested that:

> 'In the important respects, Dembowska's spectral reflectance is identical to that of laboratory measurements of highly metamorphosed ordinary chondritic meteorites.'

and that:

> 'The shape and position of the absorption band suggests a high olivine content with a pyroxene/olivine proportion most similar to that of type LL6 chondrites...'

and finally that:

> 'Dembowska is ... identified as having surface mineralogy similar to ... the ordinary chondrites.'

We would note (as above) that the behavior of the continuum of the 349 Dembowska spectral curve differs significantly (i.e., linear) from a well-developed (i.e., highly metamorphosed) silicate assemblage with a significant (>25%) pyroxene component (See Section IV).

The current interpretation of the spectrum of 349 Dembowska would indicate that the surface material of this body is similar to an olivine achondritic assemblage (olivine with minor pyroxene and metal) and unlike any known type of chondritic meteorite. It is possible to produce a chondritic assemblage with the observed mineralogy from a parent material with a high iron and

magnesium abundance relative to silicon (e.g., FeO + MgO/SiO_2 >2.0 (molar)) so that olivine is the dominant mafic silicate phase. The C3 chondrites meet these conditions but contain a relatively abundant opaque phase (carbon). Thus a similar spectral reflectance curve could be obtained from a carbon-free carbonaceous (C3) assemblage, although no such assemblage is present in terrestrial meteorite collections. A higher resolution 0.3-2.5μm spectrum would provide a basis for distinguishing between these former (probable) and latter (possible) alternatives. The pyroxene accompanying the olivine in these two assemblages would be quite different.

Type 'F' Asteroidal Spectra

The type 'F' (Flat) asteroidal spectra (Figure 6G) are characterized by a very low spectral contrast over the visible and near IR portion of the spectrum (∿0.4-1.1μm). The normalized spectral reflectance is close to 1.0 for this region. The decrease of reflectance into the UV portion of the spectral curve begins at a relatively short wavelength (∿0.36 - 0.43μm). The characterization of the surface materials of these asteroids is constrained by two spectral parameters: (a) the lack of spectral contrast through the visible and near-IR region where most meteoritic minerals exhibit marked spectral contrast (e.g., absorption features and sloped continua) and (b) the relatively short wavelength position of the onset of the blue-UV spectral falloff. Two general classes of material can meet these criteria.

1. The normal spectral contrast of a typical meteoritic silicate assemblage can be suppressed either by the presence of a spectral blocking (opaque) phase or by some physical property of the material, such as particle size. The spectral contrast exhibited in a reflectance curve is a maximum at some mean photon path length (depending on the optical density of the mineral phases) and decreases as the path length is varied away from this optimum. This effect can be produced by three types of material. (a) A spectral blocking phase (carbon, magnetite or other opaque phases) present in an assemblage can absorb most or all light which would otherwise pass through

the mineral crystals and escape to become a component of the reflected light. For example, carbon compounds and opaque oxides common in the carbonaceous chondrites are primarily responsible for the relatively low spectral contrast characterizing these meteorites. A surface made up of such an assemblage would be relatively opaque and have a low albedo. (b) The mean particle size of the material can be so small, relative to the optimal particle size for maximum spectral contrast, that the number of scattering interfaces (grain boundaries), encountered by a photon to accumulate a path length approaching a fraction of the optimal path length, is many more than the number which would scatter most of the light out of the material. The light scattered by such a surface is mostly a non-wavelength-dependent spectral component. Such a surface will have a very high albedo, very low opacity and very low spectral contrast. The bright, white reflectance of snow is an example of this effect. (c) The mean particle size can be so large that the probability is negligible that any photon, irrespective of wavelength, can transit a mineral grain without being absorbed. That is, that the mean distance between scattering boundaries is many optical depths for all wavelengths of interest. An example of this effect is obsidian, black volcanic glass, which is opaque in centimeter-sized fragments but is reasonably transparent in millimeter or smaller grains. A surface material of this character would be opaque and have a low albedo. For our purposes let us refer to these three alternatives as 'silicate with a spectral blocking

phase', 'very fine-grained silicate' and 'very coarse-grained silicate' respectively.

2. A second general class of materials which exhibit the spectral characteristics of the type 'F' spectra are those minerals which intrinsically do not exhibit significant spectral contrast in their reflectance curves. There are two types of such material.

(a) The material may be devoid of the transition metal ions (Fe^{2+}, Fe^{3+}, Ti^{3+}, etc.) which produce the crystal field and charge transfer absorptions in this spectral region. Such materials will have very low optical densities below the approximately 3 eV (<0.4μm) threshold energy of the inter-ionic electron transfer between the various silicon, oxygen and metal ions of the silicate lattice. Such a material will have a high albedo, low opacity and very little spectral contrast in the visible and near-infrared with a rather abrupt UV falloff beginning near 0.4μm. The iron-free enstatites of the enstatite achondrites are meteoritic examples of such 'transition-metal-free silicates'.

(b) The material may consist of an opaque phase such as carbon or magnetite which has no transmitted component for any reasonable particle size (e.g., >0.1 micron). Such material would have a flat spectral curve (low albedo, very high opacity). No specific meteoritic examples of assemblages composed exclusively of such an 'opaque phase' are known. Rather, such material is present in small amounts in the 'silicate with spectral blocking phase' assemblages.

Spectrally, the 'very fine-grained silicate' and 'transition metal-free silicate' characterizations are equivalent

except that in the latter case, the optical density of the silicate is so low that no significant wavelength-dependent absorption can be achieved, even at large particle sizes (e.g., <5mm). For these two cases the mean particle size is much less than an optical depth. A similar relationship exists for the cases of 'very coarse-grained silicate' and 'opaque phase' assemblages, where the mean particle size is many optical depths at all wavelengths of interest. The distinction between these cases is worth maintaining since they represent real compositional and particle size (reasonable vs. extreme) differences.

Turning specifically to the interpretation of the type 'F' asteroidal spectra, several of these alternatives can be ruled out on the basis of available data. The alternatives of 'very fine-grained silicate' and 'transition metal-free silicate' both with high albedos can be ruled out for any low albedo asteroids or any asteroids with a deep negative branch of the phase-polarization curve (P_{min} >1.0%). The 'very coarse-grained silicate' alternative seems quite unlikely (at least until all more reasonable alternatives have been ruled out) since very special conditions are required to produce naturally a fragmental surface devoid of fine particles. Very large crystals (0.5 - 5.0 cm, depending on the silicate) are quite rare in meteorites but could be formed if the thermal history permits a long crystallization or metamorphic events. The preservation of such a coarse assemblage against fracturing under the lowest proposed impacting flux onto an asteroidal surface, especially

that of a belt asteroid, seems unlikely. Also, the existence of a negative branch in the phase-polarization curves of an asteroid has been interpreted to imply a rather fine-grained or 'dusty' surface, an observation inconsistent with the 'very coarse-grained silicate' model to explain the type 'F' spectral reflectance curves.

Of the remaining two alternatives for most of these objects, the 'opaque phase' assemblage is actually a limiting case of 'silicate with spectral blocking phase', distinguished by the abundance of the opaque phase. The interpretation of a specific 'F' type asteroidal spectra (after exclusion of the other alternatives) is for the most part a process of identifying or characterizing the opaque phase and its abundance and distribution. By the very nature of the spectra, the identification of the non-opaque phases takes place as a second stage or not at all.

1 CERES - The low albedo (5.4%) and the deep negative branch of the phase-polarization curve (P_{min} = -1.67%) indicate that the surface is dark and composed of relatively opaque powdered material. The relatively strong UV falloff shortwards of 0.4μm (∿40%) in the spectral reflectance curve of this asteroid indicates a sharp increase in the mean optical density of the surface material. This is a non-trivial observation and provides the main criteria for evaluating the nature and distribution of the opaque phase as well as the non-opaque phase.

Unless all more likely assemblages are contraindicated, it is reasonable to dismiss the possibility that this is a

surface composed only of an opaque phase. The relatively high albedo of 1 Ceres compared to that of either carbon or magnetite or any material which meets our definition of 'opaque' (albedo $\lesssim$2%) would eliminate such materials by themselves from contention. It is useful to consider what can be said about the non-opaque phase. Since no definitive silicate absorption features are evident in the spectrum of 1 Ceres, let us consider the three general classes of non-opaque minerals or mineral assemblages present in meteorites. These can be defined in terms of chemical characteristics which are directly related to their optical properties: (a) the highly oxidized (Fe^{2+} + Fe^{3+}), hydrated, iron-rich clay minerals or layer-lattice-silicates which comprise the matrix of the CI (C1) and CM (C2) carbonaceous chondrites, (b) the oxidized (Fe^{2+}) mafic silicates (olivine, pyroxene) typical of the ordinary chondrites and the achondrites, and (c) the transition metal-free silicates (enstatite - Fs_0, forsterite - Fa_0) of the highly reduced enstatite chondrites and achondrites, and C2 olivine inclusions. The oxidation state of the transition metal cations (especially iron) control the general optical properties of the minerals formed by the iron-magnesium-silicon-oxygen system which dominates the non-volatile fraction of the solar system. These general optical properties can be utilized as indicators of the non-opaque mineralogy of these asteroid surface materials.

In the iron-rich clay minerals, the multivalent iron assemblage gives rise to a series of intense charge transfer absorptions (Fe^{2+} - Fe^{3+} and Fe^{3+}) shortwards of 0.7μm (Hunt and Salisbury, 1970; Mao and Bell, 1974b;

Huguenin, 1974) which cause a rapid decrease in reflectance towards shorter wavelengths. This steeply sloping spectral curve is evident in the spectra of the C2 (CM) meteorites (Figure 4i). Even in the presence of ∿5% opaque carbon and magnetite, these charge transfer absorptions impose a blue-UV absorption below 0.55μm.. In order to move this absorption edge to the 0.4μm position in the spectral reflectance curve of 1 Ceres, the spectral contribution of the opaque phase must be increased several fold. This is shown schematically on Figure 7. This might be accomplished either by significantly increasing the total abundance of the opaque carbon phases or by significantly decreasing the optical density or grain size (and hence effective optical density) of the non-opaque phase. The albedo of the assemblage will decrease rapidly when the spectral contribution of the opaque phase is increased. The 5.4% albedo of 1 Ceres is very difficult to reconcile with the 2% albedo expected in the case of a (meteoritic) clay mineral with spectral contrast suppressed by an abundant opaque phase.

An assemblage with a mafic silicate as the major non-opaque phase avoids these problems. In such an assemblage, as in any well-developed mafic mineral, the charge transfer absorptions in the blue and UV, while still significant, are much less intense than the absorptions seen in the Fe^{2+} - Fe^{3+} clay minerals. Thus, for mafic mineral assemblages, only a relatively small amount of opaque material is required to suppress the visible and IR spectral contrast and to dominate the spectral curve

beyond 0.4μm. It must be noted that most of the higher grade C-type chondrites do not contain sufficient amounts of an opaque phase to accomplish this. It is necessary to have on the order of 5-15% of the opaque phase (depending on the particle sizes). The meteorite Karoonda is an example of such a high opaque phase assemblage, consisting of olivine with ∿10% magnetite. The albedo of this meteorite (∿9%) is comparable to that of 1 Ceres and significantly higher than the albedo expected for a C2-type clay mineral mixed with sufficient opaque phase to shift the UV absorption edge to near 0.4μm. It should be noted that the meteorite Karoonda appears to be a very highly metamorphosed (recrystallized) member of the C30 (CO) group and should perhaps be classified C5 (Van Schmus, 1969). It is grouped with the carbonaceous chondrites on a bulk chemical basis (magnesium/silicon ratio) and contains only a spectrally insignificant trace of carbon.

The third class of non-opaque phases are those with almost no transition metal ions in the silicate. Among the meteoritic assemblages, this class is represented by the extremely reduced enstatites of the enstatite chondrites and achondrites and by the iron-free olivine inclusions of C2 chondrites. Since these minerals are equilibrated at extremely low oxygen fugacity, it seems highly unlikely that they could retain any significant component of the opaque oxide minerals (e.g., magnetite) which contain oxidized transition metals. Carbon is present only in trace amounts in these assemblages.

Johnson and Fanale (1973) modeled a carbonaceous spectrum from a mixture of montmorillonite and carbon. This model spectrum was a reasonable match to the spectrum of 1 Ceres. However, there is a major discrepancy in the match with the C-type meteorite spectra, the position of the blue-UV absorption edge, which is a result of the difference between a terrestrially derived clay mineral (montmorillonite) and those found in the low grade C-type (C1-C2, CI and CM) meteorites. Terrestrial clay minerals or layer lattice silicates are derived from feldspars or mafic minerals by a cation leaching process and hydration, which produces a hydrated aluminum (or magnesium) silicate strongly depleted in iron (e.g., Loughnan, 1964; Deer et al., 1965). The resulting spectra exhibit only 'water' absorption bands near 1.4 and 1.9μm with the very steep absorption edge in the reflectance curve shortwards of 0.5μm as a result of charge transfer absorptions. This relatively low optical density material, which really must be considered to be a transition-metal-free silicate of class 3, was utilized by Johnson and Fanale (1973) in their model spectrum.

By contrast, the layer lattice silicates of the C1 (CI) and C2 (CM) meteorites seem to have resulted from a hydration (but no strong leaching) of the metal oxides and silicates in the solar nebula. As a result the layer lattice silicates of these meteorites contain a significant iron component (∿30-40% - Fredriksson and Keil, 1964; Fuchs et al., 1973). These meteoritic clay minerals will thus have the charge-transfer dominated spectra of the class 1 Fe^{2+}-Fe^{3+} assemblages discussed above. Johnson and Fanale (1973) have thus shown that an opaque phase plus a

transition metal-free silicate can produce a Ceres-like spectrum, but the silicate that they chose is not appropriate to the C-type chondrites (C1) they attempted to model.

Thus, based on the spectral reflectance curve and especially the short wavelength position of the UV falloff, and considering the intermediate albedo and deep negative polarization, the surface material of 1 Ceres is most probably an assemblage of well-developed transition metal silicates with an abundant opaque phase, similar to the very high grade C-type meteorite Karoonda. The opaque phase is most probably magnetite. There are minor but significant spectral differences between 1 Ceres and Karoonda which indicate mineralogical and/or petrological differences which cannot be interpreted at the present time.

It would be possible to produce an iron-poor clay mineral assemblage, similar to that modeled by Johnson and Fanale (1973), by hydration of an iron-poor parent material (e.g., enstatite, forsterite). However, the C2 chondrites which contain abundant forsterite inclusions (Wood, 1967) do not contain clay minerals derived from these minerals but only those with uniformly high iron contents (McSween and Richardson, 1977). An opaque-rich low-iron clay assemblage must be regarded as an unlikely, but possible.

Since the spectral reflectance curve of 1 Ceres has been interpreted by a number of previous investigators, it is relevant to compare briefly our methodology and results. Chapman and Salisbury (1973) attempted to match the spectrum of 1 Ceres to laboratory spectra of a number of meteorites and concluded that among their selection, no meteorites matched the spectrum of

1 Ceres, although certain opaque-rich basalts reported by Ross et al. (1969) were similar. Johnson and Fanale (1973) compared the spectrum of 1 Ceres to the spectra of several carbonaceous chondrites and a 'carbonaceous' construct. They concluded that 1 Ceres did not match any known meteorite or ordinary mineral assemblage but that their simulation of C1 meteoritic material did match well. As discussed above, their model does not represent C1 meteorites. McCord and Gaffey (1974) concluded that this spectrum indicated a surface dominated by opaques (e.g., carbon) and probably represented some kind of carbonaceous surface material. Chapman et al. (1975) suggested that the relatively low density of Ceres would rule out the basaltic alternative (see also, Morrison, 1976), but indicated that the spectrum of Karoonda was a good match to that of Ceres. However, the mineralogy of Karoonda (Mason and Wiik, 1962) and the opaque-rich basalt (identified only as from Oregon but most probably a sample of the extensive Snake River Basalts) are identical for spectral purposes. Both consist of abundant low optical density silicates (olivine, feldspar, pyroxene) with very abundant magnetite. Chapman (1976) distinguished Ceres from other 'C'-type asteroids and designated it 'C*' (along with several other 'F' and non-'F' spectra). He suggested that the surface material was similar to Karoonda or possibly to an opaque-rich basalt. Based on the analysis of the optical properties of general mineralogical assemblages, we have concluded that that the surface material of 1 Ceres is most probably a well developed assemblage of olivine and magnetite, but that an opaque-rich, iron-poor clay mineral assemblage cannot be ruled out.

2 PALLAS - The relatively low albedo (7.4%) and deep negative branch of the phase-polarization curve (P_{min} = -1.35%) indicates a dark surface of relatively opaque material. The wavelength position of the blue-UV absorption edge (∿0.43μm) is slightly longer than that in 1 Ceres but it is still significantly shorter than typical of the Fe^{2+} - Fe^{3+} clay mineral (C1, C2) meteorites. Following the same line of arguments as for 1 Ceres, the albedo argues against an ultra-primitive (opaque-rich) clay mineral assemblage. Thus, the surface material is most probably an opaque-rich, low optical density silicate assemblage.

The spectral behavior shortward of 0.45μm is very different from that of 1 Ceres, in that the normalized reflectance decreases by about 15% and then remains approximately constant with a reflectance near 6-7% (assuming an overall albedo ∿7.4%). This spectral

behavior indicates that the optical density of the non-opaque phase increases sharply over the spectral interval from ∿0.5μm down to ∿0.38μm and thereafter remains approximately constant. The edge of the absorption band in the non-opaque phase at 0.38μm should provide a diagnostic clue to the nature of this phase. At the present time we cannot identify this phase unambiguously although possible candidates include Ni-olivine and the iron oxide mineral geothite. Until we can obtain spectra with somewhat better photometric precision and spectral resolution for 2 Pallas, as well as additional laboratory measurements, it will not be possible to specifically identify the non-opaque phase. We can state with assurance that the albedo and 0.43μm edge of the blue-UV absorption feature would rule out the typical low grade carbonaceous chondritic mineral assemblage (opaques plus Fe-rich clay mineral assemblage). The best characterization of the surface material of 2 Pallas is of a low optical density silicate assemblage (olivine, iron-poor clay?) with abundant opaques.

85 IO and 335 ROBERTA - The spectra for these asteroids share all the diagnostic spectral properties of 1 Ceres. Based on the same considerations discussed with respect to Ceres, the surface material of those bodies should be either a Karoonda-like assemblage of a low optical density mafic silicate assemblage with abundant opaques or an ultra-primitive, very high carbon, low metamorphic grade C-type assemblage or an opaque-rich, iron-poor clay mineral assemblage. A low albedo (∿2%) and deep P_{min} (∿2.0%) would favor

the second alternative, a relatively high albedo (∿5-10% and a relatively shallow P_{min} (∿0.0-0.5%) would support the first or third alternatives. On the basis of the 1 Ceres example, the opaque-rich mafic silicate assemblage is more probable. Improved spectra (resolution and signal-to-noise), albedo data and/or phase-polarization data will serve to select between these alternatives and to characterize specifically the mineral assemblages of the surfaces of these bodies.

704 INTERAMNIA and 213 LILAEA - The apparent lack of spectral contrast (the discrepancy between these data and the 'U' filter data is bothersome) is indicative of an opaque-dominated assemblage or a transition metal-free silicate. An improved spectrum (resolution and photometric precision) and albedo or phase-polarization data are needed to choose between these alternatives.

In summary the 'F' type asteroids (1 Ceres and 2 Pallas) seem to represent an opaque-rich, low optical density mafic silicate assemblage analogous to high grade (C4-C5) chondrites, although an opaque-rich, iron-poor assemblage cannot be ruled out. The other four spectra of this group are consistent with this interpretation, but the lack of albedo or phase-polarization data does not permit the exclusion of the other possible types of surface material discussed above. The two well-characterized surface materials are most consistent with a material which has been subjected to a significant thermal event in the presence of oxidizing environment (similar to Karoonda) but probably has not been melted.

Type 'T' Asteroidal Spectra

These spectra are characterized by minimal spectral contrast through the red and IR, a sharp absorption band edge near 0.5μm, a strong blue-UV absorption feature and a weak, variable but persistent absorption feature in the spectral region 0.6-0.7μm. The long wavelength position and sharpness of the 0.5μm absorption edge separates these spectra from the type 'F' spectra discussed above. On cursory examination, these spectra exhibit an apparently smooth transition ('T' = Transitional) from 'F' type spectra into the 'R' type spectra as the absorption edge becomes less distinct and migrates toward longer wavelengths and the overall spectral contrast increases.

Utilizing the line of reasoning developed with respect to the type 'F' spectra, the low spectral contrast in the red and IR would imply either an opaque-rich assemblage or a transition-metal-free assemblage. The uniformly very low albedos (3-6%) measured for a number of members of this group eliminates the latter choice. The surface material of these asteroids is thus best characterized as an assemblage whose red and infrared spectral contrast has been suppressed by an opaque phase.

The spectra provide at least two clues to the general identity of the non-opaque portion of the assemblage. The relative sharpness of the absorption edge between the blue-UV and the red-IR portions of the spectra coupled with the relatively strong blue-UV absorption indicates that the optical density or absorbance of the non-opaque phase increases rapidly over the

interval below 0.6μm, in order to overwhelm the effect of the opaque phase. As discussed in the section on type 'F' spectra, this very sharp and rapid increase of optical density to very high values at blue and UV wavelengths is characteristic of the complex series of charge transfer absorptions which take place in an assemblage with multivalent states of transition metals. This effect accounts for the sharp absorption edge and strong absorption feature of the blue-UV spectral reflectance curve of the low metamorphic grade carbonaceous chondrites (C1-C2, CI and CM). The intensity of this absorption is at least an order of magnitude greater in the type 'T' asteroid spectra and the C1 & C2 meteorite spectra than in the spectra of mafic transition-metal silicates (e.g., olivine, pyroxene).

The weak absorption feature in the 0.6-0.7μm spectral region is persistent in this spectral group. The specific characteristics of this feature (or features) such as central wavelength position, half-width and symmetry cannot be defined in any realistically quantitative fashion in the available spectra since the amplitude of the feature is near the noise level in the available spectra. To define these parameters, spectra with higher spectral resolution and better photometric precision will be needed. The intensity of the feature, however, provides an important clue as to the nature of the transition(s) giving rise to it. The transition increases the bulk optical density of the surface material enough to decrease a 3-6% reflectance by about 0.5%. The intensity of the required transition can

be appreciated when one considers that the relationship of optical density (OD) and percent reflectance (R) can be shown by an equation of the form:

$$OD \sim e^{\frac{(B)}{(R-C)}}$$

where B ∿ 20% and C ∿ 2%. When the reflectance (R) is in the range of 3-6%, a small change in the reflectance corresponds to a very large change in the optical density. Based on approximate comparisons to the optical density variations of Fe^{2+}-Fe^{3+} minerals, the optical density ($\log_{10} I_0/I$) of the non-opaque phase near 0.6-0.7μm must be on the order of 2.0 for reasonable particle sizes.

The absorption features in the 0.6-0.7μm region have been an area of investigation and controversy for several years. The major problem lies in the fact that a variety of crystal field and charge transfer transitions can and do take place in this spectral region. We can rule out the relatively weak 'forbidden' crystal field transitions of the appropriate transition metal ions (e.g., Ti^{3+}, Mn^{3+}, etc.) except where the symmetry of the cation site makes the transition 'allowed.' The strong titanium absorption feature in the spectrum of a titanium pyroxene from the meteorite Allende is sufficiently intense, but the specific nature of the transition (and hence the likelihood of the existence of this mineral in an assemblage of any given oxidation state and equilibrium state) is still unsettled. For example, Burns and Huggins (1973) assign the strong 0.6μm absorption in this mineral to a d-shell electronic transition in Ti^{3+}

in a distorted octahedral crystal site. Dowty and Clark (1973a, b) and Mao and Bell (1974a) assign this transition to a Ti^{3+}-Ti^{4+} charge transfer transition. The oxidation-reduction state of an assemblage governs the relative abundance of the valence states of these transition metal ions. The assignment of a specific electronic transition to the 0.6-0.7μm feature in the type 'T' asteroids and the assignment of a general mineralogical assemblage cannot be checked until we have a better understanding of the possible electronic transitions involved.

Alternatively, the iron oxide minerals goethite (αFeOOH) and lepidocrocite (γFeOOH) exhibit strong, ∿0.7μm absorption features which have been assigned to crystal field transitions in Fe^{3+} ions (Mao and Bell, 1974b). The laboratory spectra of terrestrial 'clay minerals' or 'layer lattice silicates' with minor iron content including talc, chlorite and serpentine (Hunt and Salisbury, 1970) exhibit absorption features (mostly weak) near 0.6μm. These may be related to the absorption features near 0.6μm in the laboratory spectra of the C2 (CM) meteorites (Gaffey, 1976), which are largely composed of such 'layer lattice silicates'.

It is . . . consistent with the present understanding of such an absorption feature in the Type 'T' asteroidal spectra, that it can arise from an electronic transition (e.g., Fe^{3+} crystal field or Fe^{2+} - Fe^{3+} charge transfer transition) in a relatively oxidized (non-reduced) assemblage similar to the C2 carbonaceous chondrites. An extension of the laboratory and theoretical work in understanding these electronic absorption

features as well as improved observational spectra (higher photometric precision and spectral resolution through this spectral region) in order to better characterize this feature (position, intensity, halfwidth, symmetry) are needed before we can significantly improve this aspect of the interpretation.

Several subgroups can be isolated within the type 'T' spectral group. These are arbitrarily designated 'TA', 'TB', 'TC', etc. Each subgroup is considered briefly below and the spectral variation from the average 'T' spectrum is emphasized and discussed.

Type 'TA' spectra (Figure 6H) are characterized by a relatively strong UV absorption (∿30% below a relative maximum near 0.5-0.6μm), a relatively strong (∿5-15%) 0.6-0.7μm feature (λ_{min}0.63-0.66μm) and very little other spectral contrast ($R_{1.0}/R_{0.56}$ = 1.00±0.05). Several measured albedos (3-6%) and P_{min} (∿1.6-1.8%) are indicated of a very dark, opaque surface material. The 0.6μm feature is stronger than typical of the C2 (CM) assemblages, but the implication is unclear for reasons discussed above. In general, the surface material of these asteroids is best characterized as an opaque-rich, Fe-rich clay mineral assemblage similar to the C1-C2 (CI, CM) carbonaceous chondrites. At least nine asteroids (19 Fortune, 48 Doris, 52 Europa, 141 Lumen, 145 Adeona, 163 Erigone, 176 Iduna, 505 Cava and 554 Peraga) are included in this group.

Type 'TB' spectra (Figure 6I) are distinguished from type 'TA' by relatively weak 0.6μm and UV absorption features. The albedos (∿5-7%) and P_{min} (∿1.3-1.7%) suggest a slightly

brighter and less opaque surface assemblage than for the 'TA' asteroids. This may represent a change in the oxidation state or metamorphic grade relative to the previous group, but without additional laboratory and theoretical information, we cannot specifically define the mineralogical variation of this surface material from that of the 'TA' asteroids. At least four asteroids (10 Hygiea, 88 Thisbe, 139 Juewa and 511 Davida) are included in this group.

Type 'TC' spectra (Figure 6J) are distinguished from type 'TA' and 'TB' by a relatively high normalized reflectance beyond the 0.6μm feature ($R_{0.85}$-$R_{1.10}$ ∿ 1.1-1.2). The position of the blue-UV absorption edge (0.50-0.53μm), low albedos (4-6%) and deep P_{min} (∿2.0%) constrain the surface material to be dark and opaque and point to an assemblage similar to low grade C-type chondrites. The 0.6μm feature is still very strong but the optical density in the 1μm spectral region is significantly less than in the type 'TA' and 'TB' spectra. This material is best characterized as a low metamorphic grade assemblage similar to the C1(CI) or C2(CM) chondrites, but with a significantly larger component of the phase producing the 0.6μm absorption feature. Until understanding of the electronic transition responsible for features in this portion of the spectrum is more advance, we cannot provide a better characterization of the surface material of these asteroids. At least four asteroids (51 Nemausa, 166 Rhodope, 194 Prokne and 654 Zelinda) are included in this group.

The preceeding three groups (TA, TB, TC) of asteroidal spectra represent assemblages dominated by opaque phases (visible-IR) and by very intense charge transfer absorptions (blue-UV). This spectral behavior is most probably the product of an opaque (carbon, magnetite) rich, relatively oxidized (Fe^{2+}, Fe^{3+}, etc.) assemblage comparable to C1 (CI) or C2 (CM) chondrites. The variable (intensity, position, symmetry) 0.6-0.7μm feature and the other spectral criteria for distinguishing the three subtypes, indicate the presence of significant variations in bulk mineralogy, reduction state and/or metamorphic grade. The determination of the specific mineralogical and petrological implications of these spectral variations must await improvements in our laboratory and theoretical understanding of opaque-rich and Fe-rich clay mineral assemblages as well as improvements in spectral precision and resolution. These improvements should be forthcoming and it should be possible to define the surface mineral compositions and abundances with relatively little uncertainty.

Several other asteroids exhibit spectra which seem to belong to one or another of the above groups, but for a variety of reasons (incomplete spectral coverage, poor precision, etc.) cannot be assigned more specifically. These (Figure 6K) include 58 Concordia, 130 Elektra, 210 Isabella, 324 Bamberga and 481 Emita. The edge of the blue-UV absorption feature (0.53-0.56μm), lack of spectral contrast, low albedo and deep P_{min} (3.6% and -1.45% respectively for 324 Bamberga) all group

these surface materials with the general TA-TB-TC asteroids, that is, an opaque-rich, Fe^{2+} - Fe^{3+} mineral assemblage analogous to C1-C2 meteoritic mineral assemblages.

Types 'TD' and 'TE' spectra are characterized by significantly greater spectral contrast shortwards of about 0.7μm than exhibited by the types 'TA, TB' and 'TC' spectra. These spectral curves are nearly flat longwards of about 0.7μm forming a plateau in the curve. The break-in-slope between the UV-visible (high spectral contrast) and the IR (minimal spectral contrast) is at significantly longer wavelengths (0.65-0.75μm) than in the 'TA-TC' spectra. It is not nearly as well defined and consists of a relatively smooth change in spectral contrast per wavelength interval. These 'TDE' spectra are distinguished from the 'RF' spectra on the basis of the normalized reflectance of the IR plateau longwards of about 0.7μm ('TD' and 'TE', $R = R_{0.7-1.1}/R_{0.56} < 1.15-1.20$ while 'RF', $R > 1.2$). The residual spectral (energy space - linear 'continuum' removed) exhibits a small but noticeable curvature on the order of 2-3 times the uncertainties. A persistent weak feature is present in the spectra near 0.65μm. Available albedos tend to be intermediate (9-16%) and P_{min}'s shallow (∿0.7%). Silicate absorption features near 1μm are absent or very weak.

A general picture of the surface material of these asteroids with 'TD-TE' spectra can be drawn from this information. The increased spectral contrast and the long wavelength position of the break in spectral slope indicates that the average optical density has decreased

significantly relative to the 'TA-TC' surface materials. The lack of well defined IR features and IR spectral contrast indicates that an opaque phase is still present though in much lower effective abundance. These conclusions, are consistent with the available albedo and phase-polarization data. The curvature of the continuum, the relatively low optical density and overall spectral shape indicate that the bulk of the material is probably a silicate. The UV-visible spectral curvature and spectral contrast indicate the presence of transition metal ions in the silicate, but the apparent absence of silicate absorption features suggests that the mean photon path length through the silicate phase is short with respect to an optical depth in the absorption feature of the silicate. For assemblages with opaques, this would imply mean distances between scattering boundaries (particle size, crystal size, spacing of inclusions, etc.) of a few tens of micrometers (10-30) for olivine (Fa_{20}) and a few microns (5-20) for pyroxene (Fs_{20}). The mean photon path length will be comparable to that in the higher temperature and weakly featured C-type meteorite (C3V(CV), C30(CO)) spectra. (The major silicate in these meteorites is olivine.) The mean photon path length through the silicate phase in the surface materials producing the 'TD' and 'TE' spectra must be shorter than typical of the lowest grade ordinary chondrites. It is also possible to exclude a well developed silicate assemblage where the optical path has been decreased by subsequent events (e.g. black chondrites - Gaffey, 1976). The black chondrites

show weak but well defined (∿10%) absorption features of the mineral phase (pyroxene) with the highest optical density in its absorption feature.

Type "TD" spectra (Fig. 6L) have relatively little spectral contrast over the interval 0.55 - 0.70μm and no indication of any 1 μm silicate absorption feature. The normalized spectral reflectance of the interval 0.8 - 1.1 μm is near unity (∿1.00-1.10).

Type 'TE' spectra (Fig 6M) have relatively high spectral contrast over the interval 0.55 - 0.70μm and indications of possible weak (∿10%) absorption features near 0.9 - 1.0 μm. (The intensity of these possible features is on the same order as the uncertainty in the data over this interval, so that with the present spectra, the position, shape and symmetry - or even the presence - of these features cannot be firmly established.) The normalized reflectance in the 1 μm region is 1.10 $\pm$ 0.10.

On the basis of reasoning described above, the surface materials giving rise to both of these spectral groups is a mafic silicate assemblage (e.g. olivine, pyroxene) with a significant but not dominant component of an opaque phase. The type 'TD' spectra seem to represent a somewhat higher effective opaque content than the type 'TE' spectra, but the silicates (judged on the basis of continuum curvature) are about equally well developed. The possible weak silicate absorption features in the 'TE' spectra could arise either from olivine or pyroxene. Improved spectra are needed to interpret the silicate mineralogy. The assignment of a silicate mineralogy can be used to strongly constrain a number of other properties of the surface material

(e.g. mean photon path lengths or particle size; abundance, distribution and nature of the opaque phase).

There appear to be subtle variations among these spectra which are not understood, but which most probably represent small but real variations in surface mineralogy and petrology from object to object in these groups. Laboratory and theoretical work to understand quantitatively the optical properties of silicate-opaque assemblages such as the C3O(CO) and C3V(CV) meteorites, coupled with improved observational spectra should be very profitable in terms of understanding the origin and evolution of these asteroids. A laboratory and theoretical investigation of the 0.6 μm feature is also important, especially since the feature in these spectra represents a significantly less intense (lower optical density) absorption than that in the 'TA-TC' spectra.

The type 'TD' and 'TE' spectra imply surface materials in many respects similar to the C3 meteorites. The details of mineralogy cannot be ascertained without further work. The 'TD' spectra include 80 Sappho, 221 Eos and 887 Alinda. The 'TE' spectra include 18 Melpomene, 28 Bellona, 82 Alkmene and 532 Herculina.

Chapman (1976, 1977 personal communication) does not distinguish between the asteroid spectra of types 'TD-TE' and 'RF' (a subset of Chapman et al., 1975 type 'S'). The selection criteria utilized here, while subtle, nevertheless appear to be petrologically significant. Zellner (1977, personal communication) notes that while the albedos of

these objects are appropriate for C3-type assemblages, the P_{min} values are too low. Considering the petrologic complexity of C3-type assemblages, the significance of this observation is unclear.

VII. Discussion and Implications

This paper discusses the interpretation of the observed spectra of approximately sixty asteroids, utilizing the wavelength dependent optical properties of meteoritic and meteorite-like mineral assemblages. The albedos (radiometric) and the depth of the negative branch of the polarization-phase curve have been used to provide an indication of the bulk optical density of the surface material, which constrains the interpretation of the surface mineralogy and petrology. A wide variety of mineralogical assemblages have been identified as asteroid surface materials. These assemblages are mixtures of the minerals found in meteorites. However, the relative abundance of mineral assemblage types present on asteroid surfaces differs radically from relative abundance of meteoritic mineral assemblages arriving at the earth's surface.

This work (McCord and Gaffey, 1974 was a first report) represents the first summary of surface mineralogy for a significant number of asteroids. The most extensive previous descriptions of asteroid surface materials were limited to classifications (spectral, albedo, polarimetric or combinations of these parameters) which, probably, lump together grossly similar rock types. The major value

of these classification approaches is to provide a rapid survey of the asteroids and to indentify special targets for further work by more sophisticated methods of characterizing surface materials. Utilizing the interpretive techniques discussed here, the following types of mineralogical assemblages have been identified. The relative abundances of various assemblages as discussed below are uncorrected for observational bias against the smaller, darker and more distant asteroids as described by Chapman et al. (1975) and Zellner and Bowell (1977).

A large fraction (∿40%) of the interpreted spectra (spectral types TA, TB, TC) indicate surface materials composed of an (spectrally) abundant opaque phase (e.g., carbon, carbonaceous compounds and/or magnetite) mixed with an Fe^{2+} - Fe^{3+} silicate (e.g. low temperature hydrated silicate or clay minerals as found in the C1 and C2 meteorites). This material is comparable to the C1 and C2 assemblages which apparently represent low temperature (<200°C) nebula condensates, with a component of high temperature mineral inclusions (olivine). A range of subtle variations of these spectra indicates that a variety of these opaque-rich clay mineral assemblages exist on asteroid surfaces. Our present limited understanding of the optical and spectral properties of such mineralogical assemblages does not permit a determination of the detailed mineralogy of the surface materials of these asteroids.

It has been suggested that several of these asteroids including 10 Hygieà (Zimmerman, 1974, personal communication), 130 Elecktra (Williams, 1973), and 511 Davida (Zimmerman and Wetherill,

1973), should be supplying a portion of the meteoritic material arriving at the earth's surface. The identification of the type TA, TB and TC asteroidal spectra with C1 or C2 carbonaceous-type assemblages severely constrains the thermal and reduction-oxidation histroy of the surface layers of these objects. If any of these asteroids can be shown to be the source body of a particular C1 (CI) or C2 (CM) meteorite in a terrestrial collection; the thermal, magnetic, major and trace element characteristics and evolution of the source body can be determined from the sample. A possible link between a specific C1 or C2 meteorite and a perticular asteroid can be evaluated by a detailed comparison of the mineralogy, petrology and mineral chemistry of the meteorite and asteroid surface material.

Approximately a quarter of the interpreted spectra (spectral types TD, TE, F) represent surface materials composed of mafic silicates (olivine, pyroxene) mixed with an opaque phase. These materials are comparable to the C3 and C4 carbonaceous chondritic assemblages. The majority (~15% of total) of these spectra (spectral types TD and TE) are characterized by a significant but not overwhelming spectral contribution by the opaque phases. These assemblages are comparable to the 'olivine + opaques' C3O (CO) and C3V (CV) meteoritic assemblages. The type 'F' spectra (~10% of total) apparently represent similar silicates (olivine) with a spectrally dominant opaque phase. An excess opaque component (such as magnetite in the C4 meteorite Karoonda) may represent either variation in the oxidation state of the nebular condensate or subsequent oxidizing conditions in these asteroids. The

highly recrystallized character of Karoonda suggests that it was derived by post-accretionary metamorphism of a C3-like parent material (Van Schmus, 1969). This could be accomplished by mild heating (~800°C) in a relatively shallow (~10 Km) layer on the surface of a parent body undergoing heating and outgasing of the interior. The flow of volatiles (especially H_2O vapor) through this warm layer would provide the necessary oxidizing conditions.

Most of the remaining spectra (about a third of the interpreted spectral) exhibit characteristics of a significant spectral contribution from metallic iron or nickel-iron. The surface materials of these asteroids (spectral types RA, RF, RR) appear to consist of assemblages of Ni-Fe, either alone or with a variety of silicates, including metal or metal plus a transition metal free silicate (e.g. enstatite or forsterite), metal plus olivine, metal plus pyroxene and metal plus olivine plus pyroxene. The surface materials interpreted from spectral types 'RF' and 'RR' might be derived either by isolation of a high temperature fraction of nebular condensate with no oxidized iron (Fe^{2+} or Fe^{3+}) or by the heating and intense reduction of lower temperature condensate. However, the majority of these metalliferous spectra (spectral type RA) appear to represent surface materials with abundant (~25-75%) metal. The apparent metal abundances in these surface materials is comparable to that in the stony-iron meteorites and represents a significant enrichment over cosmic abundance. This would require a mobilization and concentration of the metal phases and/or the specific silicate phases, by a differentiation process in a molten parent body.

This implies the heating of the parent material to temperatures in excess of the melting point of the appropriate mafic and Ni-Fe minerals (1400-1800°C). In this model, the calcic pyroxene assemblage determined for the surface material of the asteroid 4 Vesta (McCord, et al., 1970; Chapman and Salisbury, 1973; Veeder et al., 1975; Johnson, et al., 1975; Larson and Fink, 1975; McFadden et al., 1977) would represent the complementary mineral assemblage derived by the concentration of the less dense mineral phases in the near surface layers of the molten body.

The range of assemblages present on asteroid surfaces is an indication of the range of processes that have acted on the asteroids and asteroid parent bodies. Most modern cosmological models assume that the solid bodies of the solar system accreted from grains precipitated by a cooling nebula of solar composition (e.g. Cameron, 1973; Cameron and Pine, 1973; Lewis, 1972). The sequence of condensation with decreasing temperature in a solar nebula has been discussed extensively (e.g. Larimer, 1967; Grossman, 1972; Grossman and Larimer, 1974). In a condensation sequence which does not involve the large scale removal of condensed matter from contact and further reaction with the nebular gas (equilibrated or quasi-equilibrated condensation model), the unmetamorphosed chondritic meteoritic assemblages (C1, C2, C3, LL 3-4, L 3-4, H 3-4, E 3-4) and the high temperature calcium-aluminum inclusions of the C-type meteorites (e.g. Allende) can be formed by accretion of direct condensation products. While the detailed sequence of mineral condensation and reaction is a function of nebular pressure, a major factor

to bear in mind is that the oxidation of iron (Fe°) to Fe^{2+} begins to take place near 750°K, well below the temperature at which essentially all the silicate and metal phases will have condensed. In these models, the magnesium end members of the olivine and pyroxene minerals condense near 1300°K but do not incorporate the Fe^{2+} cations until the nebula has cooled below 750°K. The sensitivity of final product mineralogy (e.g. Fe^{2+} distribution) to nebular conditions and processes (e.g. isolated regions, gas-dust fractionation) and to accretionary and post-accretionary processes, can provide a key to utilizing mafic silicate mineralogy as a probe of the evolutionary histroy of certain regions of the solar system.

The asteroid surface materials consisting of mixtures of an opaque phase and an Fe^{2+} - Fe^{3+} silicate must represent a condensate or modification under conditions where Fe^{2+} can be oxidized to Fe^{3+} (e.g. approximately 400-450° K in contact with the solar nebula). Unless special conditions are invoked, a significant amount (2-4%) of carbon in various forms will be included in the condensate. In any significant post-accretionary thermal event, this carbon, based on the carbon-to-iron ratio seen in the C1 and C2 meteorites, is sufficient to reduce all of the trivalent iron to the bivalent state. The specific upper limit to any post-accretionary thermal event is a complex function of the carbon content and iron oxidation state of the parent material, the maximum temperature, heating rate and interval, thermal gradient in the parent body, and gas pressure and diffusion rate in the parent body (Lewis, 1976, personal communication). Assuming that the conditions for the C1 and C2

meteorites were in effect on these asteroids, it can be guesstimated that this asteroid surface material has not exceeded about 700°K for long periods of time (e.g. 10^6 years). Theoretical and experimental work on the thermal metamorphism and reduction of low temperature (>350°K) nebular condensate in a post-accretionary situation (e.g. out of contact with the nebular gases) is needed.

The terrestrially available analogues, and possible samples, of this material are the C1 and C2 chondrites. The composition of the mineral phases of many of these meteorites were established prior to accretion and the high temperature mafic inclusions show no evidence of alteration by the low temperature matrix (Van Schmus, 1969; Fuchs et al., 1973; Kerridge and MacDougall, 1976). Fuchs et al. (1973) suggest that the C2 meteorite Murchison has not been heated above about 250°C (520°K) since its accretion. The relevance of these meteoritic analogues cannot be evaluated until definite links between specific asteroids and specific meteorite samples can be established.

The asteroid surface materials which are opaque-mafic silicate assemblages could be produced either as a direct nebular condensate between 750°K and 350°K (e.g., below the point where Fe^{2+} can be produced but above the point where the silicates become hydrated in condensation models) or by thermal metamorphism of a high or low temperature condensate (e.g. heating, dehydration and reduction of C2-like assemblages or oxidation and magnetite formation in metal-silicate assemblages). Although there are definite mineralogical and petrological differences between

assemblages derived from these two alternatives (e.g., mineralogical homogeneity and composition, opaque phase composition and distribution), the presently available spectral data and present interpretive sophistication does not permit the determination of mineralogy precisely enough to distinguish between these choices.

The meteoritic analogues of this material, the C3 and C4 chondrites, seem to consist of accretions of intermediate temperature nebular condensate with Fe^{2+} diffused into the silicates which have undergone a range of themal metamorphic events from very little or none (C3) to very strong (C4) (Van Schmus, 1969). These assemblages have not been produced by the thermal metamorphism and reduction of C1 or C2 parent material (Van Schmus, 1969). Whether these asteroidal surface materials also represent a similar restricted sequence, can only be established by further work.

The type 'RR' and 'RF' spectra may represent metal plus transition metal-free (TMF) silicate assemblages. The meteoritic analogues of such materials are the enstatite chondrites which appear to be direct agglomerations of nebular condensate at high temperature or low oxygen partial pressure or both (e.g. Larimer, 1967; Grossman and Larimer, 1974), where Fe^0 cannot be oxidized to Fe^{2+} in any significant abundance. If the slope of the continuum in these metal-rich spectra is related to the metal particle size in the asteroidal substrate. then some of these objects would have gone through a thermal event at or above the melting point of the metal phase, permitting the growth of large metal particles. Such coarse metal-TMF silicate assemblages have not been found in terrestrial collections, but the complementary light mineral assemblage, the enstatite achondrites, do exist.

The surface materials associated with the type 'RA' spectra exhibit well developed Fe^{2+} silicate absorption features. This material could be derived from an asteroidal object accreted below 750°K or from an object accreted above 750°K which has been exposed to a subsequent oxidizing episode. The latter possibility would require the inclusion of an 'oxidizing' phase (e.g. hydrated silicates), with the high temperature accretionary product.

In the former case, the material below 750°K will include virtually all of the condensable metal and silicate phases and would resemble some type of ordinary or carbonaceous chondritic material (i.e., metal:silicate$\sim$1:4-100). The metal-rich Fe^{2+} silicate asteroid surface materials would be produced from this condensate by magmatic differentiation during a very high temperature ($\sim$1400-1800°C) thermal event. The meteoritic analogues for these asteroid materials would be the differentiated meteorites which contain Fe^{2+} silicates (e.g., eucrites, howardites, diogenites, mesosiderites, pallasites, nakhites, angrites and chassignites).

There is evidence for three definable asteroid populations, with different condensation, accretion or thermal histories.

(1) The opaque + Fe^{2+}-Fe^{3+} assemblages (spectral types TA, TB, TC) and their meteoritic analogues, C1 and C2 chondrites, accreted from material apparently condensed at low temperature (<400°K) from the solar nebula. These materials have experienced weak or minimal post-accretionary thermal events.

(2) The opaque + mafic silicate assemblages (spectral types TD, TE, F) and their meteoritic analogues, the C3 and C4 chondrites,

accreted from nebular condensate between 750°K and 350° K. The C4 meteoritic materials and the type 'F' asteroidal surface materials appear to be the result of a post-accretionary metamorphic episode sufficient to mineralogically alter C3-like parent material but not to melt it.

(3) The metal-rich differentiated asteroid surface assemblage (and most of the differentiated meteorites) accreted from material condensed below 750°K, and have experienced intense heating events permitting magmatic differentiation to occur.

VIII. Distribution of Asteroid Materials

The distribution of the types of mineral assemblages with respect to orbital elements or size of body can provide insight into the nature of the asteroid formation and modification processes. Chapman, et al. (1975) and Chapman (1976) have drawn several conclusions based on these distributions of their 'C' and 'S' type asteroids. These conclusions are based on the assumption that the 'C' type surface materials are 'carbonaceous', this is, low temperature, primitive assemblages. However, as can be seen on Table 3, the surface materials analogous to the C2 and C4 meteoritic mineral assemblages have been generally classified 'C', while many of those analogous to the C3 assemblages have been classified 'S'. Thus although most main belt 'C' objects are apparently primitive and most main belt 'S' objects appear differentiated, groups 'C' and 'S' do contain both primitive and modified objects.

C-2

The C2-like surface materials which dominate the main asteroid belt population appear to be relatively rare on the earth-crossing and earth-approaching asteroids (Apollo and Amor objects). Spectral reflectance curves have been interpreted for two Amor asteroids (433 Eros ∿ H5-6 or L5-6 assemblage - Pieters et al., 1976 and 887 Alinda ∿ C3 assemblage) and for one Apollo asteroid (1685 Toro ∿ L6(?) - Chapman et al., 1973b). Gehrels et al. (1970) utilized several indirect methods to define a wavelength dependent brightness curve for the earth-crossing asteroid 1566 Icarus which indicated the presence of an absorption feature in the region of 1μm (pyroxene?). Zellner et al. (1975) provided the UBV colors for two additional objects (1620 Geographos and 1864 Daedalus), both type 'S'. Zellner and Bowell (1977) indicate that of about 12 Apollo or Amor objects only 1 is of type 'C'. While our reservations with regard to the meteoritic specificity of the 'C-S' classification system are unchanged, we can view 'C' and 'S' as approximately 'C2' and 'not-C2'.

The distribution of the mineralogic groups with respect to semi-major axis is shown of Figure 8A. These assemblages can be grouped according to post-accretionary thermal history into two

groups: (a) apparently unmodified low temperature, surface materials (types TA, TB, TC ∿ C2) and intermediate temperature surface materials (type TD, TE ∿ C3), and (b) apparently metamorphosed or differentiated assemblages (types RA, A, F). The distribution of these materials with respect to semi-major axis is shown on Figure 8b. These distributions have not been corrected for observational bias which favors brighter objects over darker objects; that is, objects with high albedos are favored over those with low albedos or objects with small semi-major axes are favored over those with large. Thus, for example, the number of TA-TB-TC objects should be multiplied by some factor depending on size and semi-major axis to compensate for their low albedos. Zellner and Bowell (1977) have discussed this bias correction process in detail.

Based on these distributions, we would verify the increase in relative abundance of the low temperature assemblages with increasing distance from the sun (Chapman et al., 1975), but would note that inside about 3.0 AU's, all types can generally be found in a region. The particular concentration of the metal plus orthopyroxene assemblage contained in spectral type 'RA-2' inside 2.5 AU's as a distribution which should be considered in light of models for heating and differentiating these objects.

We would disagree, at least on the basis of our limited number of examples, with the suggestion (Chapman, 1976) that the low temperature assemblages (∿his 'C' type) avoid the Kirkwood Gaps significantly more than other asteroids. We find no well defined behavior of this sort. Zellner and Bowell (1977) have shown that the apparent avoidance arises from observational bias.

It has been suggested (Chapman, et al., 1975) that the variation of relative abundance of the 'C' and 'S' type asteroids with semi-major axis may represent effects of a thermal gradient in the condensing solar nebula, and that the orbital elements have been mixed to give the present distribution.

Williams (1976) has suggested that the majority of present belt asteroids are those members of a much larger population which are stable against perturbation effects by Jupiter. Williams (1976, personal communication) also suggests that these bodies are in very much the same orbits in which they were accreted, that is, that no large scale (e.g. $\gtrsim$0.1 AU) orbital mixing by perturbations should have taken place. The numerical calculations of Lecar and Franklin (1973) would seem to support this general concept. In such a situation small scale mixing of orbital elements would occur dominantly when collisions occur between asteroids. Williams (1976) indicates that asteroids which are fragments of collisions can be recognized by the clustering of their orbital elements after correction for planetary perturbations. He also notes that some of the collisional groups so far recognized (e.g. 221 Eos) consist of one major body and a number of much smaller bodies rather than several large bodies.

If we accept the concept that the present asteroidal orbits are similar to the original orbits, we perceive a very interesting situation when we consider the low and intermediate temperature asteroidal materials and their meteoritic analogues. The

low temperature and the 'TD' and 'TE' type intermediate temperature asteroidal assemblages could have been formed by accretion of direct condensation of the condensation products of a cooling solar nebula. All of the meteoritic analogues of this material apparently formed in this manner. Or alternatively, these asteroidal materials may represent alteration products (hydration and oxidation or heating and reduction) of nebular condensate in response to some heating and outgassing event.

If these asteroid surface materials represent direct condensates, of which the C1, C2 and C3 meteorites are examples, the coexistance of these assemblages throughout the inner two-thirds of the asteroid belt must be explained in terms of the isolation of the higher temperature fractions from further reaction with the nebula as it cools. This would be accomplished by accretion of some of the nebular condensate at each temperature onto the surfaces of planetesimals. Turekian and Clark (1969) have discussed such inhomogeneous accretion models. Under this model, the asteroids would accrete as concentric structures with high temperature condensate cores grading out to surfaces of low temperature condensate. The low temperature surface materials would be found on asteroids which have retained their original surface layers or which began accretion late in the condensation sequence. Intermediate temperature materials and high temperature condensate (e.g. E4) assemblages would be exposed by the erosion and mass loss of the overlying layers by small impact events (Marcus, 1969; Dohnanyi, 1969) or by collisional exposure of asteroid cores. The amount of each temperature fraction incorporated into a particular proto-asteroid will depend on the time of initial

appearance of the core body, on the density of condensed matter in the region and on the rate and efficiency of accretion as a function of cooling and condensation rates in the nebula. The removal of some condensate from the nebula at higher temperatures modifies the condensation sequence (inhomogeneous condensation), but the magnitude of this modification depends on the type and amount of material isolated from contact with the nebula.

If these low and intermediate temperature asteroidal materials can be shown to originate by this inhomogeneous accretion mechanism, then the amount of each thermal fraction exposed in a particular portion of the asteroid belt would provide a measure of some of the parameters discussed above. Constraining these parameters would provide a significant insight into the details of the condensation and accretion sequence in this region of the solar nebula.

Alternatively, the opaque-mafic silicate assemblages, analogous to C3 materials (spectral types 'TD' and 'TE'), may have been produced by the thermal metamorphism of low temperature condensate. The differentiated asteroid surface materials and meteorites are evidence of much more intense thermal events than required to metamorphose C1 or C2 type materials. While this is a quite plausible model for the origin of these asteroidal assemblages, it would imply that there are no samples of these asteroidal materials in terrestrial meteorite collections. The C3 meteorites, while petrologically and mineralogically similar, would not have derived from any of these asteroids but from another source. It would also imply that if one large compositional subdivision of the main belt asteroids were not supplying any measurable portion

of the meteoritic flux, it would be unlikely that any large portion of the meteoritic flux could be derived from main belt asteroidal sources.

This would be an unattractive hypothesis in light of our knowledge and concepts of the meteorite parent bodies. The meteorite parent bodies must have been large enough to account for the cosmic ray exposure ages and cooling rates of the meteorites and to survive erosion and a collisional destruction over the age of the solar system and be in orbits stable against perturbation and subsequent sweep-up or expulsion from the solar system. These requirements would seem to necessitate either relatively large parent bodies in long-term stable orbits (e.g., asteroid belt orbits) or constantly renewed from an exterior source (e.g., cometary nuclei). It seems difficult, if not impossible, to reconcile the low-temperature, volatile-rich character of cometary nuclei with the high temperature post-accretionary origin of the differentiated meteorites. Anders (1975) has presented arguments against the cometary origin of stony meteorites. Wetherill (1976) has argued for a cometary origin for most meteorites and presumably high temperature or inner solar system material ejected by gravitational perturbations early in solar system history would be contained in these cometary objects.

It is evident that the dominant 'C2'-type assemblage of the main belt are under-represented among the Apollo and Amor objects by about two orders of magnitude (∿1/10 instead of ∿10/1). This discrepancy implies that the Apollo and Amor asteroids are not randomly derived from the population of the main belt. If this population anomaly is not a recent or temporary event, then the source region which replenishes this inner solar system population must be both restricted and strongly depleted in 'C2'-type asteroidal materials. This suggests that these asteroids may be derived from the innermost portions of the belt, perhaps inside 2.0 a.u.'s. Wetherill (1977) has suggested that objects formed closer in to the sun (e.g., ordinary chondritic assemblages) may have been stored at the inner edge of the belt and may represent the source of these objects. The cometary hypothesis (Opik, 1963, 1966; Wetherill and Williams, 1968) for the origin of the Apollo and Amor asteroids cannot be ruled out on the basis of the available spectral data. Chapman (1977) reaches similar conclusions with respect to the origin of these asteroids.

The distribution of surface mineralogies with respect to the size of the bodies can provide information relevant to this question. The distribution for the types and groups discussed above is shown on Figure 9. Two significant factors should be

noted. Firstly, the largest sized object of the 'TD' and 'TE' (∿C3) group is significantly smaller than that of the 'TA-TB-TC' (∿C2) group. This would tend to support the concept that the C3 type material was isolated in the interiors of bodies with C2-type surfaces (inhomogeneous accretion). Secondly, the largest sized body among 'thermalized' objects (RA, A, F) is significantly larger than that of the 'unthermalized' or 'primitive' objects (TA-TB-TC, TD, TE). This would imply that the size of the parent body has a strong influence over any post-accretionary heating episode. The cutoff in size below which heating did not take place appears to be approximately 300-500 Km. Bias correction should enhance this discrepancy.

Thus, without eliminating either the 'inhomogeneous accretion and condensation' or the 'post-accretionary alteration' models for the origin of the low and intermediate temperature asteroidal assemblages, we believe that the weight of the evidence slightly favors the former alternative. However, as previously stated, improved observational data coupled with increased sophistication in interpreting the opaque-rich spectra, would provide evidence to support one or the other concept. The former alternative is particularly attractive in that it indicates that these asteroids will preserve nebular condensate from each pressure-temperature interval in an essentially pristine form.

The other major question arising from the evidence of asteroid surface materials concerns the nature of the heating and differentiation event producing the differentiated asteroidal materials. Any proposed heating mechanism must explain why heating has been

so selective among the asteroids. Two selective heating mechanisms have been proposed. Sonett et al. (1970), Sonett (1971) and Briggs (1976) have shown that heating can be induced in small inner solar system bodies by the solar magnetic field trapped in the intense solar wind during a T Tauri phase of solar evolution. Briggs (1976) has shown that the magnitude of the heating event for a particular body is dependent on electrical conductivity of the material making up the body. The variations in this parameter between agglomerations of nebular materials (C1, C2, C3O, C3V meteorites) can lead to variations of approximately 10^5- 10^6 in heating rates, between C1 (lowest heating rate) and C3O (highest rate) material, in a given moving electrical field.

Short-lived nuclides, especially Al^{26}, have been suggested as an early intense heat source for accreted bodies (Reeves and Adouze, 1969). The intensity of this heat source would depend on the amount of Al^{26} incorporated into a body, and since the Al^{26} can be produced in portions of the nebula exposed to cosmic rays, variations in relative abundance across the nebula are reasonable. Schramm et al. (1970) placed an upper limit on the abundance of Al^{26} decay products in a number of terrestrial, lunar and meteoritic samples and concluded that no significant heating would be contributed by the original abundance of Al^{26}. Recently, Lee et al. (1976) has identified an Al^{26} excess in the meteorite Allende. The possible contribution by this mechanism is as yet undetermined.

While we evaluate these possible mechanisms for providing the energy necessary for the melting and differentiation episode, we

should also consider the minerological and petrological implications for the undifferentiated meteorites and asteroidal materials. In an asteroidal mass heated to the melting point of its constituate phases at some depth in its interior, several significant events will take place. A thermal gradient will be established in the body from some elevated temperature in the deep interior grading down to approximately black body temperature at the surface. Any hydrated mineral assemblages located in a region where the temperature is relatively high will dehydrate and the water vapor will migrate toward the surface. As this oxidizing vapor passes through the overlying layers, it will react with their mineral assemblages as the pressure-temperature conditions in each region permits. The metamorphosed and oxidized C4 meteorite Karoonda probably originated by the action of water vapor on C3O parent material at an elevated temperature. The spectral type 'F' opaque plus mafic silicate assemblages would be examples of this material if our interpretation is accurate (1 Ceres, 2 Pallas).

In addition to water, at the elevated temperatures, the carbon phases present in the nebula condensate (C1$\sim$3.5%, C2$\sim$2.4%, C3$\lesssim$1%, H, L, LL3$\sim$0.3%, E4$\sim$0.4%) will react with oxidized phases by reactions of the form: $FeO + C \rightarrow Fe + Co$ or $2FeO + C \rightarrow 2Fe + CO_2$.

These two reactions operate in different temperature regimes, the former at higher temperatures than the latter. Thus the carbon monoxide gas formed in high temperature regions will migrate out to a lower temperature region and can precipitate half of the

carbon to produce the stable gas phase at the lower temperature (CO_2). The ureilite-type assemblages with well developed mafic silicates (olivine) and a high carbon content may have developed their pre-shock assemblages in this manner. A carbon-mafic silicate assemblage analogous to C4 Karoonda, might also develop by this mechanism.

It is also instructive to consider the physical effect of developing a significant volume of a vapor phase in the interior of an asteroidal body. The reaction of 0.1% by weight of carbon would develop a volume of vapor (at STP) corresponding to 6 times the volume of the source material. By way of comparison, the subsolidus heating of ordinary chondritic assemblages, grade 3 to grade 6, represents approximately a 0.2-0.3 wt.% depletion of carbon (Moore and Lewis, 1967). In a rapid heating event in a relatively impermeable (slow gas diffusion) body the internal pressure may exceed the lithostatic pressure resulting in the development of gas driven eruptive activity and eruptive breccias.

The foregoing discussion should be indicative of the types of conclusions and concepts which can be derived by a logical follow-through on the implications of the processes known to be operating or to have operated. The development of a well defined quantitative model for these types of processes would be very useful.

IX. Summary and Conclusions

We have discussed the utilization of general and specific diagnostic spectral features and parameters to interpret most of the published high quality reflectance spectra of asteroids. This provides the most complete and sophisticated mineralogically- and petrologically-based interpretation of the

surface materials of these asteroids. A range of mineral assemblages similar to certain meteorite classes have been identified. These include:

a) opaque-rich Fe^{2+}-Fe^{3+} silicate assemblages analogous to the low temperature nebular condensate making up the C1 and C2 carbonaceous chondrites,

b) opaque-mafic silicate assemblages analogous to C3 meteorites,

c) opaque-rich mafic silicate assemblages analogous to C4 meteorites,

d) metal-rich assemblages with a variety of silicates analogous to the stony-irons, irons and/or enstatite chondrites.

There is evidence of a selective high temperature event which melted and permitted the differentiation of certain asteroid parent bodies as some function of distance from the sun or proto-sun and of size of the proto-asteroid. The asteroidal surface materials, formed at low and intermediate temperature analogous to the C1 and C3 or C3 meteorites, either have not undergone any significant post accretionary thermal event as is the case for their meteoritic analogues or have undergone a significant post-accretionary heating event but do not supply any of the terrestrially recovered meteorite flux. Based on meteoritic evidence, the former alternative is favored.

Possible candidates for the source bodies of the following meteorite groups have been identified: eucrites, C1 or C2, C3, C4, E4 and E6 and/or irons, pallasites, mesosiderites and,

possibly chassignites. Any definite assignments of meteorite specimens to asteroid source bodies must at least await improvements in observational data and in interpretive sophistication to provide more detailed mineralogical and petrological data on the asteroid surface materials.

The sophistication achievable in the interpretation of observational spectra is dependent on the spectral coverage, resolution and photometric precision and on the qualitative and quantitative understanding of the functional relationship between the mineralogy of a material and its optical and spectral behavior. The present observational data consists of a) low spectral resolution and coverage, high signal-to-noise data (UBV photometry), b) intermediate resolution, broad spectral coverage, intermediate signal-to-noise data (0.3-1.1 μm filter photometry), and c) high resolution IR spectra applicable to only the brightest asteroids (interferometry). Several new systems are under development which promise improved spectra. Improved observations of previously observed objects will provide improved characterizations of the surface material of these objects.

The definition of a functional relationship between the mineralogy of a material and its optical and spectral properties has shown significant advances in the last decade. However, the magnitude and complexity of the task, as well as the magnitude of rewards, are only now becoming fully apparent. As each improvement in interpretive technique is made, it can be applied to improve the prior interpretation of data. The real gains in

sophistication will come only when the aspects of crystal physics, mineralogy and petrology and optics are considered as a gestalt. Progress, though slow, is being made, and this is the area where extra effort is most likely to provide the most immediate results.

Acknowledgements

The authors would like to thank a number of individuals whose discussions and comments proved very helpful in the preparation of this manuscript, including Dr. John Adams, Dr. Clark Chapman, Dr. Torrence Johnson, Dr. Dennis Matson, Dr. George Wetherill, and Dr. Ben Zellner. This work was supported by NASA grants NGR 22-009-583 and NSG 7310.

REFERENCES

Adams, J.B. (1974) Jour. Geophys. Res. 79, 4829-4836

Adams, J.B. (1975) in Infrared and Raman Spectroscopy of Lunar and Terrestrial Minerals (c. Karr ed.) Academic Press, New York, pp. 91-116

Adams, J.B. and Filice, A.L. (1967) Jour. Geophys. Res. 72, 5705-5715

Adams, J.B. and McCord, T.B. (1970) Proc. Lunar Sci. Conf. 1st, p. 1937-1945

Allen, D.A. (1970) Nature 227, 158-159

Allen, D.A. (1971) in Physical Studies of Minor Planets (T. Gehrels ed.) NASA SP-267, pp. 41-43

Anders, E. (1964) Space Sci. Rev. 3, 583-714

Anders, E. (1971) in Physical Studies of Minor Planets (T. Gehrels ed.) NASA SP-267, pp. 429-446

Anders, E. (1975) Icarus 24, 363-371

Arnold, J.R. (1965) Astrophys. J. 141, 1548-1556

Bell, P.M. and Mao, H.K. (1973) Geochim. Cosmochim. Acta 37, 755-759

Bell, P.M., Mao, H.D. and Rossman, G.R. (1975) in Infrared and Raman Spectroscopy of Lunar and Terrestrial Minerals (ed. C. Karr), p. 1-38, Academic Press, New York

Binns, R.A. (1970) Min. Mag. 37, 649-669

Bowell, E. and Zellner, B. (1973) in Planets, Stars and Nebulae Studied with Photopolarimetry (T. Gehrels ed.) Univ. of Arizona Press, Tucson, Arizona, pp. 381-404.

Briggs, P.L. (1976) M.S. Thesis, Massachusetts Institute of Technology, Cambridge, Mass., 63 pp.

Burns, R.G. (1970a) Amer. Mineral. 55, 1608-1632

Burns, R.G. (1970b) Mineralogical Applications of Crystal Field Theory, Cambridge University Press, New York

Burns, R.G. and Huggins, F.E. (1973) Amer. Mineral. 58, 955-961

Cameron, A.G.W. (1973) Icarus 18, 407-450

Cameron, A.G.W. and Pine, M.R. (1973) Icarus 18, 377-406

Chapman, C.R. (1972) Ph. D. Thesis, Massachusetts Institute of Technology, Cambridge, Mass., 391 pp.

Chapman, C.R. (1976) Geochim. Cosmochim. Acta 40, 701-719

Chapman, C.R. (1977) in The Interrelated Origin of Comets, Asteroids and Meteorites (A.H. Delsemme, ed.) University of Toledo Publications

Chapman, C.R., McCord, T.B. and Johnson, T.V. (1973a) Astron. Jour. 78, 126-140

Chapman, C.R., McCord, T.B. and Pieters, C. (1973b) Astron. Jour. 78, 502-505

Chapman, C.R. and Salisbury, J.W. (1973) Icarus 19, 507-522

Chapman, C.R., Morrison, D. and Zellner, B. (1975) Icarus 25, 104-130

Chapman, C.R. and Morrison, D. (1976) Icarus 28, 91-94

Cruikshank, D.P. (1977) Icarus 30, 224-230

Cruikshank, D.P. and Morrison, D. (1973) Icarus 20, 477-481

Cruikshank, D.P. and Jones, T.J. (1977) Icarus 31, 427-429

Deer, W.A., Howie, R.A. and Zussman, J. (1963) Rock Forming Minerals: Vol. 3 Sheet Silicates Longmans, Green and Co., London

Dodd, R.T. (1976) Earth Planet. Sci. Lett. 30, 281-291

Dohnanyi, J.S. (1969) Jour. Geophys. Res. 74, 2531-2554

Dollfus, A. (1971) in Physical Studies of Minor Planets (T. Gehrels ed.) NASA SP-267, pp. 95-116

Dollfus, A. and Geake, J.E. (1975) Proc. Lunar Sci. Conf. 6th 3, 2749-2768

Dowty, E. and Clark, J.R. (1973a) Amer. Mineral. 58, 230-242

Dowty, E. and Clark, J.R. (1973b) Amer. Mineral. 58, 962-964

Dunlap, J.L. (1974) Astron. Jour. 79, 324-332

Dunlap, J.L., Gehrels, T. and Howes, M.L. (1973) Astron. Jour. 78, 491-501

Egan, W.G., Veverka, J., Noland, M. and Hilgeman, T. (1973) Icarus 19, 358-371

Fredriksson, K. and Keil, K. (1964) Meteoritics 2, 201-217

Fuchs, L., Olsen, E. and Jensen, K.J. (1973) Smithsonian Contrib. Earth Sci. 10, 39 pp.

Gaffey, M.J. (1974) Ph.D. Thesis, Massachusetts Institute of Technology, Cambridge, Mass., 355 pp.

Gaffey, M.J. (1976) Jour. Geophys. Res. 81, 905-920

Gaffey, M.J. and McCord, T.B., (1977) in The Interrelated Origin of Comets, Asteroids and Meteorites, (A.H. Delsemme, ed.) University of Toledo Publications

Gehrels, T., Roemer, E., Taylor, R.C. and Zellner, B.H. (1970) Astron. Jour. 75, 186-195

Gradie, J. and Zellner, B. (1977) Science 197, 254-255

Green, H.W., Radcliffe, S.V. and Heuer, A.H. (1970) EOS Trans. Am. Geophys. Union 51, 341 (abstract)

Grossman, L. (1972) Geochim. Cosmochim. Acta 36, 597-619

Grossman, L. and Larimer, J.W. (1974) Rev. Geophys. and Space Physics 12, 71-101

Hansen, O.L. (1976) Astron. J. 81, 74-84

Hansen, O.L. (1977) Icarus 31, 456-482

Hapke, B. (1971) in Physical Studies of Minor Planets (ed. T. Gehrels), NASA SP-267, pp. 67-77

Herndon, J.M., Rowe, M.W., Larson, E.E. and Watson, D.E. (1976) Earth Planet. Sci. Lett. 29, 283-290

Huguenin, B. (1974) Jour. Geophys. Res. 79, 3895-3905

Hunt, G.R. and Salisbury, J.W. (1970) Mod. Geol. 1, 283-300

Johnson, T.V. and Fanale, F.P. (1973) Jour. Geophys. Res. 78, 8507-8518

Johnson, T.V., Matson, D.L., Veeder, G.J. and Loer, S.J. (1975) Astrophys. J. 197, 527-531

Jones, T.J. and Morrison, D. (1974) Astron. Jour. 79, 892-895.

Keil, K. (1968) Jour. Geophys. Res. 73, 6945-6976

Keil, K. and Fredriksson, K. (1964) Jour. Geophys. Res. 69, 3487-3515

Kerridge, J.F. and MacDougall, J.D. (1976) Earth Planet. Sci. Lett. 29, 341-348

Kozai, Y. (1962) Astron. Jour. 67, 591-598

Larimer, J.W. (1967) Geochim. Cosmochim. Acta 31, 1215-1238

Larson, H.P. (1977) in The Interrelated Origin of Comets, Asteroids and Meteorites, (A.H. Delsemme, ed.) University of Toledo Publications

Larson, H.P. and Fink, U. (1975) Icarus 26, 420-427

Larson, H.P., Fink, U., Treffers, R.R. and Gautier, T.N. (1976) Icarus 28, 95-103

Lecar, M. and Franklin, F.A. (1973) Icarus 20, 442-436

Lee, T., Papanastassiou, D.A. and Wasserburg, G.J. (1976) Geophys. Res. Lett. 3, 109-112

Levin, B.J., Simonenko, A.N. and Anders, E. (1976) Icarus 28, 307-324

Lewis, J.S. (1972) Icarus 16, 241-252

Loughnan, F.C. (1969) Chemical Weathering of the Silicate Minerals Am. Elsevier Pub. Co., New York

Lyot, B. (1934) Compte-Rendus Acad. Sci. 199, 774-777

Mao, H.K. and Bell, P.M. (1974a) Carnegie Inst. Wash. Yearbook 74, 448-492

Mao, H.K. and Bell, P.M. (1974b) Carnegie Inst. Wash. Yearbook 74, 502-507

Marcus, A.H. (1969) Icarus 11, 76-87

Mason, B. (1971) Meteoritics 6, 59-70

Mason, B. and Wiik, H.B. (1962) Amer. Mus. Novitates No. 2115, 10 pp.

Matson, D.L. (1971) in Physical Studies of Minor Planets (T. Gehrels, ed.) NASA SP-267, pp. 45-50

Matson, D.L. (1972) Ph.D. Thesis, California Institute of Technology, Pasadena, Calif., 235 pp.

Matson, D.L., Johnson T.V. and Veeder, G.J. (1977a) in The Interrelated Origin of Comets, Asteroids and Meteorites, (A.H. Delsemme, ed.) University of Toledo Publications

Matson, D.L., Johnson, T.V. and Veeder, G.J. (1977b) Proc. 8th Lunar Sci. Conf., in press

McCord, T.B., Adams, J.B. and Johnson, T.V. (1970) Science 168, 1445-1447

McCord, T.B. and Chapman, C.R. (1975a) Astrophys. Jour. 195, 553-562

McCord, T.B. and Chapman, C.R. (1975b) Astrophys. Jour. 197, 781-790

McCord, T.B. and Gaffey, M.J. (1974) Science 186, 352-355

McFadden, L., McCord, T.B. and Pieters, C. (1977) Icarus 31, 439-446

McSween, H.Y. and Richardson, S.M. (1977) Geochim. Cosmochim. Acta 41, 1145-1161

Moore, C.B. and Lewis, C.F. (1967) Jour. Geophys. Res. 72, 6289-6292

Morrison, D. (1973) Icarus 19, 1-14

Morrison, D. (1974) Astrophys. J. 194, 203-212

Morrison, D. (1976) Geophys. Res. Lett. 3, 701-704

Morrison, D. (1977a) Astrophys. Jour. 214, 667-677

Morrison, D. (1977b) Icarus 31, 185-220

Morrison, D. (1977c) in The Interrelated Origin of Comets, Asteroids and Meteorites, (A.H. Delsemme, ed.) University of Toledo Press

Morrison, D. and Chapman, C.R. (1976) Astrophys. Jour. 204, 934-939

Nash, D.B. and Conel. J.F. (1974) Jour. Geophys. Res. 79, 1615-1621

Opik, E.J. (1963) Adv. Astron. Astrophys. 2, 219-262

Opik, E.J. (1966) Adv. Astron. Astrophys. 4, 301-336

Peterson, C. (1976) Icarus 29, 91-111

Pieters, C., Gaffey, M.J., Chapman, C.R. and McCord, T.B. (1976) Icarus 28, 105-115

Reeves, H. and Audouze, J. (1969) Earth Planet. Sci. Lett. 4, 135-141

Reid, A.M. and Cohen, A.J. (1967) Geochim. Cosmochim. Acta 31, 661-672

Ross, H.P., Adler, J.E.M., and Hunt, G.R. (1969) Icarus 11, 46-54

Salisbury, J.W. and Hunt, G.R. (1974) Jour. Geophys. Res. 79, 4439-4441

Schaudy, R., Wasson, J.T. and Buchwald, V.F. (1972) Icarus 17, 174-192

Schramm, D., Tera, F. and Wasserburg, G. (1970) Earth Planet. Sci. Lett. 10, 44-59

Sonett, C.P. (1971) in Physical Studies of Minor Planets (T. Gehrels ed.) NASA SP-267, pp. 239-245

Sonett, C.P., Colburn, D.S., Schwartz, K. and Keil, K. (1970) Astrophys. Space Sci. 7, 446-488

Sytinskaya, N.N. (1965) Soviet Physics-Astronomy 9, 100-104

Turekian, K.K. and Clark, S.P. Jr. (1969) Earth Planet. Sci. Lett. 6, 346-348

Van Schmus, W.R. (1969) in Meteorite Research (P. Millman, Editor) pp. 480-491, D. Reidel Publishing Company, Dordrech, Holland

Van Schmus, W.R. and Wood, J.A. (1967) Geochim. Cosmochim. Acta 31, 747-765

Vdovykin, G.P. and Moore, C.B. (1971) in Handbook of Elemental Abundances in Meteorites (B. Mason, Ed.) Gordon and Breech, New York, pp. 81-91

Veeder, G.J., Johnson, T.V. and Matson, D.L. (1975) Bull. A.A.S. 7, 377

Veeder, G.J., Matson, D.L., Bergstralh, J.T. and Johnson, T.V. (1976) Icarus 28, 79-85

Veverka, J. (1970) Ph.D. Thesis, Harvard University, Cambridge, Mass., 288 pp.

Veverka, J. (1971a) Icarus 15, 11-17

Veverka, J. (1971b) Icarus 15, 454-458

Veverka, J. (1973) Icarus 19, 114-117

Veverka, J. and Noland, M. (1973) Icarus 19, 230-239

Wetherill, G.W. (1974) in Ann. Rev. Earth Planet. Sci. (F.A. Donath, ed.) Vol. 2, 303-331

Wetherill, G.W. (1976) Geochim. Cosmochim. Acta 40, 1297-1317

Wetherill, G.W. (1977) Proc. 8th Lunar Sci. Conf., in press

Wetherill, G.W. and Williams, J.G. (1968) Jour. Geophys. Res. 73, 635-648

White, W.B. and Keester, K.L. (1966) Amer. Mineral. 51, 774-791

White, W.B. and Keester, K.L. (1967) Amer. Mineral. 52, 1508-1514

Williams, J.G. (1969) Ph.D. Thesis, Univ. Cal. Los Angeles

Williams, J.G. (1973) EOS Trans. Amer. Geophys. Union 54, 233 (abstract)

Williams, J.G. (1976) Abst. I.A.U. Coll. #39, Relationships Between Comets, Minor Planets and Meteorites, Lyon, France, August 17-20, 1976, p. 19

Wisniewski, W.Z. (1976) Icarus 28, 87-90

Wolff, M. (1975) Appl. Optics 14, 1395-1405

Wood, J.A. (1967) Geochim. Cosmochim. Acta 31, 2095-2108

Zellner, B. (1975) Astrophys. Jour. Lett. 198, L45-L47

Zellner, B., Gehrels, T. and Gradie, J. (1974) Astron. Jour. 79, 1100-1110

Zellner, B., Wisniewski, W.Z., Andersson, L. and Bowell, E. (1975) Astron. Jour. 80, 986-995

Zellner, B. and Gradie, J. (1976a) Astron. Jour. 81, 262-280

Zellner, B. and Gradie, J. (1976b) Icarus 28, 117-123

Zellner, B. and Bowell, E. (1977) in The Interrelated Origin of Comets, Asteroids and Meteorites, (A.H. Delsemme, ed.) University of Toledo Publications

Zellner, B., Leake, M., Lebertre, T. and Dollfus, A. (1977a) Proc. 8th Lunar Science Conf. (in press)

Zellner, B., Andersson, L. and Gradie, J. (1977b) Icarus 31, 447-455

Zellner, B., Leake, M. and Morrison, D. (1977c) Geochim. Cosmochim. Acta., in press

Zimmerman, P.D. and Wetherill, G.W. (1973) Science 182, 51-53

TABLE 1

Asteroids considered to be possible sources of portions of the terrestrial meteorite flux on a dynamical basis.

Asteroid	Mechanism*	Reference	Mineral Interpretation
6 Hebe	SRP	1	Yes
8 Flora	SRP	1	Yes
10 Hygiea	RP	4	Yes
31 Euphrosyne	RP	2	No
89 Julia	SRP	1	No
108 Hecuba	RP	2	No
130 Elektra	SRP	1	Yes
175 Andromache	RP	2	No
511 Davida	RP	2	Yes
530 Turandot	RP	3	No
805 Hormuthia	RP	3	No
814 Tauris	RP	2	No
927 Ratisbona	RP	3	No

*SRP = collisional ejection of fragments of asteroid into nearby orbital resonance with the secular perturbations of the planets (Secular Resonant Perturbations)

RP = collisional ejection of fragments into a resonance with Jupiter (e.g., Kirkwood Gaps) with perterbations by Jupiter (Resonant Perterbations)

REFERENCES 1. Williams, 1973, also Wetherill, 1974

2. Zimmerman and Wetherill, 1973

3. Wetherill, 1974

4. Zimmerman, 1974, personal communication

Table 2

Asteroid	Orbital Parameters a(AU)	e	i (degrees)	Albedo(a) (%)	Pmin(b) (%)	Diameters(a) (Km)
1 Ceres	2.767	0.08	10.6	5.4	1.67	1003
2 Pallas	2.769	0.24	34.8	7.4	1.35	608
3 Juno	2.670	0.26	13.0	15.1	0.75	247
4 Vesta	2.362	0.09	7.1	22.9	0.55	538
6 Hebe	2.426	0.20	14.8	16.4	0.80	201
7 Iris	2.386	0.23	5.5	15.4	0.70	209
8 Flora	2.202	0.16	5.9	14.4	0.60	151
9 Metis	2.386	0.12	5.6	13.9	0.70	151
10 Hygiea	3.151	0.10	3.8	4.1	-	450
11 Parthenope	2.453	0.10	4.6	12.6	0.70	150
14 Irene	2.589	0.16	9.1	16.2	-	158
15 Eunomia	2.642	0.19	11.7	15.5	0.70	272
16 Psyche	2.920	0.14	3.1	9.3	0.95	250
17 Thetis	2.469	0.14	5.6	10.3	0.65	109
18 Melpomene	2.296	0.22	10.1	14.4	-	150
19 Fortuna	2.442	0.16	1.6	3.2	1.65	215
25 Phocaea	2.401	0.26	21.6	18.4	-	72
27 Euterpe	2.347	0.17	1.6	14.7	0.60	108
28 Bellona	2.776	0.15	9.4	13.2*	-	126*
30 Urania	2.365	0.13	2.1	14.4	0.75	91
39 Laetitia	2.769	0.11	10.4	16.9	0.70	163
40 Harmonia	2.267	0.05	4.3	12.3	0.75	100
48 Doris	3.114	0.06	6.5	-	-	-
51 Nemausa	2.366	0.07	10.0	5.0	1.95	151
52 Europa	3.092	0.11	7.5	3.5	-	289
58 Concordia	2.699	0.04	5.0	-	-	-
63 Ausonia	2.395	0.13	5.8	12.8	0.65	91
79 Eurynome	2.444	0.19	4.6	13.7	-	76
80 Sappho	2.296	0.20	8.7	11.3	-	83
82 Alkmene	2.763	0.22	2.8	13.8	-	65
85 Io	2.654	0.19	11.9	4.2	-	147
88 Thisbe	2.768	0.16	5.2	4.5	-	210
130 Elektra	3.111	0.21	22.9	5.0*	-	173*
139 Juewa	2.783	0.17	10.9	4.0	1.30	163
140 Siwa	2.732	0.21	3.2	4.7	-	103
141 Lumen	2.665	0.21	11.9	2.8	1.75	133
145 Adeona	2.674	0.14	12.6	-	-	-
163 Erigone	2.367	0.19	4.8	-	-	-
166 Rhodope	2.686	0.21	12.0	-	-	-
176 Iduna	3.168	0.18	22.7	-	-	-

192	Nausikaa	2.403	0.25	6.9	16.5	-	94
194	Prokne	2.616	0.24	18.5	2.7	-	191
210	Isabella	2.722	0.12	5.3	-	-	-
213	Lilaea	2.754	0.15	6.8	-	-	-
221	Eos	3.014	0.10	10.8	-	-	-
230	Athamantis	2.383	0.06	9.4	10.0	-	121
324	Bamberga	2.682	0.34	11.2	3.2	1.45	246
335	Roberta	2.473	0.18	5.1	-	-	-
349	Dembowska	2.925	0.09	8.3	26.0	0.35	144
354	Eleonora	2.797	0.12	18.4	14.8	0.55	153
433	Eros	1.458	0.24	10.8	17.4	0.70	23
462	Eriphyla	2.872	0.09	3.2	-	-	-
481	Emita	2.743	0.16	9.8	-	-	-
505	Cava	2.686	0.24	9.8	-	-	-
511	Davida	3.187	0.17	15.8	3.7	1.70	323
532	Herculina	2.771	0.17	16.3	10.0	0.75	150
554	Peraga	2.375	0.15	2.9	3.9*	-	101*
654	Zelinda	2.297	0.23	18.2	3.2*	-	128*
674	Rachele	2.921	0.20	13.6	-	-	-
704	Interamnia	3.057	0.15	17.3	3.3	-	350
887	Alinda	2.516	0.54	9.1	16.6	0.75	4
1566	Icarus	1.078	0.83	23.0	16.6*		1*
1685	Toro	1.368	0.44	9.4	12.4*		3*

a) Albedos and diameters by the radiometric technique as summarized by Morrison (1977c). Those indicated by an asterisk are regarded as of marginal certainty.

b) Depth of the negative branch of the phase-polarization curve (P_{min}) as summarized by Chapman et al. (1975).

TABLE 3

Asteroid Surface Materials: Characterizations

Asteroid	Spectral Type	Mineral Assemblage (a)	Meteoritic Analogue (b)	CMZ Type (c)
1 Ceres	F	Sil(O), Opq(M)*	C4 (Karoonda)	C (C*)
2 Pallas	F	Sil(O), Opq(M)*	C4 (Karoonda)	U (C*)
3 Juno	RA-1	NiFe ∿ (Ol∿Px)	Ol-Px Stony-Iron	S
4 Vesta	A	Cpx	Eucrite	U
6 Hebe	RA-2	NiFe>Cpx	Mesosiderite	S
7 Iris	RA-1	NiFe, Ol, Px	Ol-Px Stony-Iron	S
8 Flora	RA-2	NiFe≳ Cpx	Mesosiderite	S
9 Metis	RF	Nife, (Sil(E))	E. Chon, Iron	S
10 Hygiea	TB	Phy, Opq(C)	Cl-C2 (CI-CM)	C (C*)
11 Parthenope	RF	NiFe, (Sil(E))	E. Chon, Iron	S
14 Irene	RA-3	NiFe, Px	Px Stony-Iron	S
15 Eunomia	RA-1	NiFe ∿ (Ol>>Px)	Ol-Px Stony-Iron	S
16 Psyche	RR	NiFe, Sil(E)	E. Chon, Iron	M
17 Thetis	RA-2	NiFe, Cpx	Mesosiderite	S
18 Melpomene	TE	Sil(O), Opq(C)	C3	S
19 Fortuna	TA	Phy, Opq(C)	Cl-C2 (CI-CM)	C
25 Phocaea	RA-2	NiFe, Px, Cpx	Px Stony-Iron	S
27 Euterpe	RA-2	NiFe, Px, Cpx	Px Stony-Iron	S
28 Bellona	TE	Sil(O), Opq(C)	C3	S
30 Urania	RF(?)	----	----	S
39 Laetitia	Ra-1	NiFe ∿ (Ol∿Px)	Ol-Px Stony-Iron	S
40 Harmonia	RA-2	NiFe > Px	Mesosiderite	S
48 Doris	TA	Phy, Opq(C)	Cl-C2 (CI-CM)	C
51 Nemausa	TC	Phy, Opq(C)	Cl-C2 (CI-CM)	C
52 Europa	TA	Phy, Opq(C)	Cl-C2 (CI-CM)	C
58 Concordia	TABC	Phy, Opq(C)	Cl-C2 (CI-CM)	C
63 Ausonia	RA-3	NiFe, Px	Px Stony-Iron	S
79 Eurynome	RA-2	NiFe ∿ Cpx	Mesosiderite	S
80 Sappho	TD	Sil(O), Opq(C)	C3	U
82 Alkmene	TE	Sil(O), Opq(C)	C3	S
85 Io	F	Sil(O), Opq(M)*	C4 (Karoonda)	C
88 Thisbe	TB	Phy , Opq(C)	Cl-C2 (CI-CM)	C
130 Elektra	TABC	Phy, Opq(C)	Cl-C2 (CI-CM)	U
139 Juewa	TB	Phy, Opq(C)	Cl-C2 (CI-CM)	C
140 Siwa	RR	NiFe, Sil(E)	E. Chon, Iron	C
141 Lumen	TA	Phy, Opq(C)	Cl-C2 (CI-CM)	C

Asteroid	Spectral Type	Mineral Assemblage (a)	Meteoritic Analogue (b)	CMZ Type (c)
145 Adeona	TA	Phy, Opq(C)	C1-C2 (CI-CM)	C
163 Erigone	TA	Phy, Opq(C)	C1-C2 (CI-CM)	C
166 Rhodope	TC	Phy, Opq(C)	C1-C2 (CI-CM)	U
176 Iduna	TA	Phy, Opq(C)	C1-C2 (CI-CM)	C
192 Nausikaa	TA-2	NiFe∿(Px>Ol)	Px-Ol Stony-Iron	S
194 Prokne	TC	Phy, Opq(C)	C1-C2 (CI-CM)	C
210 Isabella	TABC	Phy, Opq(C)	C1-C2 (CI-CM)	C
213 Lilaea	F	Sil(O), Opq(M)*	C4 (Karoonda)	C
221 Eos	TD	Sil(O), Opq(C)	C3	U
230 Athamantis	RF	NiFe, (Sil(E))	E. Chon., Iron	S
324 Bamberga	TABC	Phy, Opq(C)	C1-C2 (CI-CM)	C
335 Roberta	F	Sil(O), Opq(M)*	C4 (Karoonda)	U
349 Dembowska	A	Ol, (NiFe)	Ol. Achondrite	O
354 Eleonora	RA-1	NiFe∿Ol	Pallasite	S
433 Eros (d)	--	Px∿Ol, NiFe	H Chondrite	S
462 Eriphyla	RF (?)	----	----	S
481 Emita	TABC	Phy, Opq(C)	C1-C2 (CI-CM)	C
505 Cava	TA	Phy, Opq(C)	C1-C2 (CI-CM)	C
511 Davida	TB	Phy, Opq(C)	C1-C2 (CI-CM)	C (C*)
532 Herculina	TE	Sil(O), Opq(C)	C3	S
554 Peraga	TA	Phy, Opq(C)	C1-C2 (CI-CM)	C
654 Zelinda	TC	Phy, Opq(C)	C1-C2 (CI-CM)	C
674 Rachele	RF (?)	----	----	S
704 Interamnia	F	Sil(O), Opq(M)*	C4 (Karoonda)	U
887 Alinda	TD	Sil(O), Opq(C)	C3	S
1685 Toro (e)	--	Px, Ol	L Chondrite(?)	U

a) Mineral assemblage of asteroid surface material determined from interpretation of reflectance spectra: NiFe (nickel-iron metal); Ol (Olivine); Px (Pyroxene, generally low calcium orthopyroxene); Cpx (Clinopyroxene, calcic pyroxene); Sil(O) (Mafic silicate, most probably olivine); Sil(E) (Spectrally neutral silicate, most probably iron-free pyroxene, (enstatite),or iron-free olivine (forsterite); Phy (Phyllosilicate, layer lattice silicate, meteoritic clay mineral, generally hydrated, unleached with abundant subequal Fe^{2+} and Fe^{3+} cations); Opq(C) (Opaque phase, most probably carbon or carbon compounds); Opq(M) (Opaque phase, most probably magnetite or related opaque oxide).

Mathematical symbols ('>', greater than; '>>', much greater than; '$\sim$' approximately equal) are used to indicate relative abundance of mineral phases. In cases where abundance is undetermined, order is of decreasing apparent abundance.

Asteroidal spectra which are ambiguous between 'TDE' and 'RF' are not characterized mineralogically.

b) Meteoritic analogues are examples of meteorite types with similar mineralogy but genetic links are not established. For example, objects designated as analogous to mesosiderites could be a mechanical metal-basaltic achondritic mixture.

c) Asteroidal spectral type as defined by Chapman, et al. (1975) and as summarized by Zellner and Bowell (1977). C* designation from Chapman (1976).

d) Pieters et al., 1976

e) Chapman et al., 1973b

FIGURE CAPTIONS

Figure 1 - Spectral albedo curves for three types of meteoritic assemblages: (1) Eucrite (pyroxene + plagioclase feldspar), (2) C3O or CO chondrite (olivine + minor carbon) and (3) C2 or CM chondrite (clay mineral + carbon) with the mineralogically significant spectral features indicated: A = pyroxene (absorption feature), B = plagioclase feldspar, C = olivine, D = Fe^{2+} - Fe^{3+} or Fe^{3+} electronic absorption feature, E = H_2O or OH, and F = 'break-in slope' or 'elbow' between visible-IR and blue-UV spectral regions. The position, bandpass (indicated by tic-marks) and wavelength coverage of the several observation data sets for asteroids.

Figure 2 - Typical spectral reflectance curves for the various asteroid spectral groups: (A) 'RA-1' - 3 Juno, (B) 'RA-2' - 8 Flora, (C) 'RR' - 16 Psyche, (D) 'RF' - 9 Metis, (E) 'A' - 4 Vesta, (F) 'A' - 349 Dembowska, (G) 'F' - 1 Ceres, (H) 'TA' - 141 Lumen, (I) 'TB' - 10 Hygiea, (J) 'TC' - 51 Nemausa, (K) 'TD' - 80 Sappho and (L) 'TE' - 532 Herculina. Spectral curve for each asteroid is displayed in several formats: Left - normalized reflectance vs. wavelength (μm), Center - normalized reflectance vs. energy (wavenumber, cm^{-1}) and Right - difference between spectral curve and a linear 'continuum' fitted through 0.43μm and 0.73μm points.

Figure 3 - Normalized spectral reflectance curves for the range of meteorite types.

Figure 4 - Spectral reflectance curves of a range of meteoritic mineral assemblages: (A) pyroxene + plagioclase feldspar (.50, .50) - Eucrite, (B) olivine + pyroxene + metal (.45, .40, .10) - L6 chondrite, (C) olivine (.90) - Olivine achondrite, (D) NiFe metal (1.00) - iron meteorite, (E) olivine + pyroxene + metal (.45, .40, .10) - L4 chondrite, (F) enstatite (Fs_o) pyroxene + NiFe metal (.75, .20) - E4 chondrite, (G) enstatite (Fs_o) pyroxene + NiFe metal (.75, .20) - E6 chondrite, (H) enstatite (Fs_o) pyroxene (1.00) - enstatite achondrite or aubrite, (I) clay mineral + carbon (.90, .03) - C2 or CM chondrite, (J) olivine + carbon (.90, .01) - C30 or CO chondrite, and (K) olivine + magnetite (.80, .10) - C4 or C5 chondrite. Format is the same as Figure 2.

Figure 5 - (A) Plot of olivine-pyroxene ratio for meteorites versus half-width at half-height for long wavelength wing of 1μ absorption feature.

(B) Plot of normalized absorption band contrast $[\sim(R_{0.75\mu m} - R_{0.95\mu m})/R_{0.56\mu m}]$ versus normalized continuum contrast $[\sim(R_{0.75\mu m} - R_{0.35\mu m})/R_{0.56\mu m}]$ for a variety of meteoritic spectra (e.g., L6, C30, etc.) and several asteroids which exhibit distinct absorption features. Asteroids indicated by circled numbers. Positions above field of meteorites indicates presence of reddening agent (e.g., NiFe metal) in surface material.

Figure 6 - Normalized spectral reflectance curves of asteroids discussed in text. Format is same as Figures 2 and 4.

(A) Spectral type RA-1: 3 Juno, 7 Iris, 15 Eunomia, 39 Laetitia and 354 Eleonara.

(B) Spectral type RA-2: 8 Flora, 6 Hebe, 17 Thetis, 40 Harmonia, 79 Eurynome, 192 Nausikaa, 25 Phacaea and 27 Euterpe.

(C) Spectral type RA-3: 14 Irene and 63 Ausonia.

(D) Spectral type RR: 16 Psyche and 140 Siwa.

(E) Spectral type RF: 9 Metis, 11 Parthenope, 230 Athamantis; possible RF: 30 Urania, 462 Eriphyla and 674 Rachele.

(F) Spectral type A: 4 Vesta and 349 Dembowska.

(G) Spectral type F: 1 Ceres, 85 Io, 335 Roberta, 2 Pallas, 213 Lilaea and 704 Interamnia.

(H) Spectral type TA: 19 Fortuna, 48 Doris, 52 Europa, 141 Lumen, 145 Adeona, 163 Erigone, 176 Iduna, 505 Cava and 554 Peraga.

(I) Spectral type TB: 10 Hygiea, 88 Thisbe, 139 Juewa and 511 Davida.

(J) Spectral type TC: 51 Nemausa, 166 Rhodope, 194 Prokne and 654 Zelinda.

(K) Spectral types TA-TB-TC: 58 Concordia, 130 Elektra, 210 Isabella, 324 Bamberga and 481 Emita.

(L) Spectral type TD: 80 Sappho, 221 Eos and 887 Alinda.

(M) Spectral type TE: 18 Melpomene, 28 Bellona, 82 Alkmene and 532 Herculina.

Figure 7 - Schematic representation of suppression of spectral contrast (continuum and absorption feature) and albedo with increasing abundance of an opaque or spectral blocking phase with (A) a relative low optical density silicate (e.g., olivine) and (B) a high optical density silicate (e.g., Fe^{2+}-Fe^{3+} meteoritic clay mineral). Particular attention is directed to the relationship between the position of the break-in-slope (BIS) and the albedo of each mixture as a function of the optical density of the non-opaque phase.

Figure 8 - Distribution of asteroid surface material groups as a function of the semi-major axis of their orbits (uncorrected for observational bias): (A) The members of each spectral group discussed in the text. (B) Groups with diverse thermal histories (Primitive - apparently unaltered by any post-accretionary heating events - TA-TB-TC, TD-TE and Thermalized - apparently heated and modified or melted and differentiated by some strong post-accretionary heating episode) versus the distribution of the first 400 numbered asteroids (as a histogram per 0.02 AU).

Figure 9 - Distribution of asteroid surface material groups as a function of asteroid diameters (uncorrected for observational bias). Primitive materials (TA-TB-TC and TD-TE) are compared to Thermalized materials (RA-1, RA-2, RA-3, A, F) to provide an indication of the upper limits to the size distributions of the original populations.

FIGURE 1

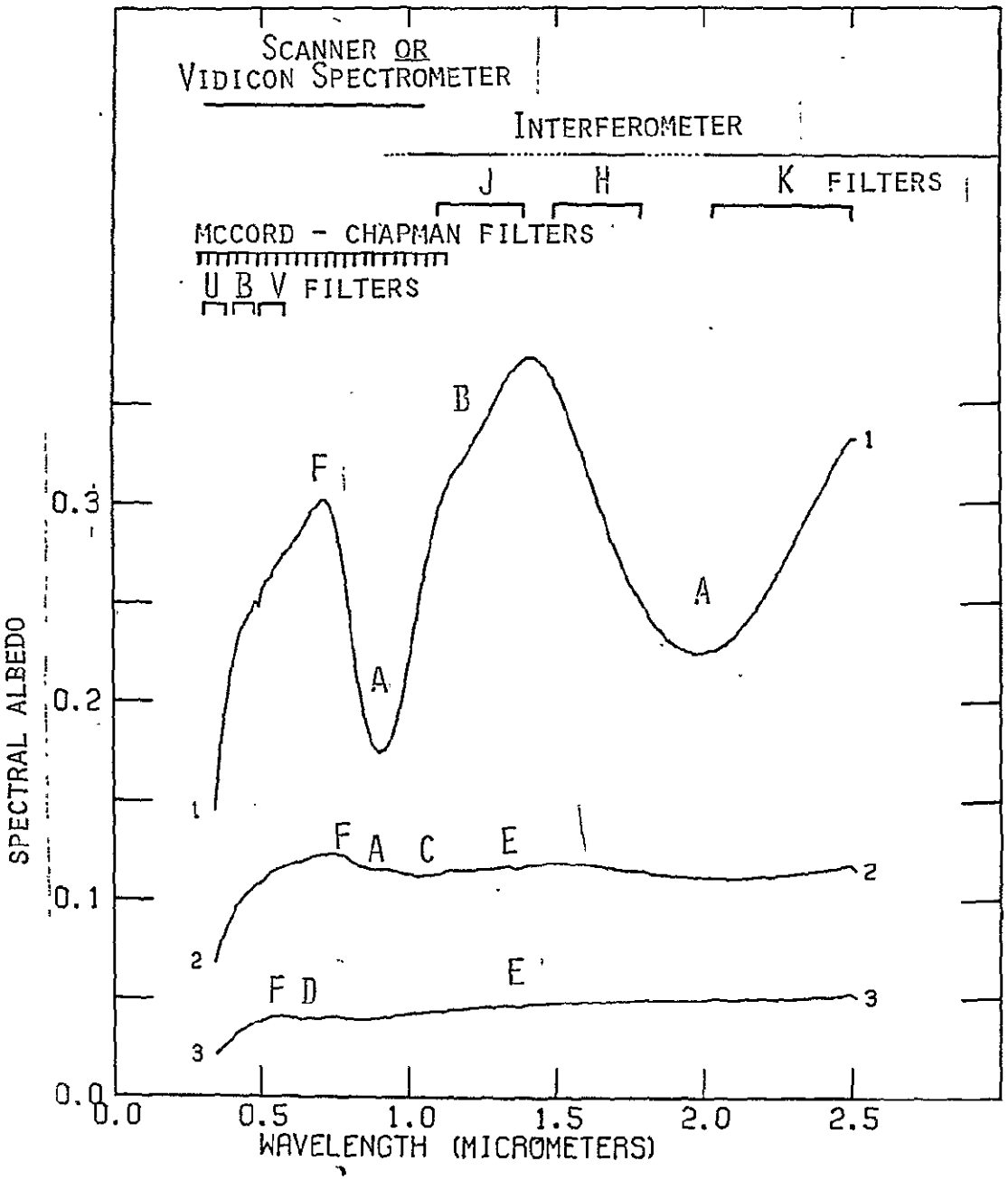

FIGURE 2

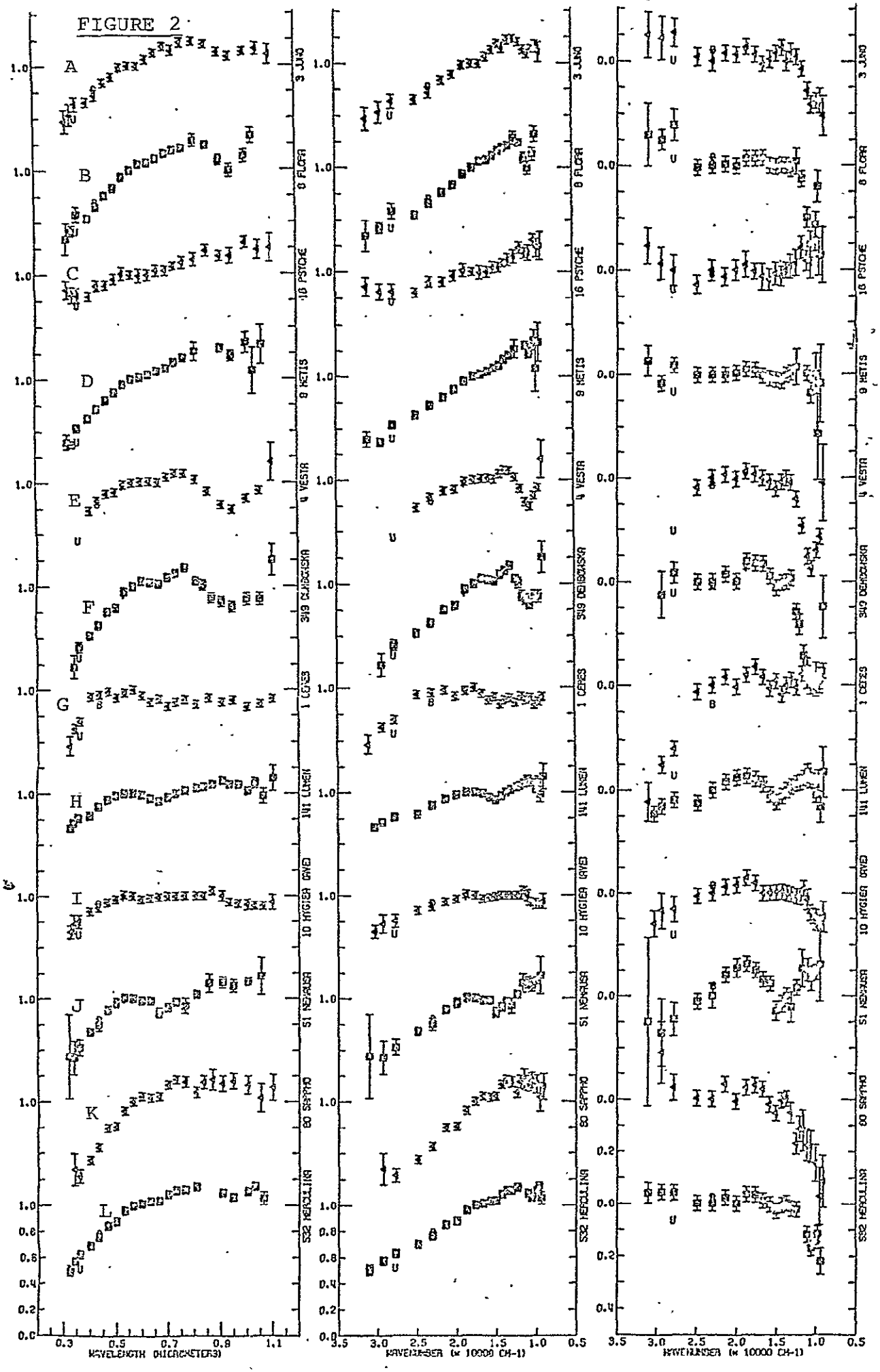
A
B
C
D
E
F
G
H
I
J
K
L
3 JUNO
8 FLORA
16 PSYCHE
9 METIS
4 VESTA
349 DEMBOWSKA
1 CERES
141 LUMEN
10 HYGIEA (2)
51 NEMAUSA
80 SAPPHO
532 HERCULINA
WAVELENGTH (MICROMETERS)
WAVENUMBER (x 10000 CM-1)

FIGURE 3

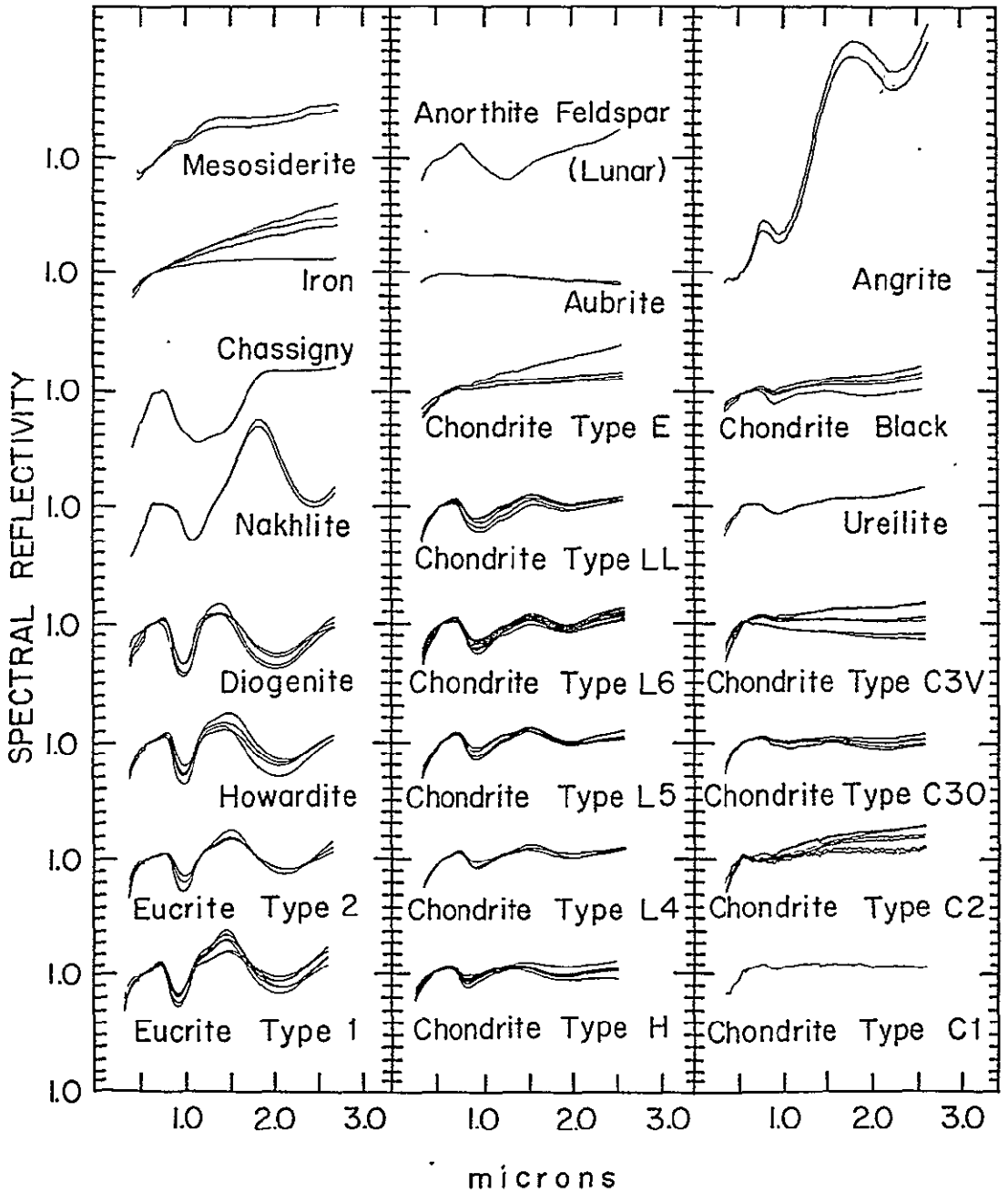

FIGURE 4

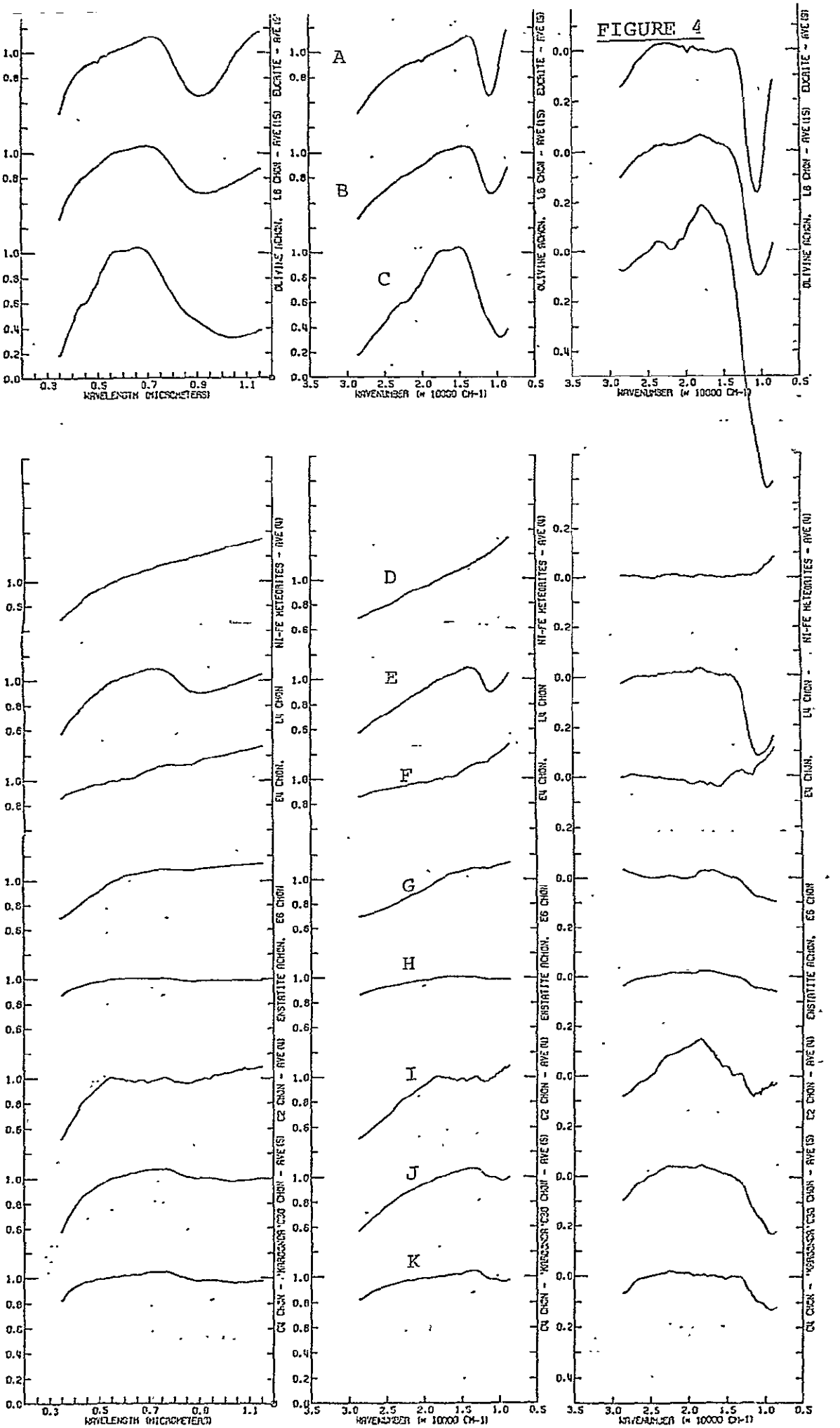
A
B
C
D
E
F
G
H
I
J
K
WAVELENGTH (MICROMETERS)
WAVENUMBER (x 10000 CM-1)
OLIVINE ACHON. L6 CHON - AVE(S) EUCRITE - AVE(S)
EU CHON. L4 CHON - AVE(N) NI-FE METEORITES - AVE(N)
C4 CHON - "KARGANOR" C30 CHON - AVE(S) C2 CHON - AVE(N) ENSTATITE ACHON. E6 CHON

FIGURE 5A.

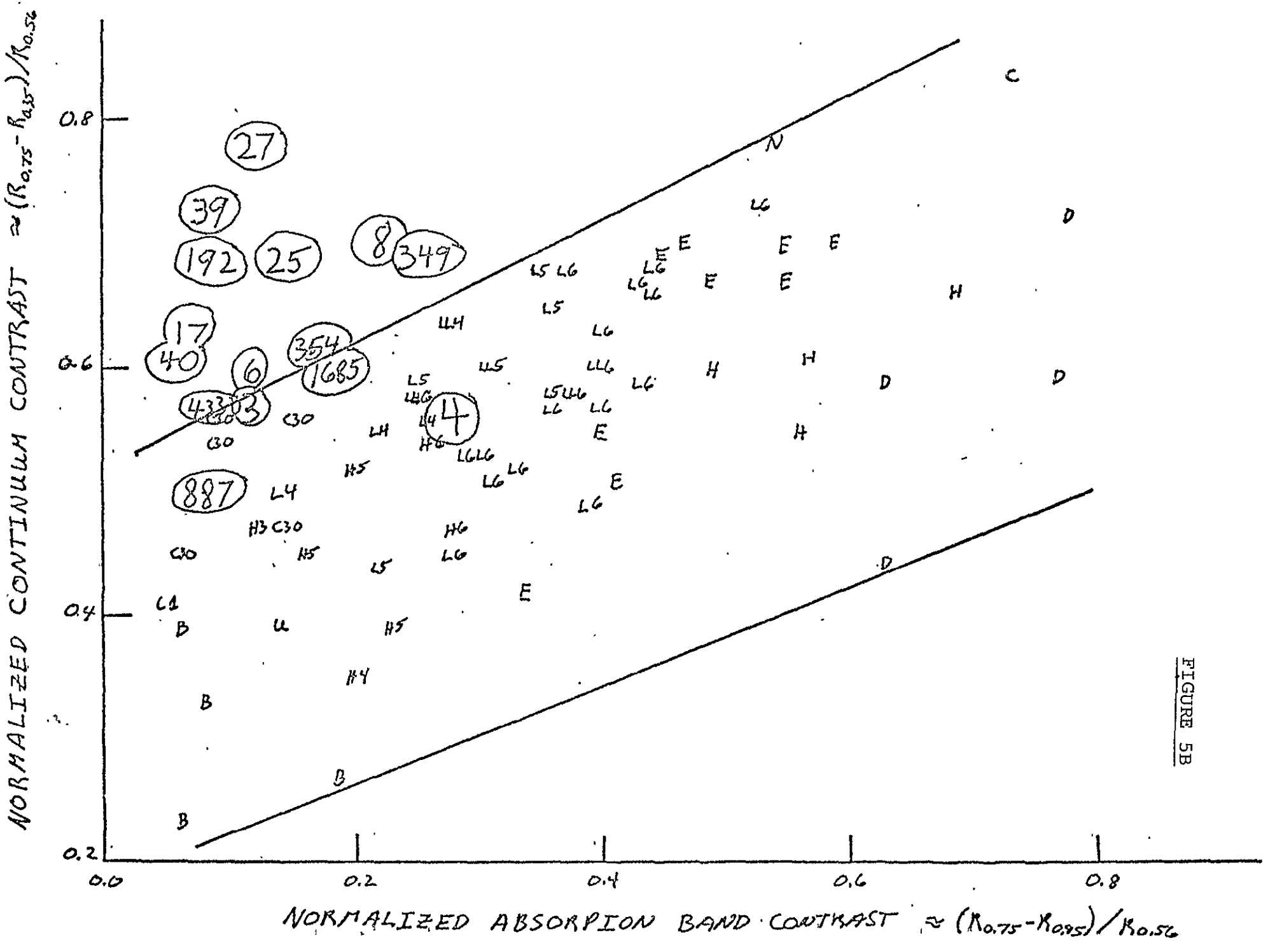
NORMALIZED CONTINUUM CONTRAST ≈ $(R_{0.75} - R_{0.45})/R_{0.56}$
0.8
0.6
0.4
0.2
0.0
0.2
0.4
0.6
0.8
NORMALIZED ABSORPION BAND CONTRAST ≈ $(R_{0.75} - R_{0.95})/R_{0.56}$
27
39
192
25
8
349
17
40
6
354
1685
433
3
4
887

FIGURE 5B

FIGURE 6A

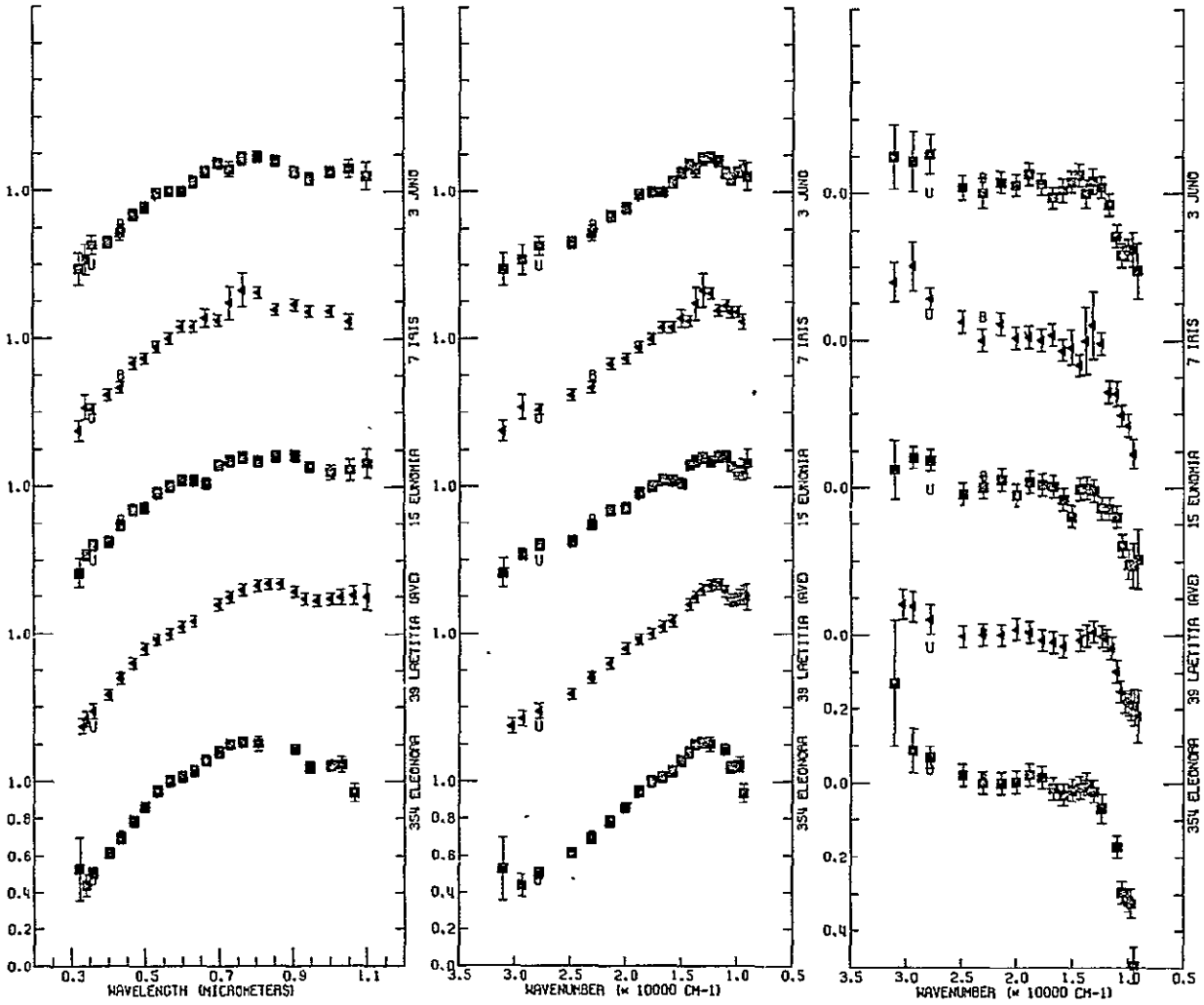

FIGURE 6B

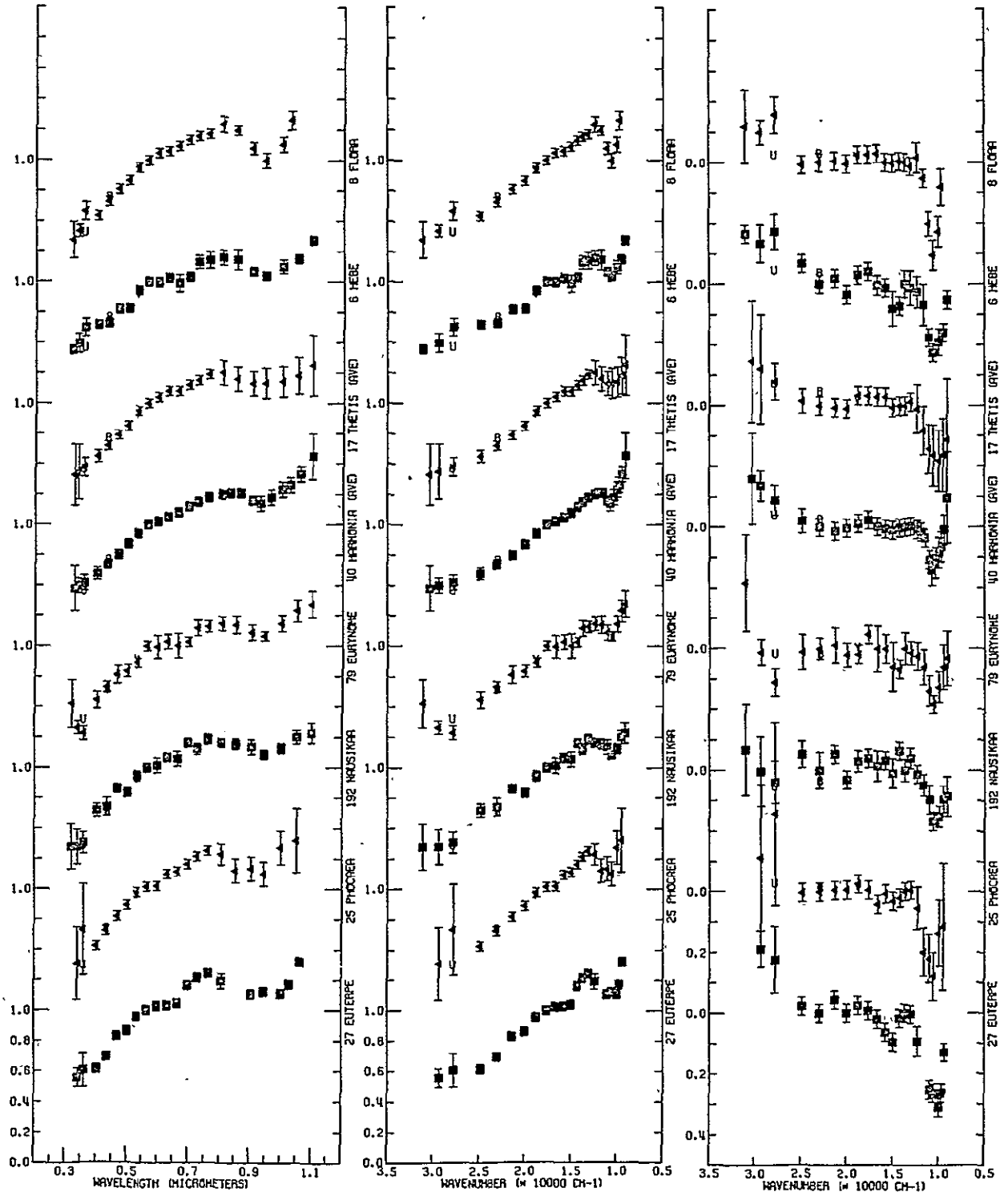
8 FLORA
6 HEBE
17 THETIS (AVE)
40 HARMONIA (AVE)
79 EURYNOME
192 NAUSIKAA
25 PHOCAEA
27 EUTERPE
WAVELENGTH (MICROMETERS)
WAVENUMBER (* 10000 CM-1)
WAVENUMBER (* 10000 CM-1)

FIGURE 6C

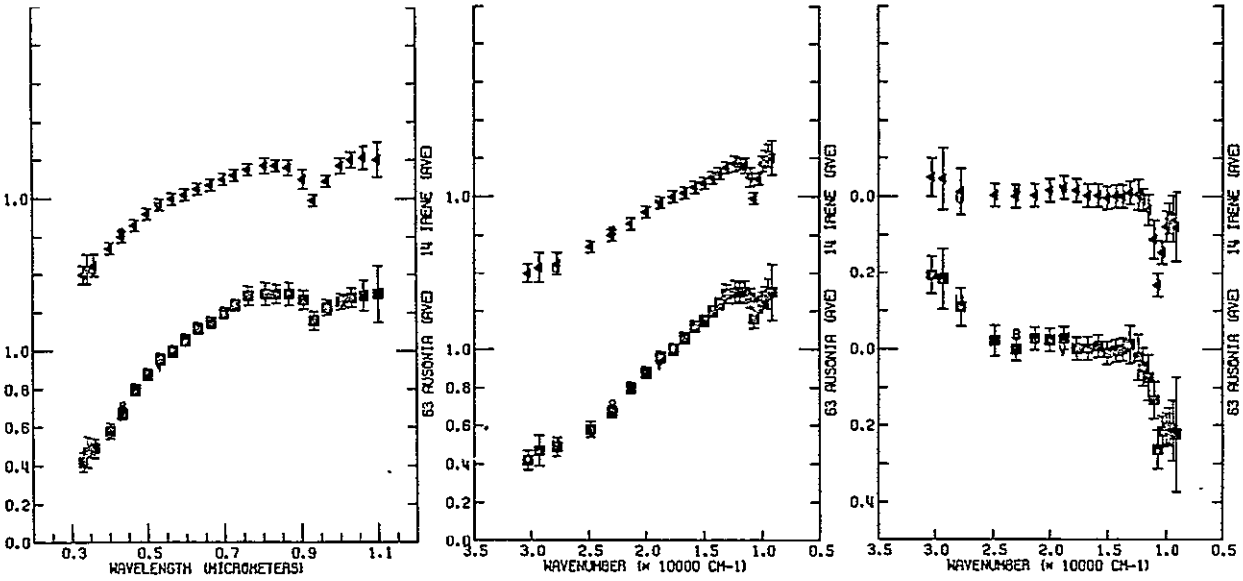

FIGURE 6D

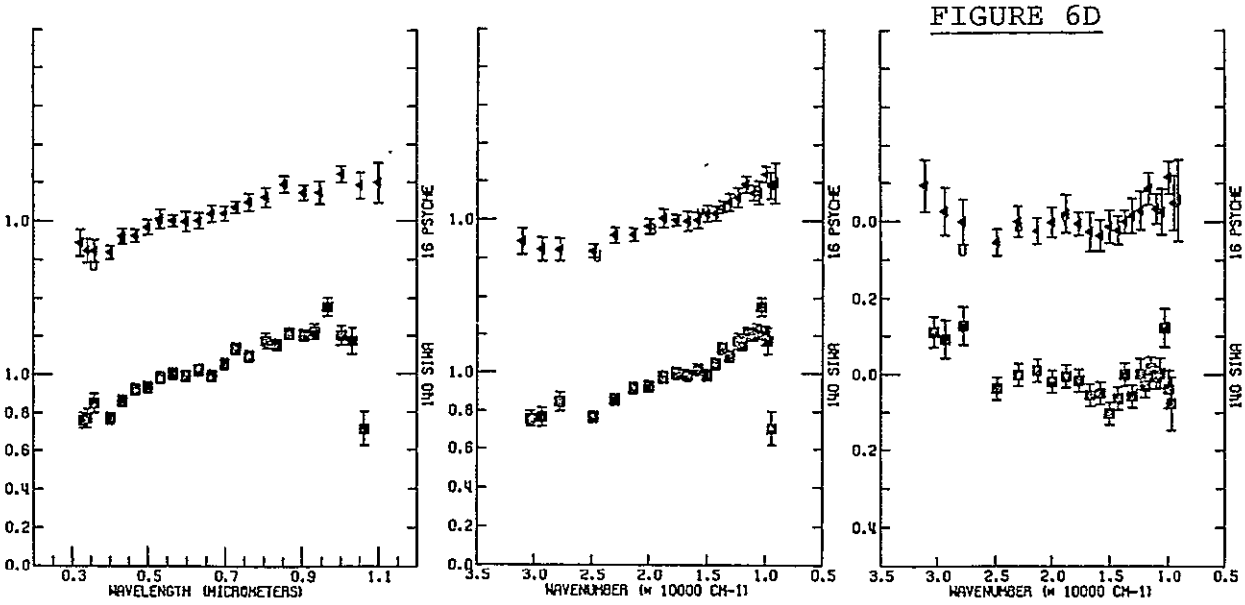

FIGURE 6E

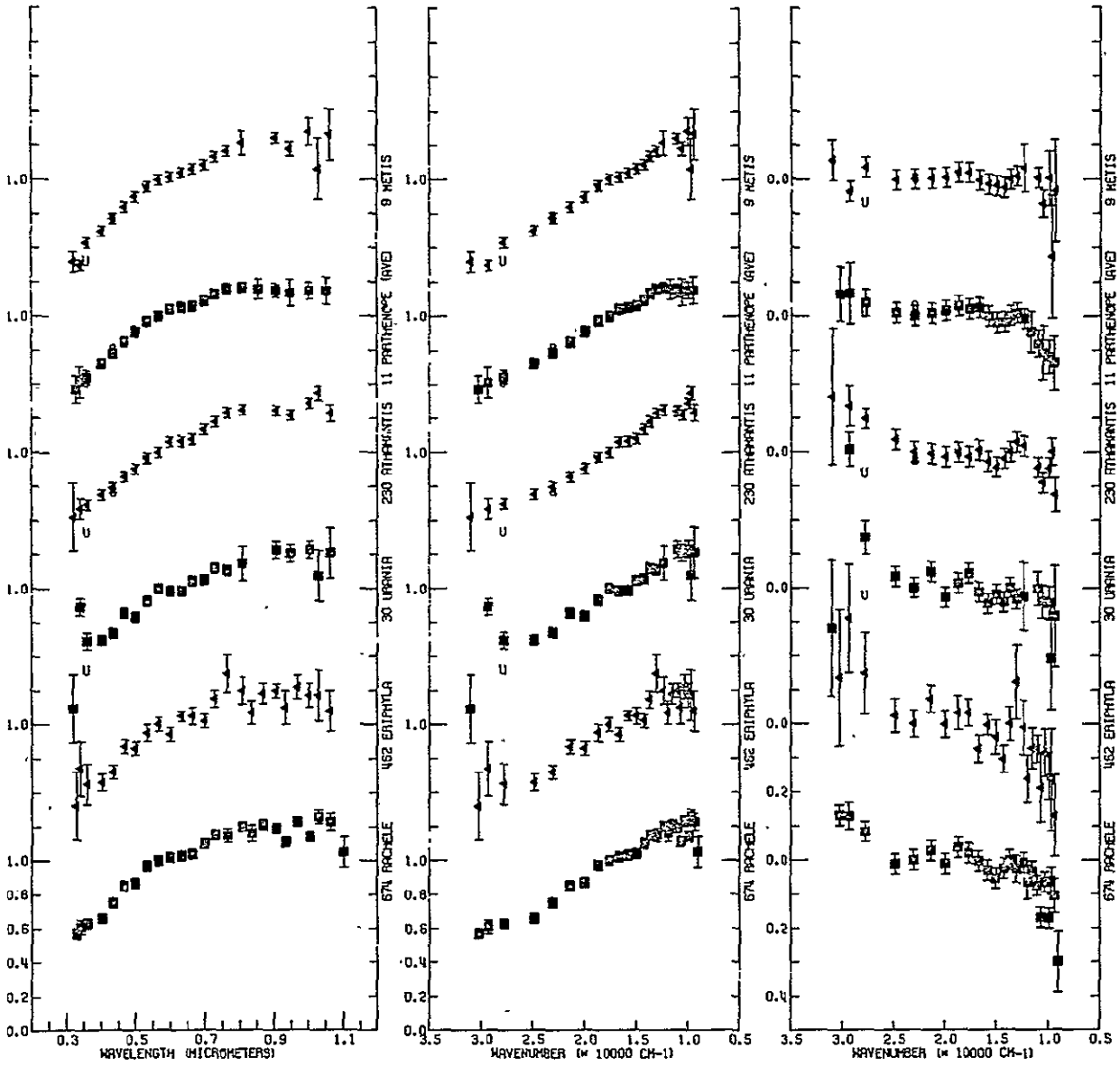

FIGURE 6F

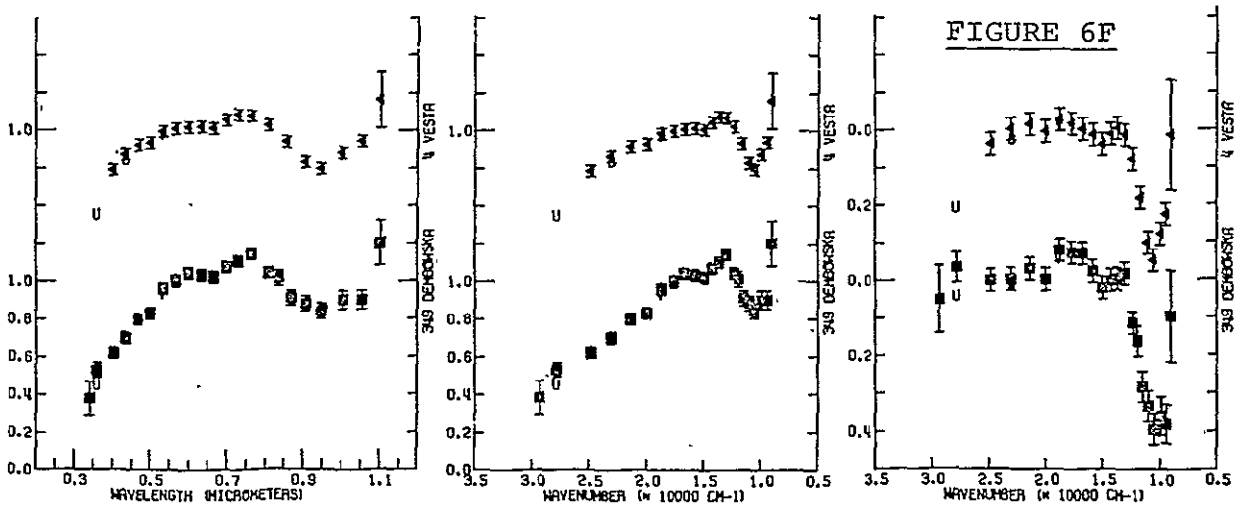

FIGURE 6G

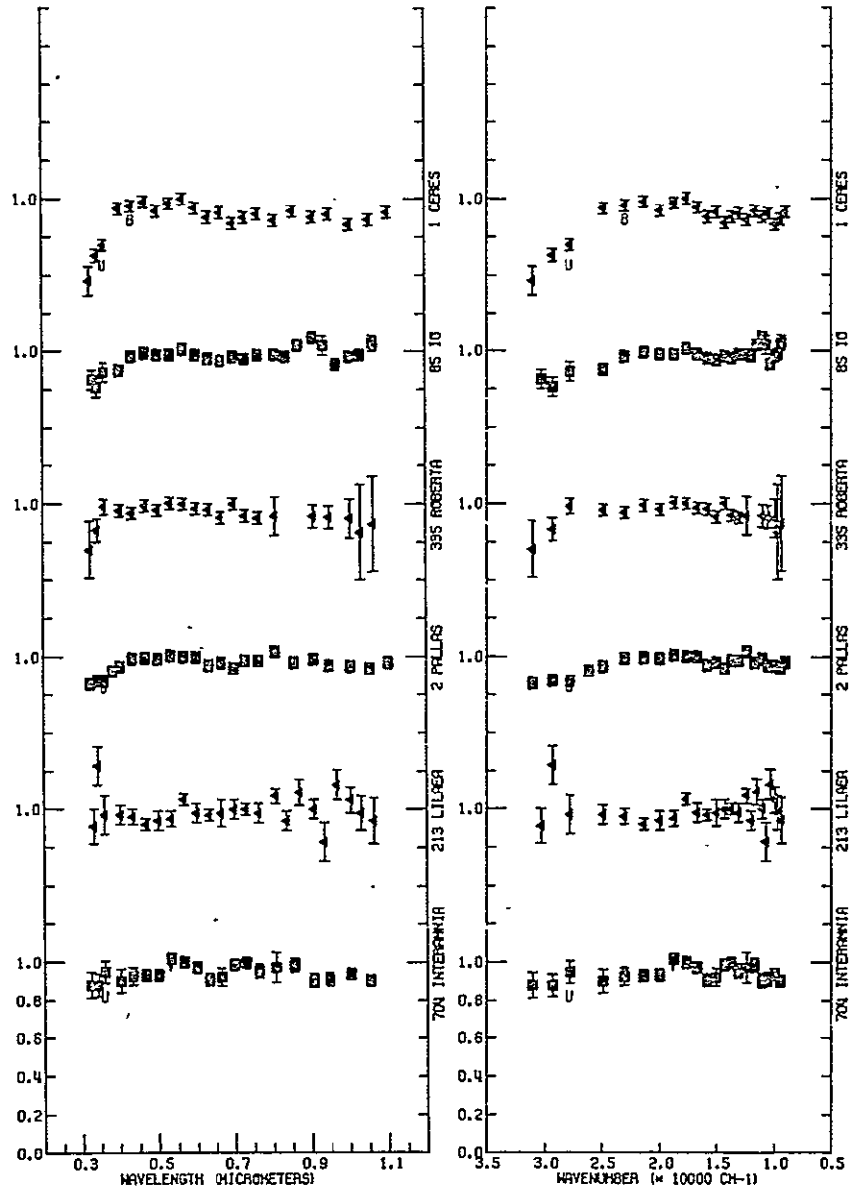

FIGURE .6H

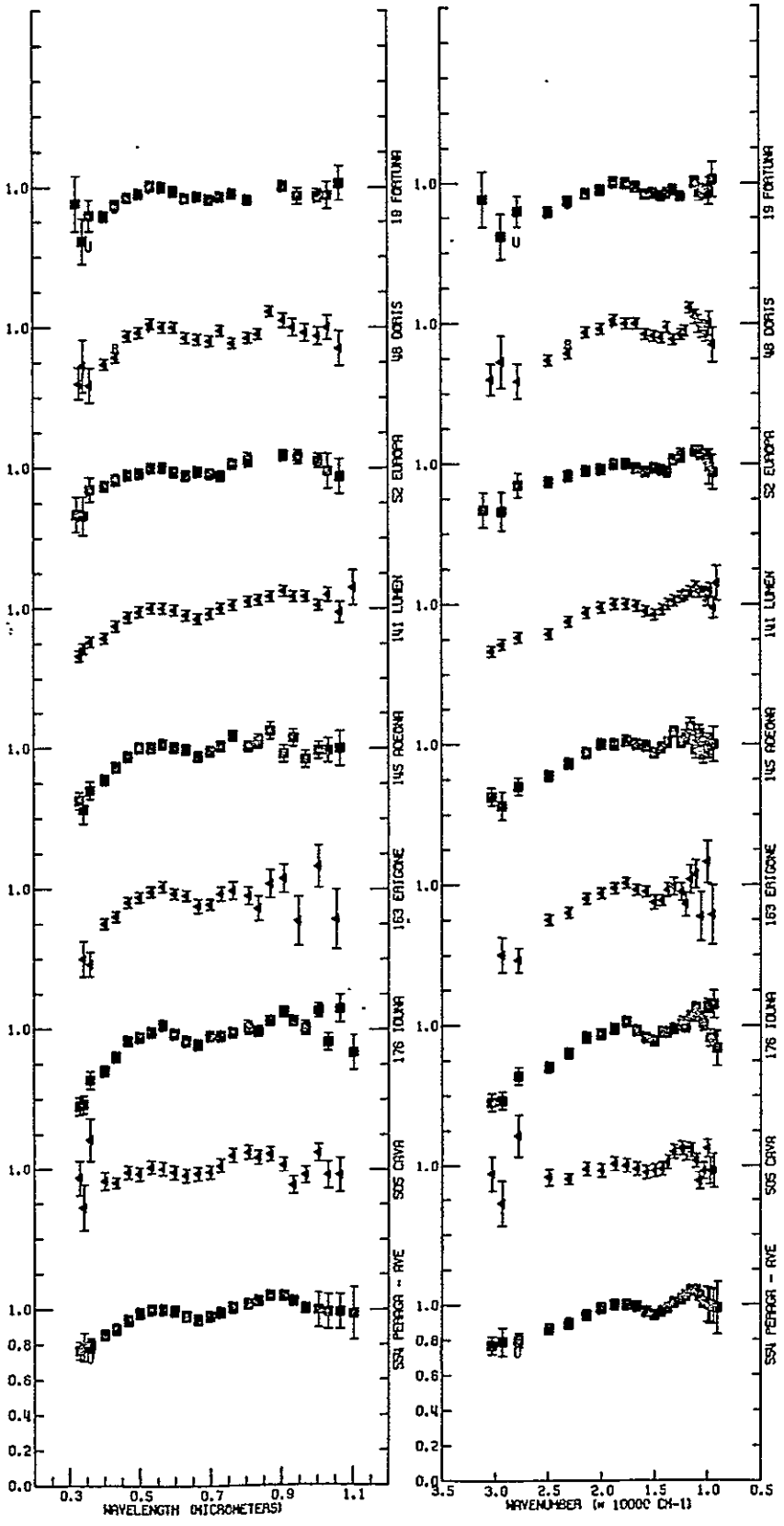
19 FORTUNA
U
48 DORIS
B
52 EUROPA
141 LUMEN
145 ADEONA
163 ERIGONE
176 IDUNA
505 CAVA
SSN PERHGR - RVE
WAVELENGTH (MICROMETERS)
WAVENUMBER (* 10000 CM-1)

FIGURE 6I

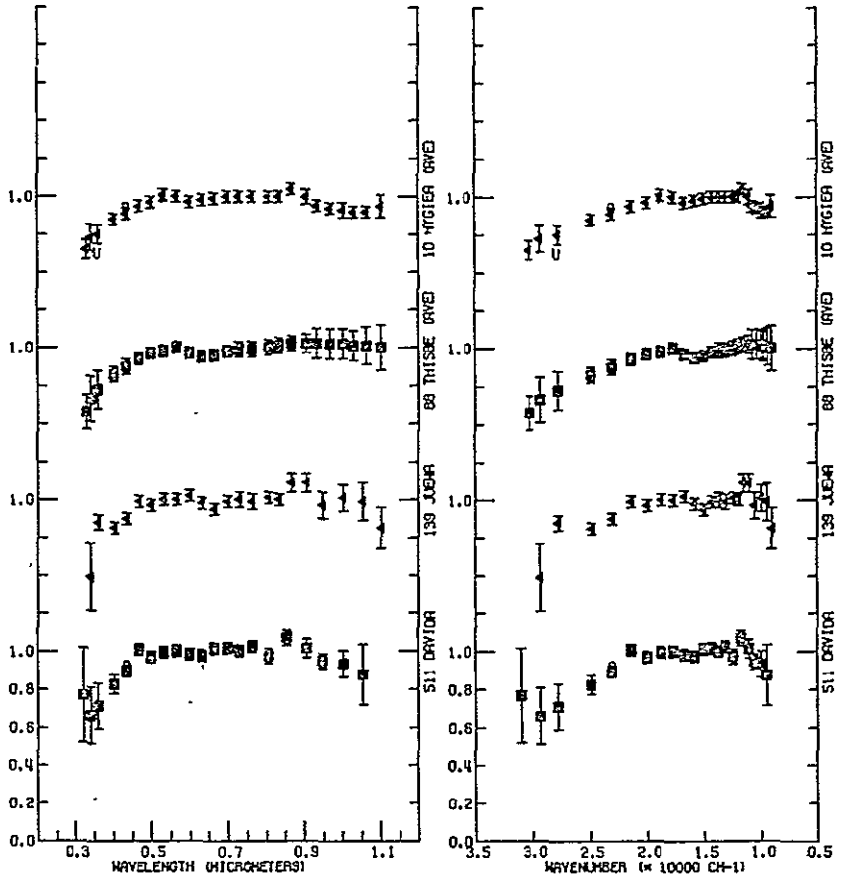

FIGURE 6J

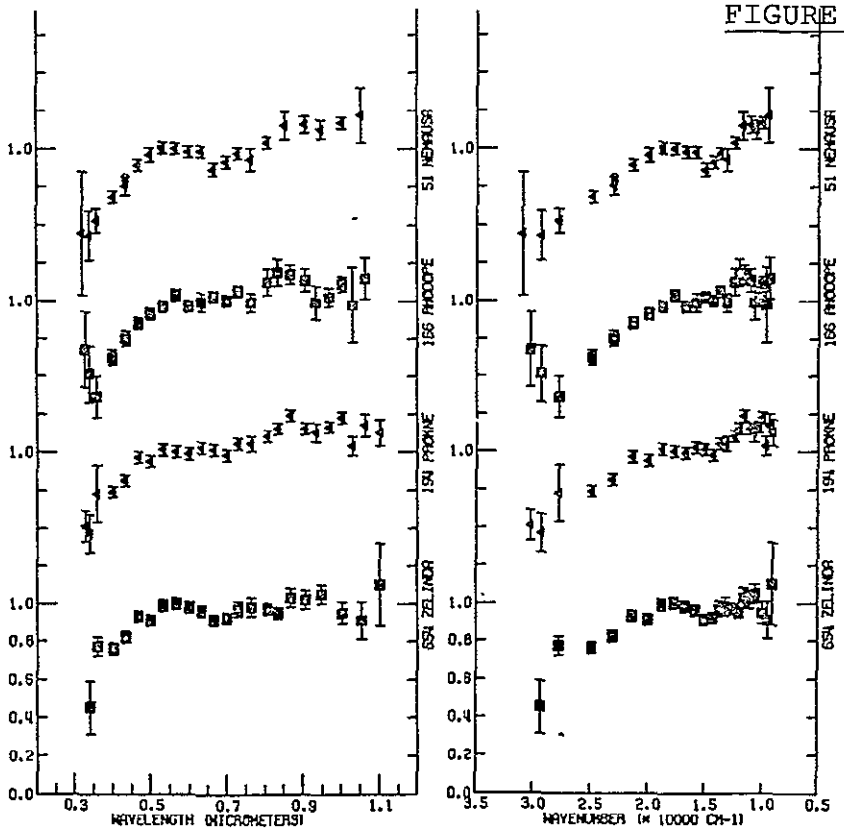

FIGURE 6K

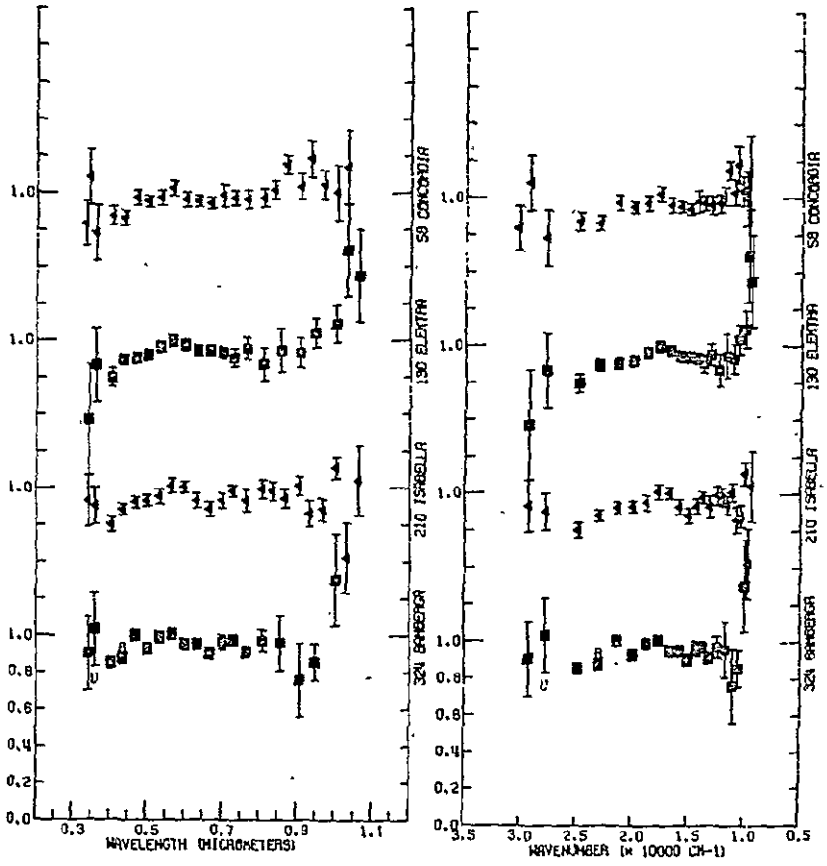
59 CONCORDIA
130 ELEKTRA
210 ISABELLA
324 BAHAMIAN
1.0
0.8
0.6
0.4
0.2
0.0
0.3
0.5
0.7
0.9
1.1
WAVELENGTH (MICROMETERS)
3.5
3.0
2.5
2.0
1.5
1.0
0.5
WAVENUMBER (* 10000 (CM-1)

FIGURE 6L

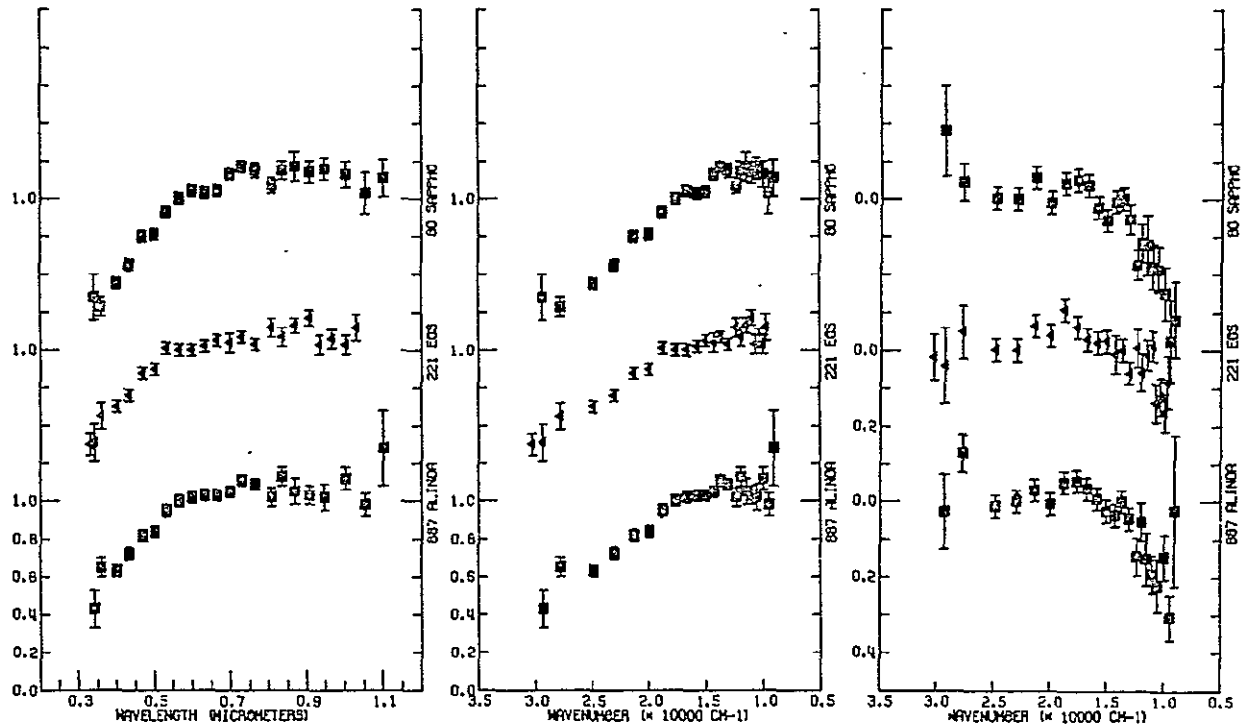

FIGURE 6M

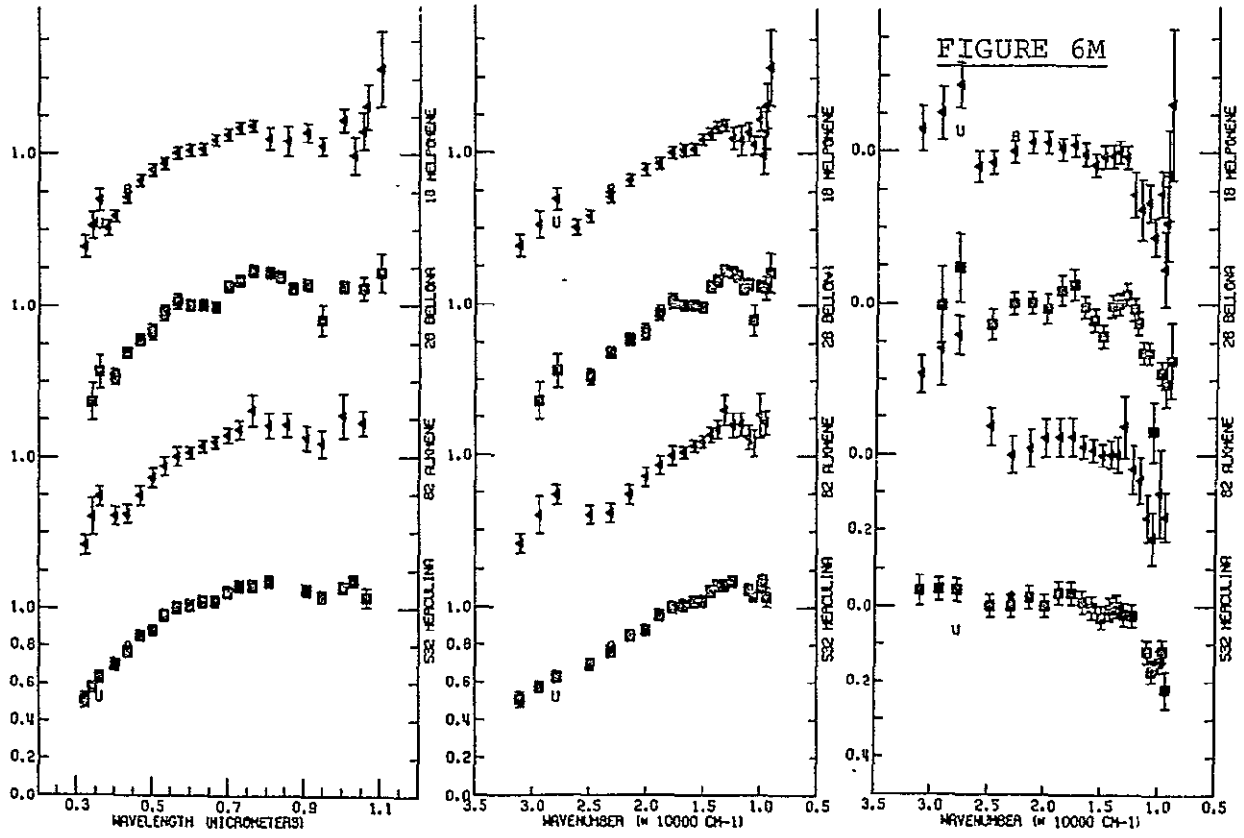

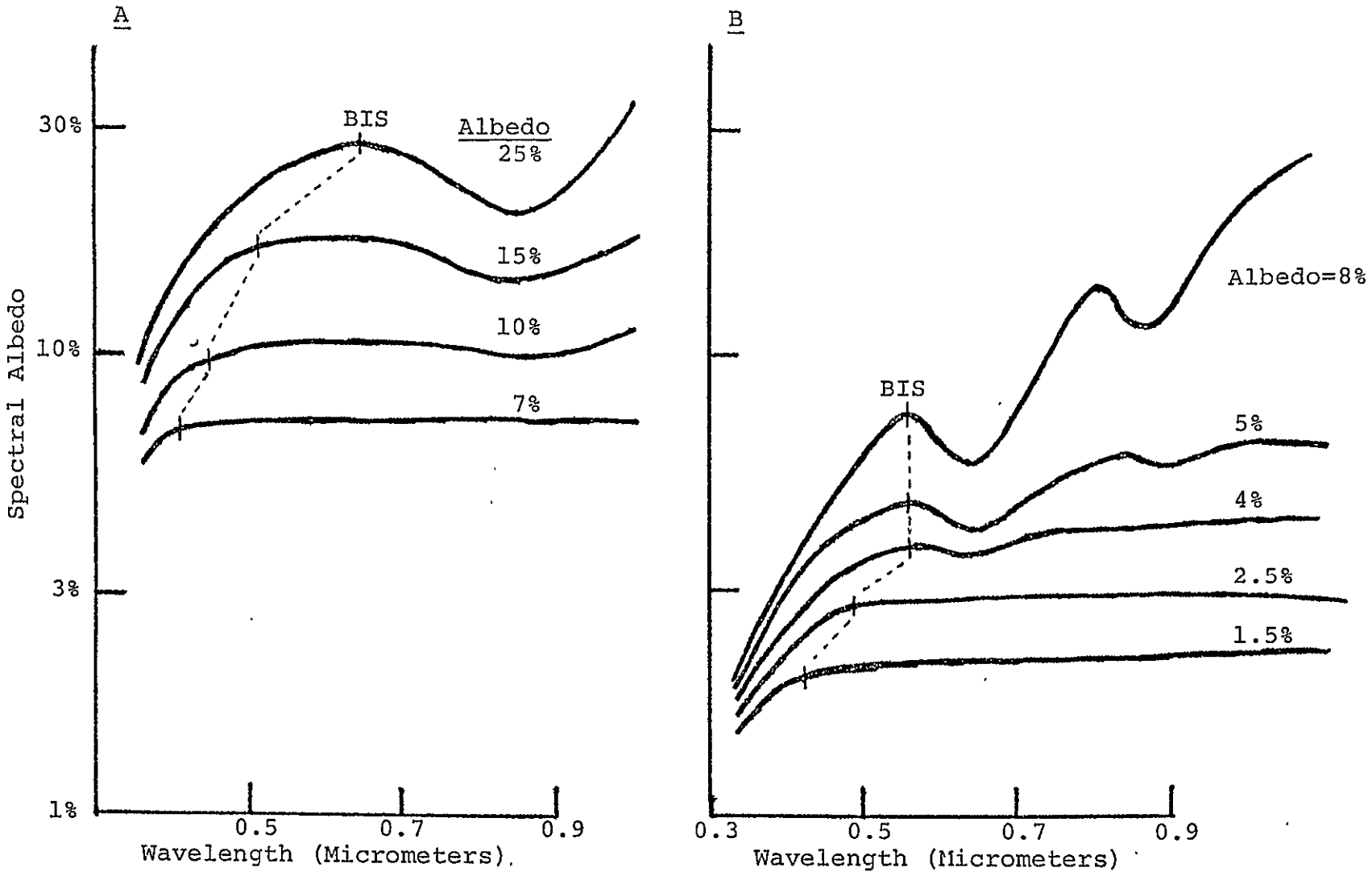
A
B
30%
10%
3%
1%
Spectral Albedo
BIS
Albedo
25%
15%
10%
7%
0.5
0.7
0.9
Wavelength (Micrometers)
BIS
Albedo=8%
5%
4%
2.5%
1.5%
0.3
0.5
0.7
0.9
Wavelength (Micrometers)

Figure 7

FIGURE 8A

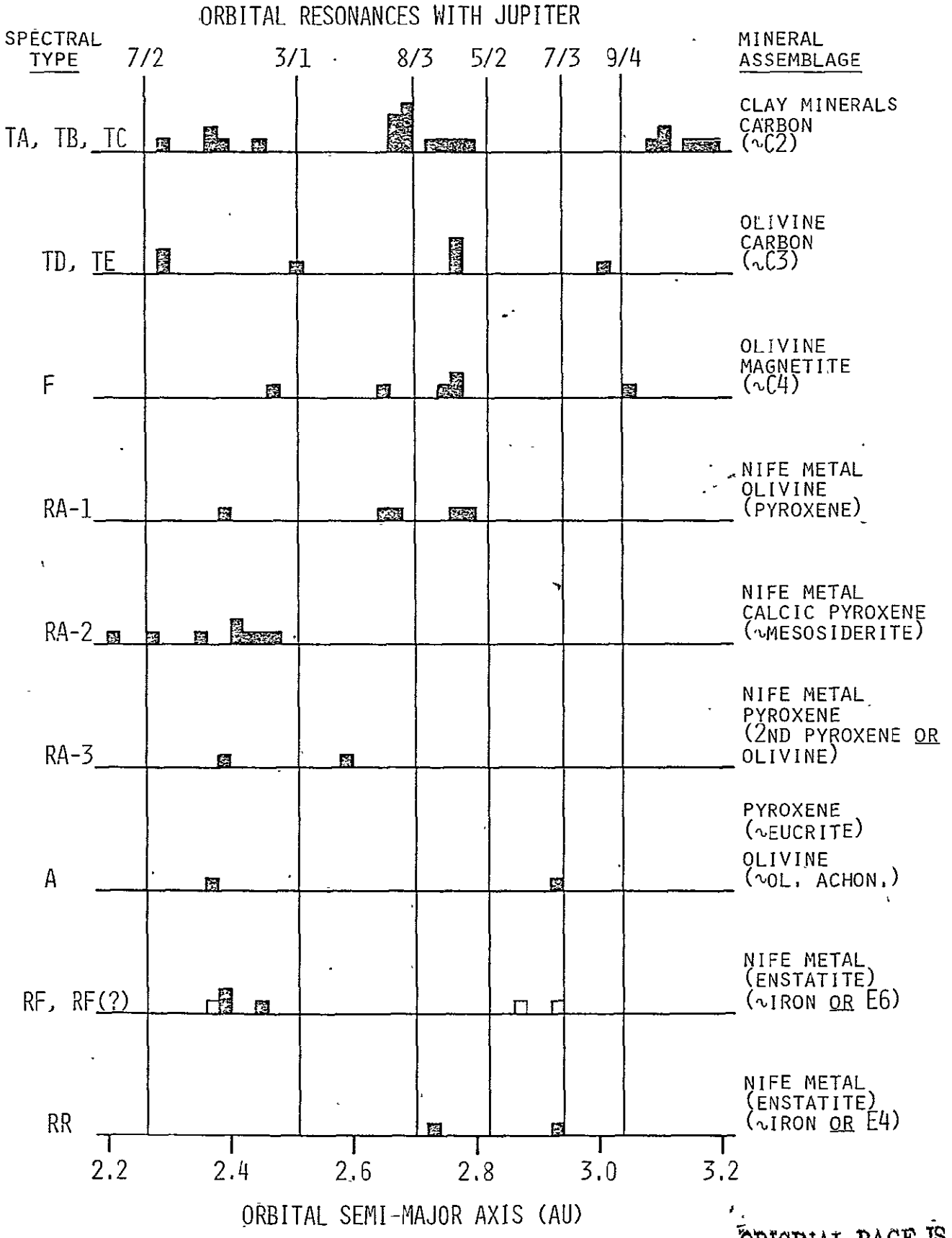

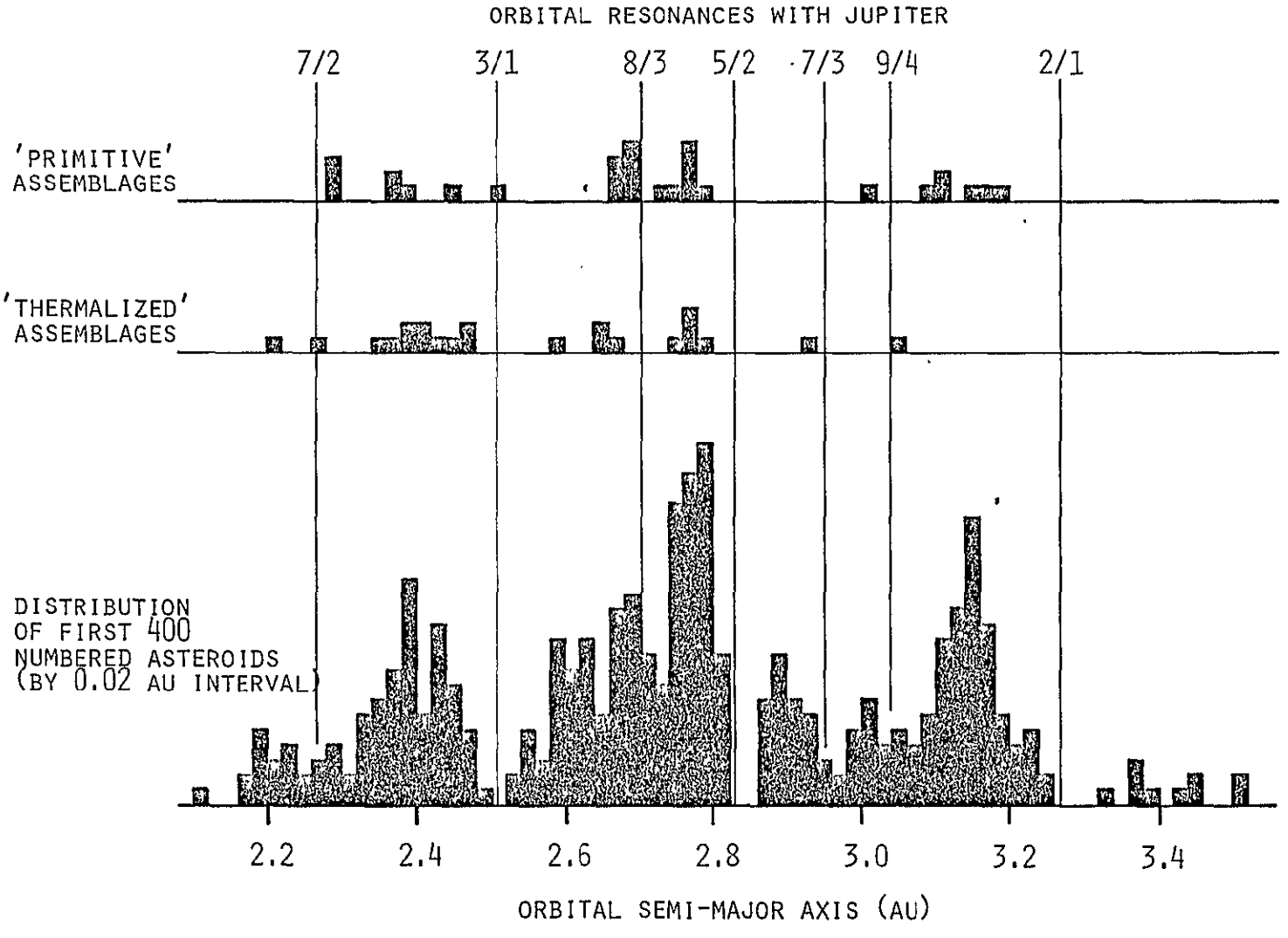
ORBITAL RESONANCES WITH JUPITER
7/2
3/1
8/3
5/2
7/3
9/4
2/1
'PRIMITIVE' ASSEMBLAGES
'THERMALIZED' ASSEMBLAGES
DISTRIBUTION OF FIRST 400 NUMBERED ASTEROIDS (BY 0.02 AU INTERVAL)
2.2
2.4
2.6
2.8
3.0
3.2
3.4
ORBITAL SEMI-MAJOR AXIS (AU)

FIGURE 8B

FIGURE 9